UNIVERSITY OF THESSALY

SCHOOL OF ENGINEERING

DEPARTMENT OF MECHANICAL ENGINEERING

Diploma Thesis

Low temperature direct ethanol fuel cells in acidic media

By

Chrysopoulou Klairy

Maistralis Antonios

Supervisor

Prof. Tsiakaras Panagiotis

Submitted in partial fulfillment of the requirements for the degree of Diploma in Mechanical Engineering at the University of Thessaly

Volos, 2022

ΠΑΝΕΠΙΣΤΗΜΙΟ ΘΕΣΣΑΛΙΑΣ

ΠΟΛΥΤΕΧΝΙΚΗ ΣΧΟΛΗ

ΤΜΗΜΑ ΜΗΧΑΝΟΛΟΓΩΝ ΜΗΧΑΝΙΚΩΝ

Διπλωματική Εργασία

Κυψέλες καυσίμου χαμηλής θερμοκρασίας λειτουργίας με απευθείας τροφοδοσίας αιθανόλης σε όξινο περιβάλλον

Υπό

Μαϊστράλης Αντώνιος

Χρυσοπούλου Κλαίρη

Επιβλέπων

Καθηγητής Τσιακάρας Παναγιώτης

Υπεβλήθη για την εκπλήρωση μέρους των απαιτήσεων για την απόκτηση του Διπλώματος Μηχανολόγου Μηχανικού

Βόλος, 2022

Approved by the Committee on Final Examination:

Advisor Dr. Tsiakaras Panagiotis (Supervisor)
Professor of Department of Mechanical Engineering
School of Engineering
University of Thessaly

Member Dr. Charalampous Georgios
Assistant Professor of Department of Mechanical Engineering
School of Engineering
University of Thessaly

Member Dr. Brouzgou Angeliki
Assistant Professor of Department of Energy Systems
School of Technological Sciences, University of Thessaly

ΕΥΧΑΡΙΣΤΙΕΣ

Με την διεκπεραίωση της παρούσας διπλωματικής εργασίας, καταφέραμε να κλείσουμε τον κύκλο των σπουδών μας. Θα θέλαμε να ευχαριστήσουμε θερμά τον καθηγητή και επόπτη μας κύριο Παναγιώτη Τσιακάρα για την πολύτιμη βοήθεια, γνώση, υποστήριξη και τις συμβουλές που μας προσέφερε καθ' όλη την διάρκεια της διαδικασίας συγγραφής της εργασίας μας καθώς και για την άμεση ανταπόκριση που μας παρείχε σε κάθε στάδιο.

Στη συνέχεια, για την ηθική και οικονομική υποστήριξη σε όλη τη διάρκεια των σπουδών τους, αφενός η Κλαίρη Χρυσοπούλου θα ήθελε να ευχαριστήσει τους γονείς της Αθανάσιο Χρυσόπουλο και Γεσθημανή Χατζηπαναγιώτου και την αδελφή της Εριφύλη, και αφετέρου ο Αντώνης Μαϊστράλης θα ήθελε επίσης να ευχαριστήσει τους γονείς του Ευάγγελο Μαϊστράλη και Ελευθερία Παπαζή και τον αδελφό του Νίκο.

Τέλος, δεν θα μπορούσαμε να παραλείψουμε το μεγαλύτερο ευχαριστώ στους φίλους μας οι οποίοι ήταν κοντά μας όλα αυτά τα χρόνια και μας έδιναν καθημερινά την υποστήριξη και την αγάπη τους, ιδιαίτερα τον τελευταίο καιρό διότι χωρίς την παρότρυνση και την ώθηση τους δεν θα είχαμε καταφέρει να φέρουμε εις πέρας αυτό το έργο.

ACKNOWLEDGEMENTS

We were able to end our academic cycle with the completion of this thesis. We would like to express our gratitude to Mr. Panagiotis Tsiakaras, our professor and supervisor, for his invaluable assistance, knowledge, support, and advise throughout the writing of our thesis and for his prompt assistance at every stage.

Next, we would like to thank our beloved parents Athanasios Chrysopoulos, Gesthimani Hatzipanagiotou and Evangelos Maistralis, Eleftheria Papazi and the rest of our family members for their moral and financial support. Important contributors during this trip were our brothers Erifili Chrysopoulou and Nikos Maistralis who were always by our side.

Finally, we could not leave out the biggest thanks to our friends who have been close to us all these years and gave us their daily support and love, especially lately because without their encouragement and push we could not accomplish this project.

ΠΕΡΙΛΗΨΗ

Η παρούσα εργασία πραγματεύεται το θέμα των κυψελών καυσίμου με απευθείας τροφοδοσία αιθανόλης σε όξινο περιβάλλον (PEMFC) και σε χαμηλές θερμοκρασίες λειτουργίας (έως 80^{o}C).

Αρχικά, (1^{ο} κεφάλαιο) γίνεται μια εισαγωγή γενικά στο ενεργειακό πρόβλημα και τις αιτίες που το προκαλούν, ενώ στην συνέχεια παρουσιάζεται μια ιστορική αναδρομή στις κυψέλες καυσίμου, οι λόγοι για τους οποίους αναπτύσσονται και χρησιμοποιούνται ευρέως, καθώς και αναφορά στην αιθανόλη ως καύσιμο και στη σύγκριση της με άλλα καύσιμα όπως η μεθανόλη και το υδρογόνο.

Εν συνεχεία (2^{ο} κεφάλαιο), γίνεται αναφορά στην ηλεκτροχημεία και τις ηλεκτροχημικές συσκευές (μπαταρίες, πυκνωτές, ηλεκτροχημικοί αισθητήρες). Αναλύεται η γενική τεχνική πάνω στην οποία στηρίζεται η λειτουργία των ηλεκτροχημικών συσκευών καθώς και οι κινητικοί και θερμοδυναμικοί νόμοι που την διέπουν. Παρουσιάζεται η αρχή λειτουργίας των κυψελών, θα αναλυθεί η μορφολογία της κυψέλης -δηλαδή τα ηλεκτρόδια , ο καταλύτης , η μεμβράνη, ο ηλεκτρολύτης, τα bipolar plates και το diffusion layer-, οι τύποι κυψελών, περιβάλλον και θερμοκρασίες λειτουργίας και τα βασικά χαρακτηριστικά τους.

Κατόπιν (3^{ο} κεφάλαιο) εξετάζονται οι κυψέλες καυσίμων με τροφοδοσία αλκοολών. Παρουσιάζεται η θεωρία που αφορά την αναμόρφωση των υδρογονανθράκων και οι τέσσερις βασικοί τρόποι με τους οποίους μπορεί να επιτευχθεί. Το επόμενο κομμάτι του κεφαλαίου αφορά τις κυψέλες καυσίμου απευθείας τροφοδοσίας αιθανόλης σε αλκαλικό και όξινο περιβάλλον καθώς επίσης και των κυψελών στερεών ηλεκτρολυτών με ανάλυση της αρχής λειτουργίας τους και των προκλήσεων που έχουν να αντιμετωπιστούν. Παράλληλα γίνεται μια σύγκριση μεταξύ των όξινων και αλκαλικών κυψελών.

Έπειτα (4^{ο} κεφάλαιο), διεξάγεται εκτενής επισκόπηση των κυψελών καυσίμου χαμηλής θερμοκρασίας λειτουργίας σε όξινο περιβάλλον. Πιο συγκεκριμένα, αναλύονται τα υλικά που χρησιμοποιούνται στις συγκεκριμένες θερμοκρασίες , οι ιδιότητες και η απόδοση τους σε διάφορες πυκνότητες ρεύματος. Το συγκεκριμένο κεφάλαιο στηρίζεται και αναπτύσσεται με βιβλιογραφική ανασκόπηση και παρουσίαση της μέχρι τώρα πορείας των κυψελών καυσίμου.

Τέλος (5^{ο} κεφάλαιο) , γίνεται λόγος για την απόδοση- σύγκριση των κυψελών , ανάλυση των αποτελεσμάτων και συμπεράσματα για την κατάλληλη επιλογή υλικών που προκύπτουν από την έρευνα και τις συγκρίσεις που διεξήχθησαν.

ABSTRACT

This essay discusses direct-fed ethanol fuel cells working at low temperatures and in an acidic environment (PEMFC) (up to 80^{o}C).

In the first chapter, the overall energy problem and its causes will be introduced, followed by a historical overview of fuel cells, the factors that led to their development and their widespread application, as well as a reference to ethanol as a fuel and a comparison to other fuels like methanol and hydrogen.

In Chapter 2, electrochemistry and electrochemical devices will be discussed (batteries, capacitors, electrochemical sensors). Analyses of the kinetic and thermodynamic rules governing electrochemical devices as well as the overall mechanism upon which they operate will be presented. Cell morphology, including the electrodes, catalyst, membrane, electrolyte, bipolar plates, and diffusion layer, as well as the types of cells, their operating environments and temperatures, and their fundamental characteristics, will all be discussed. The principle of how cells work will also be presented.

The discussion of fuel cells with alcohol feed follows in Chapter 3. The theory governing the reforming of hydrocarbons will be discussed, along with the four primary methods by which it can be accomplished. Direct-fed ethanol fuel cells in alkaline and acidic environments as well as solid electrolyte fuel cells will be covered in the following section of the chapter along with an analysis of their operating principles and the difficulties they encounter. The comparison of acidic and alkaline cells will take place concurrently.

Chapter 4 will provide a thorough discussion of low-temperature fuel cells that operate in an acidic environment. The materials employed at these temperatures, their characteristics, and their performance at different current densities will be examined. A literature review and a summary of the development of fuel cells to date serve as the foundation of this chapter.

In the last section (Chapter 5), the performance comparison of the cells will be covered, along with an analysis of the findings and recommendations for the best choice of materials based on the research and comparisons conducted.

Table of Contents

List of Figures

List of Tables

CHAPTER I

1. Introduction

1.1 Energy crisis, fuel cells and biofuels

One of the most serious problems confronted by the mankind during the last decades is the so-called energy crisis. Although the energy crisis has been the consequence of a complex combination of many factors, the ever-increasing world's population, and the overexploitation of fossil-fuel resources can be considered among the most important. Energy is crucial in almost every human activity, and as a result, implications of the crisis have now social and political repercussions and energy is a means of exerting international leverage [1]. Corollaries of this worldwide phenomenon are the greenhouse gas emissions, climate change, extreme weather conditions, and acid rain. Due to all these factors, mankind attempts to examine alternative energy sources and has come a long way by developing devices that operate with solar energy, hydrogen, wind power, biomass, geothermal energy and ocean wave energy [2]. Alternative fuels also known as advanced fuels, are substances that can be used instead of conventional fuels. The conventional fuels that are used today are fossil fuels, such as petroleum, coal, natural gas, propane, and nuclear substances like uranium.

One of the most remarkable and promising developments is the electrochemical device of fuel cell (FC) that produces electrical power directly from fuel through an electrochemical process and is also used for storage. Fuel cell technology possesses unique benefits that almost no other device can provide. The first benefit associated with the use of FCs is energy security, since the device is operating with fuels that are available almost in every country and thus, it reduces imports of fuels and their price, which is also a result of the broad range of fuels that can be used. Fuel cells provide a steady power supply, and they work in a low-temperature environment with no moving parts which are two important features of their application and reliability. The elimination of gas emissions, along with their low cost and quiet operations give another advantage that makes FCs standing out. Moreover, in contrast with thermodynamic devices, fuel cells have been regarded as highly efficient devices with a range of 70% to almost 100% efficiency (with heat recovery) and a supplement to this fact is that they also work in a wide range of power ratings in stationary and portable applications [3]. In addition to the previous advantages, fuel cells are characterized by long lives and zero environmental impact [4]. The first application of this technology was made with hydrogen fuel cells which produce electricity using hydrogen (H_2) as fuel. Nowadays progress on fuel cells leads to many capabilities on the fuels that

can be used depending on the type of fuel cells. Non-alcohol fuel cells work with hydrazine, ethylene, dimethyl-ether, etc. and alcohol fuel cells use methanol, propanol and ethanol.

At this point, it is worth making a reference to biofuels, liquid, gaseous or solid, which are mainly produced from biomass. Biomass is the energy source that comes from organic matter and is regarded as a viable alternative to fossil fuels, as well as the world's fourth greatest accessible energy resource. Biomass may alternatively be described as a natural and affordable energy storage technology that can be used at any time. Biofuels are preferred over conventional fuels because of their biodegradability and their environmentally friendly nature.

1.2 Introduction of ethanol as fuel

Bioethanol is the most popular fuel used in the transportation sector as biofuel aiming and contributing to the reduction of gas emissions. As an organic chemical compound with molecular type C_2H_5OH belongs to the alkanol category. In environmental conditions it has the form of a volatile, flammable, and colourless liquid, consisting of an ethyl group (C_2H_5) linked to a hydroxyl group (OH). It is an excellent alternative fuel option as it is abundantly available, low cost, low toxic, with desired physicochemical features as well as high energy density. Also, it is used either blended with gasoline in low or high percentages on internal combustion engines, or exclusively, as a fuel-on-fuel cells. Methanol, like ethanol, is among the most widely known and used alcohol fuels, however, its high toxicity and corrosion aspects due to the high-temperature performance render ethanol a more suitable fuel for fuel cells. Moreover, over the years, as regards transportation, there has been an evolution of hydrogen cars, but hydrogen has storage restrictions as well as lack of distribution infrastructure.

Bioethanol [5] is distinguished into three categories named as “generations” depending on the source of the product. First generation comes from feedstock, sugar-based such as sugarcane, sugar beet, fruits, sweet sorghum and starches such as corn, wheat, rice, and potato. Second generation bioethanol is based on lignocellulosic crops such as wood, straw and grasses, while the third generation biofuel is extracted from algae biomass [6]. The first-generation biofuels seemed to be very eco-friendly as they don’t harm the environment, however sustainability concerns about the use of feedstocks as a fuel and not as a food, lead scientists to search for the second and third generation biofuels mentioned above. The production process depends on the crop used, but generally it consists of three basic steps: the acquisition of a mass that contains sugars which can be fermented, conversion of sugars via fermentation and lastly, separation of ethanol and after that purification. These three processes are achieved via pretreatment, hydrolysis, and fermentation.

Pretreatment is a very important step since the production yield depends on the product of the operation. It contributes to the process by boosting the fermentation, resulting in higher amounts of produced sugar, and it facilitates the next operation, hydrolysis. There are various ways of pretreatment but the most common are; physical pretreatment which usually refers to the operation of milling the biomass into smaller sizes, and chemical pretreatment which refers to ozonolysis acid hydrolysis or alkaline hydrolysis. Other methods are biological and physicochemical pretreatment.

After the first treatment, the hydrolysis process follows, where feedstocks are converted into fermentable sugars. There are two methods of conducting this process. The first one is, acidic hydrolysis which is the most known and used operation and is separated in two different methods dilute and concentrated, while the second one is enzymatic hydrolysis. Acid hydrolysis is divided into two subcategories, dilute and concentrate, acidic dilute hydrolysis is the most common operation, and it is held at higher temperatures in a low acid concentration, however there is a drawback, because it produces larger quantity of inhibitors in comparison with concentrated hydrolysis. Concentrated hydrolysis is held at lower temperatures in a high acid concentration and in a smaller period of time it can generate higher sugar recovery up to 90% in comparison to acid hydrolysis which cannot have these amounts of recovery and as a result it increases the operation cost. As for the enzymatic hydrolysis, enzymes are responsible of the transformation of feedstocks into fermentable sugars.

Fermentation processing is divided into three main categories: i) separate hydrolysis and fermentation (SHF), ii) simultaneous saccharification and fermentation (SSF) and iii) simultaneous saccharification and co-fermentation (SSCF). SHF is less preferred than the other two processes because the operations of hydrolysis and fermentation occurs in different tanks and as a result it is less efficient, more expensive and has higher processing time.

Sugar-based ethanol from sugarcane and sugar beet is extracted by the procedure of milling, fermentation, and distillation. As for the starch the process is the same with the addition of gelatinization and hydrolysis. According to surveys, it involves the lowest production cost. Ethanol's performance is based on the total efficiency of conversion, which depends on the nature of biomass, the conditions of the process and the microorganisms used. According to a study [7], sugarcane expanses in comparison with corn and sugar beet are more efficient as greenhouse emissions are reduced by 40%. Furthermore, sugarcane's expenses in comparison with corn and sugar beet are reduced by 60% and 75% respectively.

CHAPTER II

2. Fundamentals of Catalysis, Electrochemistry and Electrochemical devices

2.1 Electrochemistry

Electrochemistry has deep roots on the 18th century, since many scientists have been involved with the study of the relation between chemistry and electricity. The first one, whose experiment gave the green light for further and extensive analysis, was the Italian Luigi Galvani in 1781. His experiment was the application of electrical current on the legs of a frog. The result was the stimulation of the frog's muscles which in his mind could be explained as: each muscle works like a Leyden jar (the first version of capacitor) where positive and negative potential exist on each muscle and fiber tissue [8].

The next scientist contributing to the evolution of electrochemistry was the Italian physicist Alessandro Volta. In 1800 Volta constructed the first device - known today as battery - called volta pile. The idea of behind this pile was that it had no need of any special oxidizer; instead, simple water flowing through the silver cathode was breaking down into hydrogen gas. The energy of a single pile was about 0.4 Volt and as a result, if more energy was required, larger devices were necessary. Volta's idea transmitted the stimulus to many scientists for further research, leading to the huge development of the battery [9].

A few weeks after Volta's invention in early 1800's (volta pile) [10, 11] the world experienced a new discovery, the conversion of electricity and chemistry as the British William Nicholson and Anthony Carlisle after multiple experiments found out that when electrical current permeates water ,it creates gaseous bubbles of H_2 and O_2. The potential of the electrodes was higher than 1.5 Volt (thermodynamic potential) and the material of electrocatalyst was Pt in order to eliminate kinetic loses. This was the first time that chemical materials changed their identity as separable substances and this reaction is the foundation of catalysis.

Continuing in the mid 1800's and specifically in 1834 Michael Faraday after a long series of experiments managed to discover many electromagnetic phenomena but also, he became famous for his two laws known as Faraday's law in electrolysis. His work is based on experiments without using mathematical equations since his lack of education deprived him of this way of studying, yet with his quantitative methods, found out that under different conditions the same amount of electricity passing through a solution decomposes the same amount of a substance [12]. In 1842 William Groove using his information about hydrogen and oxygen reaction on a platinum surface, managed to build the first fuel

cell in a sulfuring acid [13]. Over the next years many significant scientists have made great contributions to electrochemistry via their findings. In 1836 John Frederick Daniell invented the constant battery which, after 100 years became the common battery [14]. In 1839, Edmund Becquerel discovered the photovoltaic effect [15] as when light reaches the surface of two brass plates dipped in a liquid produces electrical current. Around 1900 Walther Nernst one of the pioneers of physical chemistry was interested in experimental data and as a result he invented the famous Nernst equation and the Nernst lamp [16]. Also, in the 19th century the research of Clausius and Williamson in electrolysis led them to the conclusion that conversion on chemical particles can occur with their physical molecular motion, a discovery that shed light on the development of the physical science. The evolution of electrochemistry continues in the last century with the presence of the universities as they significantly contribute to the progress of this science [17].

The science of Electrochemistry is a well-established sector, originating from the conjunction of two main fields of nature, science chemistry and electricity, that have come together to develop new approaches to important issues such as sustainable energy sources. Theoretical and applied electrochemistry, are the two primary branches of electrochemistry. The first branch, theoretical, is concerned with the study of chemicals and procedures. Electrochemical cells are divided into two main categories. The first one is galvanic cells and the second, electrolytic cells. Regarding galvanic cells, chemical reactions occur on the surface of the two electrodes; one reaction occurs on the anode and the other on the cathode. The place which the oxidation takes place is called anode and it is the positive pole of an electrolytic cell but also, a negative pole of a galvanic cell. On the other hand, reduction occurs on the cathode which is the opposite sign, as for the electrolytic cell is the negative pole and for the galvanic cell, the positive [18]. Applied electrochemistry investigates the phenomena of metal structure corrosion as well as protection methods. It examines the design and operation of devices that generate electric current and are utilized in everyday life (accumulators-Galvanic cells). In recent years, electrochemistry has experienced rapid expansion and gained a lot of traction among researchers in both, academia, and industry, due to increasing environmental awareness since there is a need for enormous electrical loads and therefore for developed for energy storage. This gap is narrowing with the indirect energy production via chemical bonds and reactions and the constant current that is provided. Accordingly, the dominant theory of electrochemistry has been established and developed based on the physical and chemical properties of ionic conductors, electronic conductors and even insulators [19]. If a chemical reaction is driven by external applied voltage or voltage is created by a chemical reaction, then there is an electrochemical reaction. More precisely,

electrochemical reactions occur by electron transfer processes that are initiated on the surface of an electrode and thus, electrochemistry analyses the phenomena that happen at the interface between an electron conductor (electrode) and an ion conductor (electrolyte solution). Furthermore, electrochemistry addresses issues that are often found in other branches of research, such as the structure and characteristics of solid electrolytes and the kinetics of ionic processes in solutions [20].

The use of electrochemistry may be found in four distinct domains: i) the production of chemicals (with catalytic reactions), ii) the production and storage of electricity, iii) corrosion, and finally iv) the environmental sector. A few examples of electrochemical applications are the following:

- Batteries, fuel cells, capacitors
- Potentiometric and galvanic sensors
- Electrolysis
- Electrosynthesis
- Metal plating and processing
- Waste treatment

Figure 1 below gives extensive examples of electrochemistry depending on the field that is applied. Apart from the depicted fields, electrochemical methods have also contributed to many medical achievements [21].

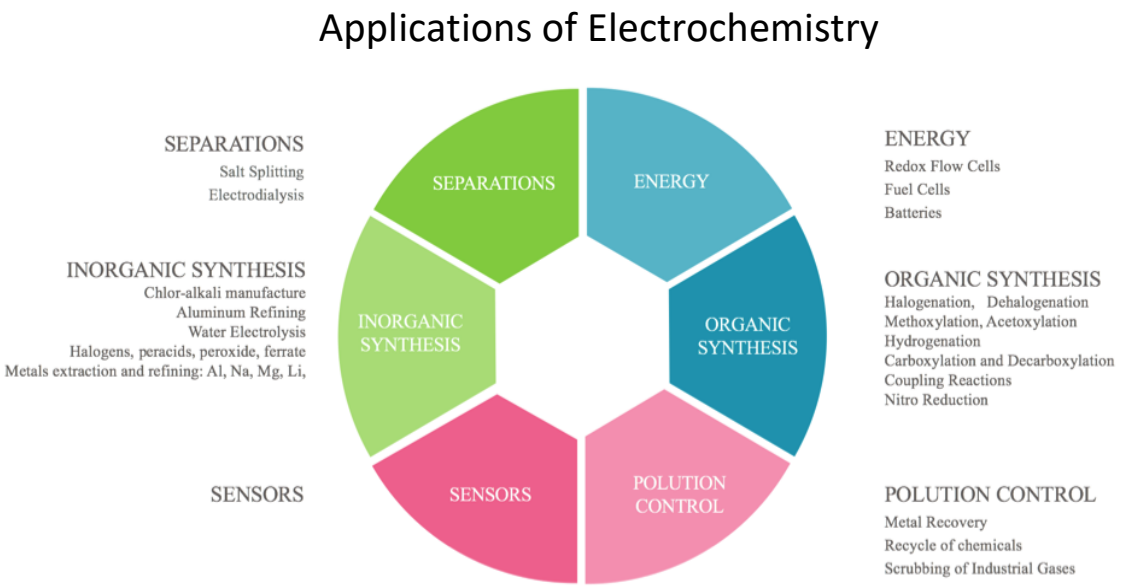

Figure 1. Applications of Electrochemistry in many different fields.

2.1.1 General Technique

Electrochemistry, as previously stated, deals with the movement of electrons as they pass through a conductor in a closed circuit, referred as an electrochemical cell. Also, electric current can occur via the movement of ions when a solution is between the anode and the cathode. The chemical reactions are taking place on the interface of the electrode/electrolyte. Electrochemical

cells are one of the fundamental breakthroughs of electrochemistry and they illustrate how principles of this science are applied. To gain insight into the chemical reactions involving many components (electrodes, electrolytes etc.) in the electrochemical cells and determine how they operate, it is important to introduce some basic terminology:

- Conductor: There are three types of conductors, ionic, electronic and mixed conductors. In general, conductor is the material that carries either ions or electronic charge carriers (holes for electrons to move through them) and thus it allows current to flow. Ionic conductors transfer energy via the movement of ionic species while electronic conductors transfer energy in the form of electric current [22, 23].
- Electrode: An electrode is an electrical conductor that makes contact with the non-metallic circuit parts of a circuit, such as an electrolyte. If in an electrochemical cell, this is also known as an anode or cathode. The domain of research of electrodes is very important as the materials are responsible for the conductivity. The requirements of these materials are durability, stable temperatures, physical, chemical, and mechanical stability.
- Anode: Is it a positive-sided electrode where the electricity moves into. It acts as an electron donor. In electrochemical cells oxidation (loss of electrons) takes place on this electrode.
- Cathode: Is a negative-sided electrode from where the electricity flows out or is given out. It acts as an electron acceptor. In electrochemical cells reduction (gain of electrons) takes place on this electrode.

When we examine galvanic cells, the exact opposite is occurring for both the anode and the cathode. Cathode is swapped by anode -now anode is negatively charged-, and vice versa as seen in **Figure 2a**.

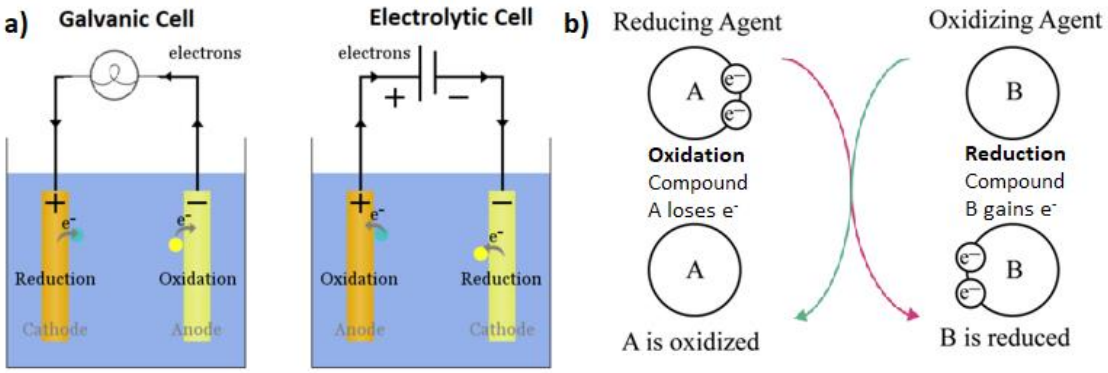

Figure 2. a) Representation of galvanic and electrolytic cell b) Illustration of a redox.

- Redox: Chemical reactions involving simultaneously oxidation and reduction processes (**Figure 2b**).

- Half-cell reaction: Is either the oxidation or reduction reaction component of a redox reaction.
- Electrolyte: In any electrochemical device, electrolyte is an ionic conductor between two electrodes which provides ionic current to support the reactions [24].

After the introduction of the fundamental terms, it is possible to provide a more extensive description of the electrochemical cell. Generally, electrochemical cells are divided into two sub-types, galvanic and electrolytic. Electricity is generated by galvanic cells while an electrolytic cell utilizes electricity to create or dissolve chemical bonds. A typical electrochemical cell consists of two electrodes, an anode and a cathode and it is divided into two main categories: galvanic cell, electrolytic cell (**Figure 2a**). Electrons move through an external circuit via an electric conductor that connects anode and cathode. Also, between the two electrodes, there's a liquid/solid solution called electrolyte that carries anions (negatively charged ions) and cations (positively charged ions) that move freely and carry the current through the electrolyte. Overall, in an electrochemical cell a pair of reactions are taking place known as redox reactions [25, 26]. The **eq. 1** below, describes redox at equilibrium:

$$R \leftrightarrows O + ne^- \tag{1}$$

where O is the oxidized species, R is the reduced species and n is the number of electrons exchanged between O and R [27]. The formula that describes the relationship between Gibbs energy and concentrations of oxidized and reduced species is given by the **eq. 2**, as:

$$\Delta G = \Delta G^O + RTln\frac{[R]}{[O]} \tag{2}$$

where R is the gas constant (8,3145 J mol^{-1} K^{-1}) and T [K] is the temperature. The most important part of this equation is that it constructs a new equation that connects Gibbs energy with the dynamic of the reaction E [V], as described from **eq. 3**:

$$\Delta G = -nFE \tag{3}$$

here E is the maximum potential between the electrodes when no current is passing through the electrochemical cell and F is the Faraday's constant (96,485 C mol^{-1}). However, if there is activity in the cell, the equation can be written as **eq. 4**:

$$\Delta G^o = -nFE^o \tag{4}$$

In this case, E^o is the standard electrode potential and ΔG^o is the standard free Gibbs energy changed. A key tenet of electrochemistry is the mathematical formula that represents the correlation between potential and concentration, given by **eq. 5**:

$$E = E^O + \frac{RT}{nF} ln \frac{[O]}{[R]} \quad (5)$$

Also, apart from the term standard potential E^O another very useful term is added in these equations and it is known as the electromotive force (emf, Ɛ), which is the maximum potential when the circuit is open and its measurement unit is Volt. In general, the cell potential is calculated by the **eq. 6**:

$$E^O_{cell} = E^O_{cathode} - E^O_{anode} \quad (6)$$

Because of the redox reactions the conversion to emf has some changes at the signs of the terms and it converts to **eq. 7**:

$$Ɛ_{cell} = Ɛ_{cathode} + Ɛ_{anode} \quad (7)$$

The electromotive force determines if a reaction is spontaneous or not. More precisely, when the emf has a positive sign then the reaction is spontaneous while when it has negative, the reaction is non-spontaneous. Moreover, in order to express the rate of the process in the terms of current, the Faraday's law provides this possibility and describes the total charge of an electrochemical cell through the **eq. 8**:

$$Q = nFN \quad (8)$$

According to this equation, the total charge (number of coulombs spent during a chemical process) is proportional to the amount of product in moles reacted per unit of electrode area (mass rate production) (N), the Faraday constant (F) and the number of electrons.

2.1.2 Kinetics

Kinetics of a chemical reaction is the study of the rates of transformation of chemical compounds from reactant species into products. Therefore, it's crucial to study and understand some of the fundamental relationships that underpin reaction kinetics. Also, they are critical for determining how much current can be generated with a standard quantity of overpotential. At the redox reactions there is also a mass transfer mechanism that takes place and completes the procedure. Electrochemical reactions are heterogeneous chemical processes and thus, transfer phenomena should be considered, beginning with overpotential.

2.1.2.1 Overpotential

As the energy system tries to stay in equilibrium, the transport of electrons from anode to cathode needs an initial energy to complete this task. Nowadays, as technology develops, it is desirable that the time of the reactions on electrochemical cells needs to be as fast as possible. This aim is achieved by the overpotential enforcement on reactions. The overcome of this

activation energy which results in a chemical reaction is called overpotential (η) and is expressed as (η) by **eq. 9** [28].

$$\eta = E - E° \tag{9}$$

whereas E is the actual cell potential and E° is the potential of equilibrium. Its operation is different on electrolytic, and galvanic cells. In electrolytic cells the power supply needed for the fulfillment of the reaction, is more than the thermodynamic equilibrium, but as for the galvanic cells, overpotential means that there are losses during the reaction and as a result less energy is produced. In both cases, the additional energy needed, is due to the conversion in thermal energy. Overpotential is the sum of three main parameters, activation overpotential η_{act}, ohmic overpotential η_o, concentration overpotential η_c as seen in **eq. 10**:

$$\eta = \eta_a + \eta_o + \eta_c \tag{10}$$

Activation overpotential (η_a) is referred to as resistance that is developed on the surface of the electrode as multiple reaction and electron transfer take place. Usually, electrons pile on the electrode and as a result the new ingoing electrons can't intrude in order to transfer from anode to cathode. Another reason that may cause overpotential could be some reactions that act upon the electrode such as catalytic decomposition and crystallization [29].

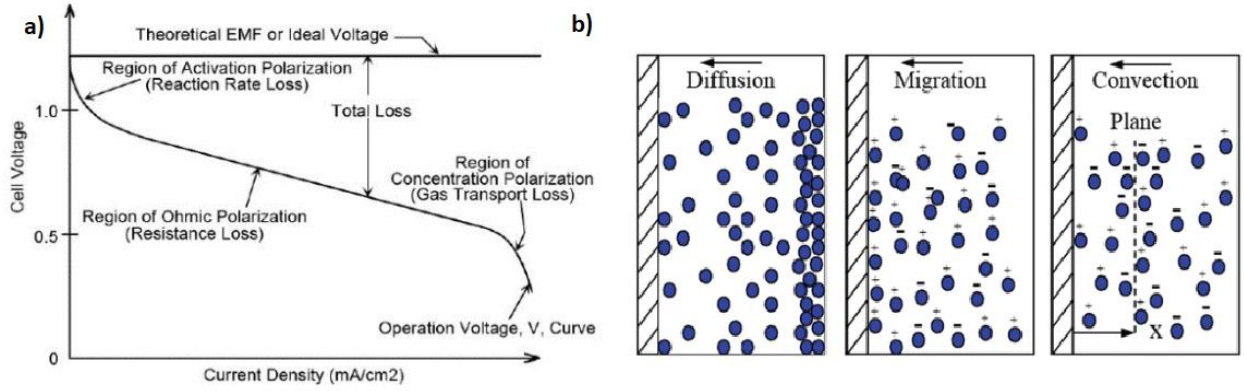

Figure 3. a) Typical curve of electrochemical cell overpotential losses; b) Main types of mass transfer [30].

Ohmic overpotential refers to the sum of the resistances of the components existing in an electrochemical cell like electrodes, membrane, electrolyte, etc. More specifically the ionic transfer through the membrane depends on the distance of the electrodes and the conductivity of the solution. Resistance can be reduced if the distance of the surfaces is short. Generally, ionic resistance is higher than electronic, except if there are semiconducting materials or there is a coat of passive film on the electrode [31]. In an electrochemical cell the main ground for research is the behavior of the current on the applied voltage where, according to Ohm's law, the voltage that is required for an electrolytic cell is described from **eq. 11**:

$$E_{cell} = E_{cell,rev} + iR_{\Omega} \tag{11}$$

where i is the current density in units (A/cm^2), referring to the total current divided by the total surface of the electrode. On the other hand, the voltage for the galvanic cell is given by **eq. 12**:

$$E_{cell} = E_{cell,rev} - iR_{\Omega} \quad (12)$$

When it comes to overpotential, the main aim is to reach as close to the ideal voltage line as possible, as seen in **Figure 3a**. The entropy is the blank area between the actual curve and the line of emf, and it corresponds to the system's losses, which are simply undesirable and must be eradicated as soon as possible. Entropy always increases when an isolated system changes, and its change is equivalent to the amount of thermal energy that can no longer be used to produce work. More precisely, when losses are reduced, the curve shifts to the top and the entropy decreases.

Mass transfer is parsed in 3 main types (**Figure 3b**)**:** diffusion, migration and convection, which in combination follow the fast speed of the reaction and as a result there is an accumulation of products on the cathode or a discharge of reactants on the anode which leads to the above-mentioned resistance. Specifically, in diffusion there is a transfer of species from higher concentration levels to lower. Migration generally contributes positively to mass transfer rate; however, it becomes undesirable when the signs between the electrode space field and the diffusion layer field are opposite. In this case potential gradient is needed to provoke the movement of charged species. Convection refers to the flow of a mass of liquid due to external forces such as gradient pressure which is caused from the difference in density levels of the anode and the cathode. The sum of these three types of mass transfer gives the total mass transfer, **eq. 13**, according to Nernst-Plank equation:

$$J_i = -D_i \nabla c_i - u_i c_i \nabla \Phi + c_i v_i \quad (13)$$

where J_i is the total flux density, the first term of the equation refers to the diffusion of the flux of the ions and comes from Fick's first law given by **eq. 14**:

$$J_i = -D_i \frac{dci}{dx} \quad (14)$$

The second term refers to the migration of the moles and the third term to the convection.

At this point it would be useful to mention that the concentration on the electrode surface depends mainly on the current applied since, it is the current that determines the speed of the reaction, as the rate of mass transfer is balanced by the external current transfer. This means that the more we increase the current density, the faster the reaction becomes and the less the electrode surface concentration. Nevertheless, this rate has a finite maximum value, named as critical current, at which the concentration on electrode surfaces is zero. The relation between concentration and current is shown by the formula below, explaining the preceding definition.

The current density (i_{cr}) of a diffusion reaction until the critical level is expressed as **eq. 15**:

$$i_{cr} = \frac{nFDc^*}{\delta} \quad (15)$$

Where D is the diffusion coefficient, c* is the concentration on the bulk of the reactant, δ is the thickness of the diffusion layer.

2.1.2.2 Butler-Volmer and Tafel Equation

The Butler-Volmer equation constitutes an important part of electrochemistry since it describes the connection between the current density that can be produced from a standard amount of overpotential applied and thus, how the voltage difference between the electrode and the bulk electrolyte affects the electrical current via an electrode. It is known that, at the state of equilibrium, the cell reaches its maximum potential. Nevertheless, when the current passes through the electrode a drop of potential is observed due to electrochemical ability. The potential drop depends on the type of the electrode (material) that determines if the electrode has fast kinetics and produces more electrons in short time, namely the kinetic rate. The chapter of kinetics, as well as the equations that underpin it, is based on the current density which is determined below by **eq. 16**:

$$i = \frac{I}{A} \quad (16)$$

Where, i is the total current and A is the electrode surface area. A redox reaction, as mentioned above, is described from **eq. 17**:

$$R \underset{k_b}{\overset{k_f}{\leftrightharpoons}} O + ne^- \quad (17)$$

Where k_b, k_f are the heterogeneous rate constants, f stands for forward (oxidation, anode) and b for backward (reduction, cathode) and they depend on the temperature (T) and the free Gibbs energy of the reaction (ΔG). The correlation between the rate constants and the parameters is given by **eq. 18** and **eq. 19**:

$$k_f = k_{o,f} e^{(-\frac{a_{red} nF\eta}{RT})} \quad (18)$$

$$k_b = k_{o,b} e^{(\frac{a_{ox} nF\eta}{RT})} \quad (19)$$

Each electrode has its own current density depending on the half-cell reaction that takes place on it and is defined by **eq. 20** and **eq. 21**:

$$i_a = k_f C_{ox} \quad (20)$$

$$i_c = k_b C_{red} \quad (21)$$

Where, C_{ox}, C_{red} refers to the concentration of the redox species. When it comes to equilibrium it applies that $i_a = i_c$. The total current density for the whole cell, including both half-cell reactions, is shown below in **eq. 22**:

$$i = nF(i_a - i_c) = nF(k_f C_{ox} - k_b C_{red}) \quad (22)$$

And in a compact type, **eq. 23**, it takes the form known as the Butler-Volmer equation:

$$i = i_0 \left\{ e^{\left(\frac{a_{ox} nF\eta}{RT}\right)} - e^{\left(-\frac{a_{red} nF\eta}{RT}\right)} \right\} \quad (23)$$

In this equation there are some undefined terms that are explained below. Firstly, the term i_0 refers to the exchange current density at equilibrium conditions and it is a physical property of each material. Also, the higher the value of i_0 the faster the electrode is and the more electrons it produces in short time. Moreover, α is the charge transfer coefficient, η is the overpotential and the term $\alpha_{ox/red} nF_\eta$ is the electrical energy of reaction and electrons. Constants a_{ox}, a_{red} are two interdependent coefficients, since $a_{ox} + a_{red} = 1$, and relate to how the applied potential affects and favours anodic over cathodic reactions and vice versa.

The first term of the Butler-Volmer equation represents the anodic current and the second one the cathodic current. The Butler-Volmer equation gives the current density when the system is at equilibrium and both terms contribute equally. However, when the system is beyond this state and oxidation or reduction takes over, the current density changes and has a different sign depending on the half-cell reaction that is occurred at a higher level and thus to the potential. More specifically, when oxidation dominates, the potential is positive (η>0), but when there is reduction, the potential is negative (η<0). As a result, because we are far from equilibrium, the one term is considered to be negligible and the current density is no longer supplied by Butler-Volmer law, and the behaviour of the system is described by Tafel equation. **Figure 4a** shows that when the voltage, so overpotential, increases, the anodic current (red line) grows as well, whereas the cathodic current (blue line) approaches to zero. The opposite behaviour is observed when the voltage has a negative value.

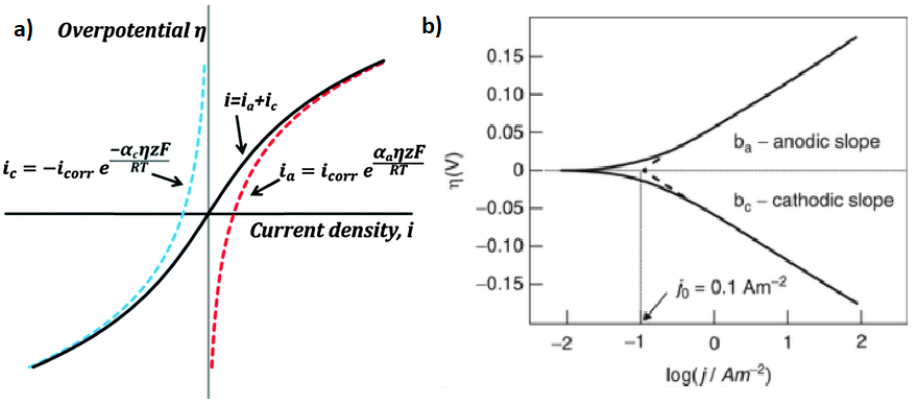

Figure 4. a) Typical I vs dependency based on the Butler-Volmer equation [32]; b) Tafel Slope for anodic and cathodic branches [33].

It is observed from **Figure 4b**, which is known as Tafel plots, that when the overpotential increases or decreases over a certain value (approximately 50 mV) the current increases exponentially and the equations for the anodic and cathodic current density can be expressed by **eq. 24** and **eq. 25**:

$$i_a = i_0 e^{\frac{\eta}{b_a}} \quad \text{for } \eta>0 \tag{24}$$

$$i_c = -i_0 e^{-\frac{\eta}{b_c}} \quad \text{for } \eta<0 \tag{25}$$

Where b_a, b_c are the Tafel slope for each condition. From the intercept of the slopes, exchange current i_0 can be calculated. Tafel slope value also indicates the number of electrons exchanged in the electrochemical reaction, thus they provide valuable information regarding the mechanism of a reaction. Tafel equation is usually presented as **eq. 26**:

$$n = b log_{10}(\frac{i}{i_0}) \tag{26}$$

2.1.3 Electrical Double Layer

Any electrode reaction, is an interfacial (heterogeneous) reaction that requires a charge transfer step, as well as a sequence of electrolyte reactant rearrangements before discharging at the electrode surface. There must be a compensatory balancing charge near the liquid phase for any charged solid surface, such as a metal electrode under potential submerged in liquid electrolyte (liquid-solid interface). As a result, the liquid phase has a small but finite volume that differs from the bulk liquid phase. More precisely, when a metal is immersed into an electrolyte (liquid), both phases carry different energy levels resulting in tension at their interface once they get into close contact and there's a spontaneous organization of charges at their interface. Due to the high dielectric constant of water, all compounds take on a negative charge when distributed in it. Ions attracted to the surface charge of metals accumulate around the particles in the liquid. The anionic surface is neutralized by cations, which create a well-ordered, immovable layer known as the surface (stationary) layer. Since, the metal's surface holds a large quantity of charge, a second layer forms due to the lower attractive force. As a result, the second layer, which is called diffusion layer, is disorganized. The two layered structure is called electrical double layer, and a potential drop is confined to only this region. The double layer is important for the study of electrode kinetics since it significantly affects the electron transfer rate [34],[35].

The electrode-solution interface has been discovered to behave like a typical electrical capacitor and models explaining the behaviour at the electrode-solution interface relate to those of capacitors. At any given potential there will be an accumulative charge on the electrode, Q_{Elec}, and an accumulative charge on the solution, Q_s. The voltage across, the interface, and the composition of the

solution, determine whether the charge on the electrode is negative or positive in relation to the solution. In all cases it is assumed that $Q_{Elec} = -Q_s$. The charge on the electrode is an excess or shortage of electrons that forms a very thin layer on the electrode surface, whereas the charge in solution is an excess of cations or anions. The array of charged species and oriented dipoles present at the electrode-solution interface is generally known as an electric double layer and is characterized by the bilayer capacitance C_{dl}, which is often a function of potential.

2.2 Fundamentals of Catalysis

2.2.1 Catalysis and figures of merit

Many chemical processes, even though they are thermodynamically permissible, cannot proceed on their own at a satisfactory rate. The basic variables that govern a reaction and allow it to be controlled are temperature, pressure, concentration and contact time. The majority of industrial reactions run under high pressure and temperature in order to achieve desirable rates of production. These conditions, though, have significant consequences such as corrosion and damage of the equipment and materials and furthermore they are energy intensive and have undesirable side reactions and products. To avoid such occurrences, technical advancements have been made that are divided into two sections that are both under the category of catalysis. Catalysis is the primary technique for achieving chemical transformations. It is a procedure where the presence of a substance (catalyst) that is not consumed during the reaction affects the rate and the result of the reaction. The first section is the application of catalysts, which are substances that speed up the reaction rates and allow them to run in lower temperatures and pressures. In reality, catalysts undergo reversible chemical changes during the process. The second section is concerned with improved methods of contacting, such as packed and fluidized catalyst beds that allow to operate in continuous flow conditions at higher efficiencies. Also, the increased focus on environmental protection has resulted in the growth of environmental catalysis, which can limit the emissions of unwanted or harmful substances in the environment [36], [37]. Catalysis is classified in two main branches, homogeneous and heterogeneous. There are five broad classes in catalysis research that depend on the catalysts that are used, biocatalysts; homogeneous catalysts; electrocatalysts; conventional heterogeneous catalysts and Ultra-high Vacuum (UHV) Surface Science. Catalysts contribute to the economy of the developing countries accounting for about one quarter of their gross domestic product. They are used in contact processes and catalytic converters as the three-way catalyst of a car [38, 39].

The energy route for converting reactants to products determines the reaction rate. Catalysts increase process in terms of productivity and energy consumption by offering an advantageous energy pathway. During catalysis the chemical bonds between the molecules are dissolved, altered, and reconstructed and then atoms are recombined into new molecules. In general, the role of the catalyst is reducing the energy barrier or activation energy of the reactants for both the forward and the reverse reactions and thus, increasing the rate of the reaction without being consumed. Because the catalysed path requires less activation energy than the uncatalyzed path, more molecules will have enough energy to react efficiently (**Figure 5a**). The energetics of the initial and final states are unaffected by the catalyst but, it accelerates their attainment and the approach to the equilibrium state predicted by chemical thermodynamics under certain conditions. More specifically, free energy and enthalpy are unaffected by the presence of the catalyst.

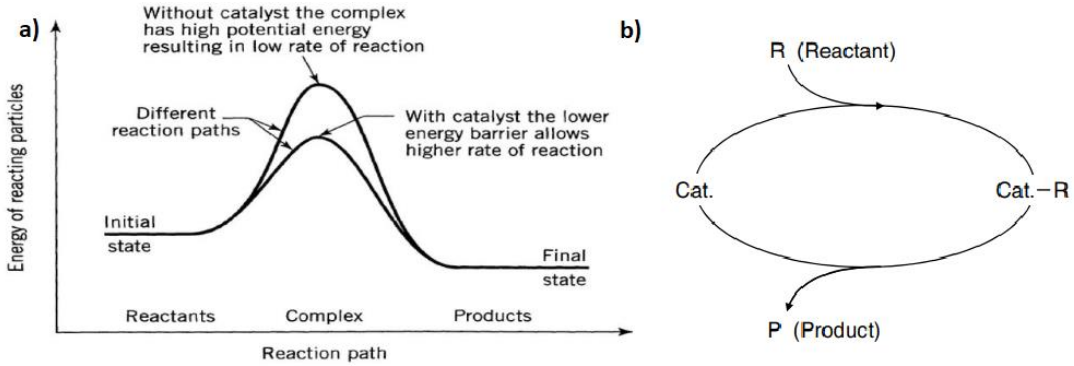

Figure 5. a) Effect of a catalyst on the activation energy. The catalyst provides a different reaction path with a lower activation energy; b) Catalytic cycle [40].

Catalysts are classified according to criteria such as structure, area of application, composition, or state of aggregation. They are classified as either homogeneous or heterogeneous. In the first case, the catalyst and the reactants are in the same phase, commonly in solutions and the catalysts are well-defined chemical compounds (molecule, ion, enzyme) dispersed in the reaction medium. It interacts with a reactant to produce an intermediate material, which decomposes or reacts with another reactant in one or more stages to renew the original catalyst and produce product.

The catalyst, in the second case, is usually a solid body, whereas the reactants are liquid or gaseous. Heterogeneous catalysis is also known as surface catalysis since the reaction takes place on the solid's surface and the catalytic activity is only visible in some areas of the catalytic surface called active sites and the reactant molecules are adsorbed onto a solid surface before they react with the catalyst to form the product [41].

Catalysis has at least four steps, and these steps combined define the catalytic cycle as displayed in **Figure 5b**. More particularly, with the reactants, the catalysts generate unstable intermediates, which break down into the next step, releasing the catalyst. It can then create an unstable intermediate with another reactant molecule, allowing the catalytic activity to continue. As a result, a catalyst or active site molecule 'reacts' with a large number of compounds [42, 43]. In the first step, adsorption of the reactant onto the surface of the catalyst where the bonds are dissolved and new bonds are created with the catalyst's active sites, then the activation of the adsorbed reactant takes place. In the next step reaction of the absorbed reactant occurs and eventually diffusion of the product from the surface into the gas or liquid phase (desorption) completes the catalytic transformation. The concept of the active site is the essential aspect to be analysed surrounding the discussion of the mechanism of catalytic reactions in heterogeneous catalytic reactions, which are complicated processes. The active site is a convergent atom or a set of similar domains on the catalyst surface where the catalytic transformation takes place. The catalytic process performance is determined by the concentration of accessible active sites per unit of surface area or volume of a catalyst. The number of active sites per unit of surface area varies by catalyst material, hence the amount of exposed surface area impacts total activity and reaction rate. Thus, increasing the number of accessible active sites by increasing the specific catalytic surface area is one strategy to improve catalyst performance hence the porous, honeycomb-like appearance is a common form of a catalyst at the surface catalysis procedure [44]. A special form of heterogeneous catalysis is the phase-transfer catalysis in which a phase-transfer catalyst, or PTC, aids in the migration of a reactant from one phase to another where the reaction occurs.

2.2.1.1 Activity, Stability, Selectivity

At this point it is crucial to discuss the three basic figures of merit for catalysts that determine its efficiency and must be considered in the selection of a catalyst. To begin with, activity is the first term to be explained. Catalytic activity refers to a catalyst's ability to accelerate a reaction. The physical contact of the reactants with the catalyst via chemisorption is what defines catalytic activity. The activity is determined by the rate of conversion, therefore, the rate that product is created or a reactant is eliminated and as a result it is measured by the specific reaction rate as follows by **eq. 27**:

$$r = \frac{1}{v_i N}\frac{dn_i}{dt} \tag{27}$$

where n_i is the number moles of reactant, t is time, N is the volume, weight or surface area of the catalyst and v_i is the stoichiometric coefficient of the reactant. The stoichiometric coefficient takes positive values when i, corresponds to a product and negative when it corresponds to a reactant.

Then onwards, the next term is selectivity. Selectivity is the ability of a catalyst to direct a reaction to yield a particular product and exclude other thermodynamically feasible products that are undesirable which lead to major gains in energy efficiency. So, the same reaction with different catalyst can yield to different products. This feature may be one of the most important variables of a catalyst that can be altered regarding the complex reactions [45]. Many parameters, such as the type of reaction and the conditions (temperature, pressure, reaction time) that might lead to different pathways during catalytic multipath reactions, can influence selectivity in addition to the type, shape, support (material with large surface that the catalyst is affixed on) and additives of the catalyst. This occurs because they influence the catalyst's chemical and thermal stabilities, as well as the reactions intermediates and surface mobility. At the molecular level, there are seven main parameters that can influence the activation energy barriers and allow reaction selectivity to be controlled. Surface structure, absorbate mobility, reaction intermediates, surface composition, charge transfer during catalysis and oxidation state of catalysis are the parameters mentioned above. To evaluate a catalyst's ability to accelerate a reaction in a specific direction, such as B production ($A \rightarrow B$), we utilize the parameter YB, which stands for selectivity as to B and is described by the relation described from **eq. 28**:

$$Y_B = \frac{C_B}{C_{A0}} \tag{28}$$

Where C_{A0} is the initial concentration of A, C_B is the concentration of the product B. Another parameter that can evaluate the catalysts selectivity is yield to B and the formula is described from **eq. 29**:

$$S_B = \frac{C_B}{C_{A0} - C_A} \tag{29}$$

Where, C_A is the concentration of A after the reaction.

Last but not least, stability is the last figure of merit for the catalysts analysis that needs to be explained. Every catalyst is defined by its Turnover Number (TON) as given **eq. 30**:

$$TON = \frac{Number\ of\ product\ molecules}{Number\ of\ active\ sites} \tag{30}$$

Turnover number refers to the number of cycles a catalyst has been through till its total deactivation which is the moment when a catalyst cannot catalyse anymore. Every new product that comes through the catalyst means that a cycle has been completed and it is known as turnover cycle. The challenge for a good development is to find the suitable conditions where the catalyst will run better in combination with the less losses. To make this clear, a catalyst can run better in low temperatures, however this is not feasible because of the low rate of the reaction in low temperatures. From the equation (10) it is clear that, the greater turnover number means more stability for the catalyst, while on the other hand. we mentioned that in theory a catalyst could last forever, but in reality, the lifetime

of a catalyst lasts from some seconds to three years depending on the usage. Besides turnover, there is another variable, named as turnover frequency or (TOF) that measures the efficiency of the catalyst and can compare the activity of catalysts equipped with different structures and compositions. TOF is expressed in units one over time (s^{-1}) as in **eq. 31**:

$$TOF = \frac{number\ of\ reactan\ converted\ or\ product\ produced}{reaction\ time \times number\ of\ active\ sites} \quad (31)$$

As it is mentioned above, deactivation of a catalyst occurs due to physical and chemical factors, it is inevitable to happen however slowing down is the main factor that can be adjusted. The three main causes of deactivation in heterogeneous catalysis are poisoning, coking and sintering and they will be analyzed briefly in the next paragraphs.

Poisoning

The first factor of deactivation refers to poisoning which is divided in two branches, selective and non-selective. Selective poisoning is the term referring to chemisorption of some substances on the active sites which are found on the feed system, and are adsorbed selectively blocking the action of the strongest active sites. Sometimes though, this kind of poisoning is desirable to adjust selectivity of catalysis. Non-selective refers to a linear relationship between catalyst activity and the percentage of active surface (or sites) that is accessible [46].

Coking

This kind of deactivation is mostly common in the petroleum industry, involving reactions with hydrocarbons where additional reactions result to the creation of carbonaceous residues which it turn up in either covering the surface of the active sites or blocking the pores of the surface [47].

Sintering

Sintering is a physical and/or thermal phenomenon that, as there is a temperature growth on the catalysis reactions, causes structural modification that leads to agglomeration and decrease in the surface to volume ratio of the catalyst. Depending on the catalyst's kind, this can lead to either a partial or complete collapse of the internal pore structure and a corresponding loss of surface area or it can lead to a loss of active sites as a result of agglomeration of distributed metal or crystallites to bigger ones. In general, this kind of deactivation usually takes place in high temperatures over 500^{o}C. Sintering can also be caused by high water partial pressures, particularly when noble metals and high activity catalysts are involved. The sintering is described by three mechanisms: i) via

the formation of active phase crystallites ii) the carrier (support) pore structure collapsing and iii) active phase's solid-state interactions with the carrier [47].

2.2.2 Fundamentals of Electrocatalysis

Electrocatalysis deals with the chemical reactions which occur at the electrode-electrolyte interface. More specifically, the phenomenon addressed as electrocatalysis, is a catalytic process involving redox reactions through the direct transfer of electrons and requires electrocatalysts (electrodes) in order to lower the overpotential of the reaction. Consequently, electric current is involved in the electrochemical process [33, 48-50]. The rate of the electron transfer in an electrocatalytic reaction depends on the electrode material, which acts as an electrocatalyst. In general, electrocatalysis facilitates conversion between electrical and chemical energy (production of chemicals) and vice versa (batteries, fuel cells, electrocatalysis devices), using electricity to realize catalysis reactions. The aim of this procedure is to offer new pathways under the same potential without inhibiting electron transfer rate. The transfer reactions on the electrode-electrolyte interface strongly depend on the nature of the electrode material. Electrocatalysis is considered as a sub-division of heterogeneous catalysis of interface reactions (**Figure 6**). Nevertheless, the two phenomena, are closely related, involving the same elementary bond breaking and making processes and share common principles in molecule transformation [49, 51-58]. Moreover, many of the most active metals that are used in electrocatalysis are also used in heterogeneous catalysis such as Pt that is known to be very active in oxidation of alcohols and reduction of O_2.

In addition to the similarities above, there are definite distinctions between the two cases of catalysis. The most significant differences between the two pertain to the presence of electrical double layer (EDL), the influence of the applied potential on the reaction rate, the change of composition on the side of the EDL and the concentration of intermediates and products. These are some features of electrocatalysis that make the activation energy of electrochemical reaction to depend on the applied potential as well as to a lesser extent on temperature. Furthermore, unique reaction environments make them distinctive. The electrochemical environment is typically harsher to catalyst stability.

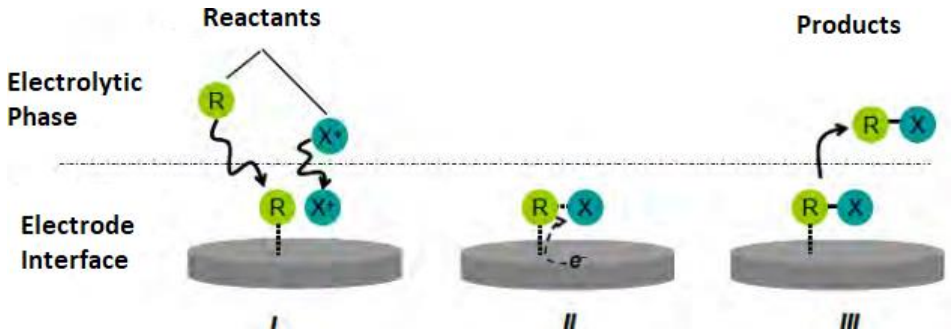

Figure 6. Displays three essential phases that take place during an electrocatalytic reaction: (I) transfer and adsorption of the reactants to the electrolyte-electrode interface, (II) electron transfer between reactant and electrode, and (III) desorption of the formed products from the electrode surface [37].

The dissolution of metal and the support are important concerns for electrolytic processes as these phenomena are enhanced under electrochemical conditions. Additionally, the presence of an electrolyte frequently hinders or improves catalytic kinetics, and at certain potentials, it can result in surface poisoning. Electrocatalysis is centred on fuel cells and specifically proton exchange membrane fuel cells, while heterogeneous catalysis spans in a wide range of chemical, automobile, petroleum, and pharmaceutical industries. When conducting electrocatalytic procedures it is desirable to have durability and activity for a long term and this contrasts with the short lifetime of most heterogeneous catalytic reactions. Since the solvent, ions, and electric fields that can dissolve a catalyst make it difficult to select one for electrocatalysis, only a few supported metals/alloys and metal oxides can be used. As a result, there's a narrow range of possibilities as compared to heterogeneous catalysis [37].

Only certain chemical processes, which may be subdivided into oxidation and reduction, can be carried out electrochemically. The reactants must be capable of either a forced or a spontaneous electron exchange with the appropriate electrodes. There are, nevertheless, also apparent advantages from electrocatalysis application namely; electrolysis can convert chemical energy into electricity which is much preferred over heat. Likewise, it can supply the necessary energy that is needed for endergonic reaction at room temperature that could be impossible otherwise. Also, by modifying the circuit's current, reaction rates may be regulated. Due to the fact that the reaction rate is dependent on the electrostatic potential drop at the electrode and electrolyte interface, there is another readily controllable parameter that may be used to affect electrocatalytic processes. Hence, in heterogeneous catalysis, the way to influence the reaction rate, is temperature while in electrocatalysis, electrode potential takes over this role by shifting electronic energies in the electrode. Lastly, by applying electrocatalysis it is possible, the anode and the cathode, to be separated by an ion-conducting

membrane to prevent convective mixing of the reactants and to enable the separation of the oxidized and reduced products [37]

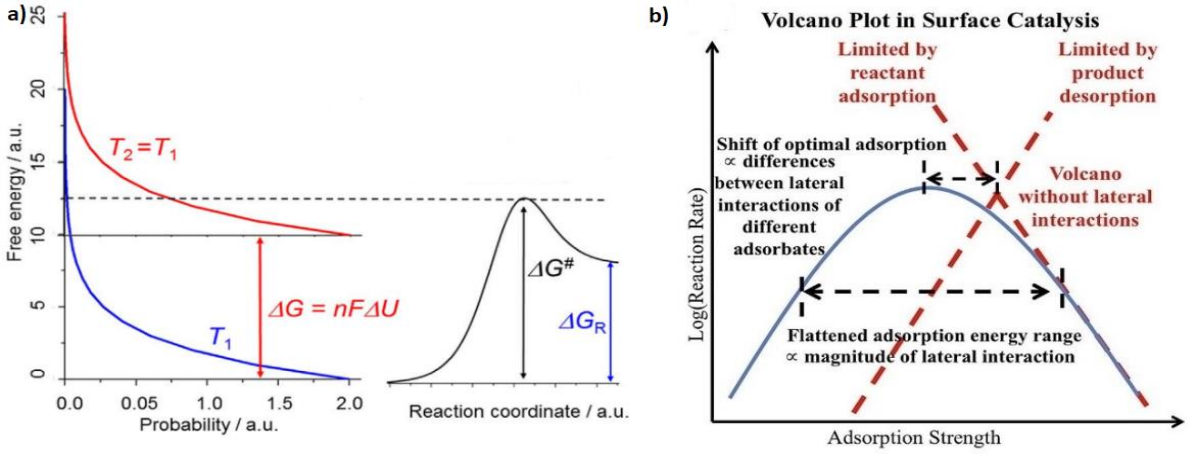

Figure 7. a) Reactions by applying electrical current; b) Relation between catalytic activity and adsorption strength. Dashed lines are based on Arrhenius law and solid line is obtained with the consideration of lateral interactions between absorbed intermediates [59].

Figure 7a illustrates schematically the process of electrocatalysis using electrical energy. More specifically, instead of increasing the temperature in the reaction system, the necessary amount ΔG is supplied in the form of electrical energy nFΔU, and as previously mentioned; electrocatalysis enables electrochemical processes, to take place at low temperatures in place of conventional catalysis. The basic processes that take place during an electrocatalytic reaction are adsorption-desorption, electron transfer, and bond breaking-formation.

2.2.2.1 Sabatier principle and volcano curve

Sabatier principle, that is usually applied to describe heterogeneous catalysis, is also used for electrocatalysis. It states that, the ideal catalytic surface for a catalytic reaction, has optimized adsorption strength for the reaction intermediate, that is neither too strong nor too weak. It has been widely used as the key criterion in designing and screening electrocatalytic materials. Schematic representation of the qualitative Sabatier principle is a curve called «Volcano Plot» and it shown below. The Volcano curve shows the qualitative dependence of electrocatalytic activity chemisorption strength of reaction intermediates.

According to **Figure 7b** above, interaction between the catalyst and the reactants must be moderated in a certain level of adsorption strength. If the interaction is too weak then the reactants will not be able to bind with the catalyst and few reactions will take place. On the other hand, if the interactions are too strong, the products formed on the catalyst cannot desorb, leaving the catalyst inhibited [60, 61].

2.2.1.2 Electrocatalysts

Electrocatalyst is a special type of catalyst that participates in electrochemical reactions and functions on the surface of the electrode or, most commonly, are the electrode itself. Electrocatalysts expedite the intermediate chemical [56, 62-66] transformation while, they also speed up the rate of electron transfer between the electrode and the reactants. They are defined by activity, selectivity and stability like all catalysts. There are two main subcategories, homogeneous and heterogeneous. The first category includes enzymes and inorganic coordination complexes. In heterogeneous electrocatalysts belong the bulk materials (platinum metals), and nanomaterials. Nanomaterials may be; nanoparticles that can be tuned with respect to their size and shape, carbon-based materials that are well-suited to the absorption of many species and have good conductivity and finally, framework materials.

2.3 Electrochemical devices

The term electrochemical devices, refers to systems that either use electrical energy in order to provoke chemical reactions, or via chemical reactions they generate electricity for general use. They are under the microscope of the scientists as their advantage is the production of direct energy from one type to another, resulting in high efficiency with very low pollutant products. As a matter of fact, comparing an electrochemical device such as a fuel cell and a battery with an internal combustion engine the efficiency for the first is around 45% to 60% and if the heat energy is captured, it can go up to 80%, in comparison with an engine where it is around 20% to 25%. Furthermore, the fact that they can contribute to mobile and stable sources of energy with low needs such as mobile phones, and high needs of energy like energy stations capable to supply power to a small city, making them appear promising for the future. The main devices of this category are; batteries, supercapacitors, fuel cells and electrolyzers.

2.3.1 Battery

The basic principle of a battery [67-76] is the transformation of chemical energy through some reactions into electrical mostly for portable devices. In fact, its functionality is so simple and efficient making it necessary for most of the devices. Li-ion batteries are the most common and have the most extensive use on portable devices. The preference comes from the combination of good performance and efficiency provided by using graphite on the anode and $LiCoO_2$ on the cathode Li-ion battery can perform a maximum output of 3.6V while the current density can reach up to 150 Wh/kg on a single cell. Despite the massive use of this battery, yet its use in EV is still under research because of some challenges

such as lifetime, safety issues and thermodynamic instability. The main parts of the battery are two electrodes, the anode and cathode, and the electrolyte or ionic conductor in the middle where the reactions take place as shown in **Figure 8**.

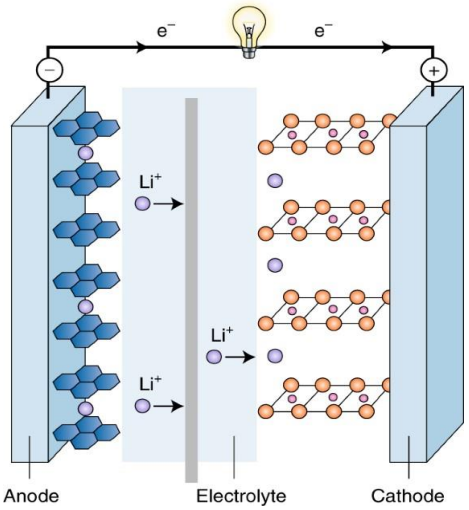

Figure 8. Electron transporting and Li-ion exchange of a battery [77].

In order to provide the required voltage and current, inside the battery there are numerous cells connected in series or parallel. Batteries are divided into two categories, rechargeable and non-rechargeable. In the second case, if larger electrical current passes through the electrodes on the opposite direction, then recharging is possible. The electrical energy provided from a battery, meaning voltage and the capacity, depends on the substances of the chemical system.

2.3.2 Supercapacitors

Supercapacitors, also known as electrochemical double layer capacitors or ultracapacitors, are energy storage devices that have high energy density compared to conventional capacitors and high-power density compared to batteries. Their structure consists of two electrodes that are close to each other and an electrolyte and a separator that allows transfer of ions. Many materials such as carbon materials, mixed metal oxides and conducting polymers have been used as supercapacitor electrodes. Supercapacitors are used when large amounts of energy must be stored and delivered repeatedly since the charge-discharge time is just a few seconds. The concept behind their operation is the storage of electrical energy in electrical double layer that is formed between the electrodes and the electrolyte [78]. As voltage is applied to the supercapacitor the anions diffuse in the pores of the positive electrode while, the positively charged cations are drawn to the negative plate throughout the charging process. Hence, charge accumulates at the electrode/electrolyte interface forming two double layers, one on the surface inside the conductor

and the other layer on the electrolyte, as shown in **Figure 9**. These two layers have a really small distance between them and they behave as a physical capacitor [78].

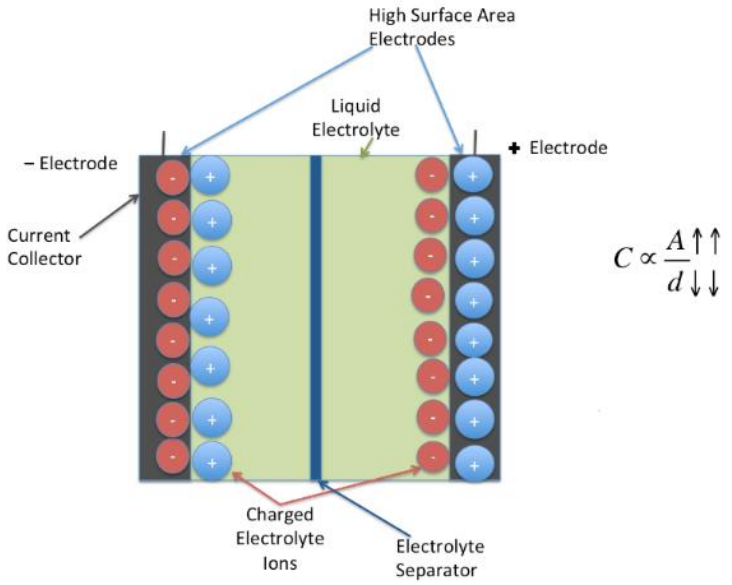

Figure 9. Schematic diagram of supercapacitor structure and working principle [79].

The formula that describes the capacitance of a supercapacitor is given by **eq. 32**:

$$C = \varepsilon \frac{A}{d} \tag{32}$$

Where A is the overlap surface of the electrode plates and d is the distance between the plates and ε is the electrolyte permittivity.

2.3.3 Fuel Cells

The operation of the fuel cell is based on the phenomenon of transforming chemical to electrical energy. The main parts that constitute a fuel cell, are two electrodes called anode and cathode, the membrane and the electrolyte where the reactions take place. The electrodes and the membrane are called membrane electrode assembly (MEA). Fuel cells also have bipolar plates which separate both electrodes from neighboring cells and they have a triple role in the system. Firstly, they ensure electron conductivity between the neighboring cells. Moreover, bipolar plates enable the transfer of reactants (gases and liquids in the case of alcohols) to the electrode catalytic sites and allow the drainage of reaction byproducts (H_2O and CO_2 in the alcohols context). Lastly, they provide thermal control within the basic cell by removing extra heat. Another important component of fuel cells is the gas diffusion layer which is placed before the anode and after the cathode electrodes and offers heat transfer. It gives the MEA sufficient mechanical support to prevent expansion due to water absorption, prevents floods by removing by-produced water from outside the catalyst layer, and provides a gas diffusion path from the flow channels to the catalyst layer.

The classification between the various types depends on the type of the catalyst, the type of fuel but also the processing of the fuel, for example outside or inside the fuel cell and lastly the temperature range of the operation. With this information in mind fuel cells are classified in low temperatures, Proton Exchange Membrane Fuel cell (PEMFC), Alkaline Fuel Cell (AFC), Phosphoric acid fuel cell (PAFC) and in high temperatures, Solid Oxide Fuel Cell (SOFC), Molten Carbonate Fuel Cell (MCFC). All these types will be briefly discussed in the following paragraphs.

2.3.3.1 Types of Fuel Cell

2.3.3.2 Proton exchange Membrane (PEMFC)

A Proton exchange membrane [80-87], [62, 88] (**Figure 10a**) uses hydrogen on the anode and oxygen on the cathode in order to produce electrical energy. Their use is focused mainly on the automotive industry as hydrogen could replace fossil fuels.

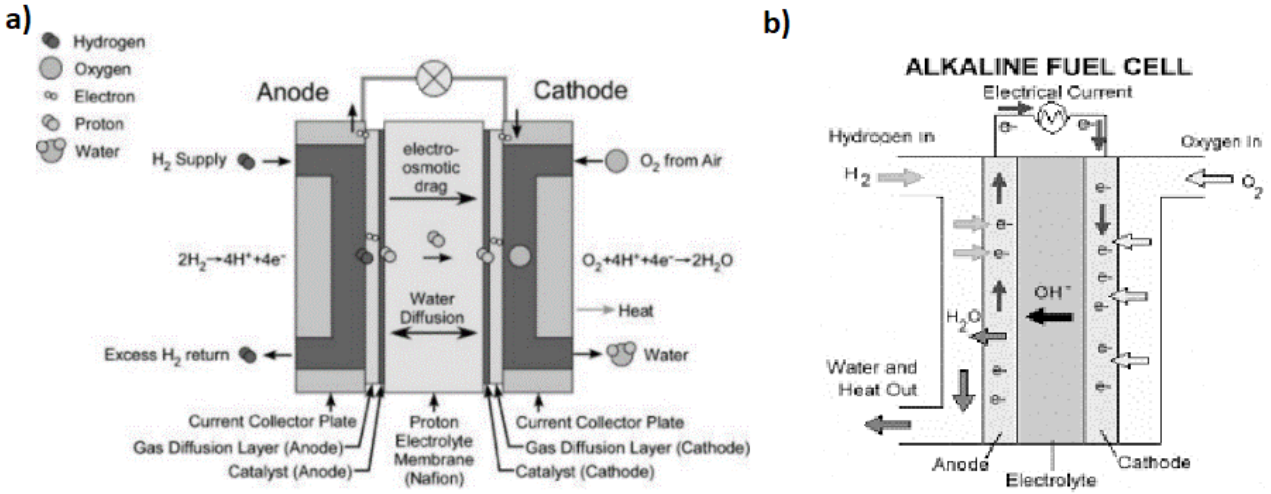

Figure 10. a) Proton Exchange Membrane [89]; b) Alkaline Exchange Membrane [90].

The temperature operation of this fuel cell is from 20° to 80° Celsius. Some advantages are that it is low weight, and sustainable to high current densities, resistant to oxidant reactions and for this reason air can be used on the cathode instead of clear oxygen which is more difficult to produce. Also, PEM can operate at low pressures of 1-2 bars and has compact structure which makes it durable over time. Its major characteristic concerning the electrolyte is that it allows the proton exchange on the membrane but blocks the electrons passage. The reactions are given by **eq. 33** and **eq. 34**:

$$\text{Anode: } H_2 \rightarrow 2H^+ + 2e^- \quad (33)$$

$$\text{Cathode: } 2H^+ + 2e^- + 1/2O_2 \rightarrow H_2O \quad (34)$$

Proton exchange fuel cells operate with feed of hydrogen, methanol, and formic acid.

2.3.3.2 Alkaline Fuel Cell (AFC)

Alkaline fuel cells were discovered for the first time by the scientist Dr. Francis T. Bacon in the 1930s, and in 1952 he constructed the first AFC [91]. A very significant use of this fuel cell was at the missions of NASA in the Apollo and space-shuttle programs in order to produce drinking water. Conventional AFCs (**Figure 10b**) use hydrogen as a fuel on the anode, oxygen on the cathode and KOH as an electrolyte, operating at temperatures between 60°C – 80°C. The choice of this electrolyte makes it friendly to non-noble metal catalysts e.g. (nickel) because it reduces the cost of production. AFC have a lot in commons with PEMFCs except the use of alkaline exchange membrane instead of acid. The half-cell reactions of AFC are shown below by **eq. 35**, **eq. 36**, **eq. 37**:

$$\text{Anode: } 2H_2+4OH^- \rightarrow 4H_2O+4e^- \quad (35)$$

$$\text{Cathode: } O_2+2H_2O+4e^- \rightarrow 4OH^- \quad (36)$$

$$\text{Overall reaction: } 2H_{2+}\ O_2 \rightarrow 2H_2O \quad (37)$$

They operate with hydrogen, methanol, ethanol, sodium borohydride, hydrazine, ethylene glycol, glycerol, ammonia, dimethyl ether, potassium formate and 2-propane.

2.3.3.3 Phosphoric Acid Fuel Cell (PAFC)

Phosphoric acid fuel cell was the first fuel cell that was commercialized. It operates at temperatures from 170°C to 210°C and was widely used as a stationary power generation, for hospitals, factories, hotels and many other buildings [92]. As implied by the name of the fuel cell, the electrolyte that is used is liquid phosphoric acid H_3PO_4 in concentration of 95%. The electrodes used are carbon with pores, containing platinum for the catalyst role coming from Pt, Fe and Co while the fuels used are natural gas, hydrogen, propane and digested gas. The efficiency of this fuel cell, when used for generating electricity, is around 37%-44%. On the contrary, when it is used for co-generation of heat and electric energy, efficiency can reach up to 85%. Because of the resistance of the electrolyte to CO_2 presence, hydrogen is usually used on the anode as a fuel which is produced from organic fuels usually hydrocarbons and alcohols while on the cathode it reacts with oxygen. The main reaction of the fuel cell is shown below by **eq. 38**, **eq. 39**, **eq. 40**:

$$\text{Anode: } H_2 \rightarrow 2H^+ + e^- \quad (38)$$

$$\text{Cathode: } ½O_{2(g)} + 2H^+ + e^- \rightarrow H_2O \quad (39)$$

$$\text{Overall: } H_2+1/2O_{2(g)} \rightarrow H_2O \quad (40)$$

2.3.3.4 Solid Oxide Fuel Cell

The operation of this fuel cell is around 750°-1000° C which makes it efficient up to 80% in co-generation of electricity and heat. Also, the power provided can range from 1 KW to some MW, a wide range of energy capable to move a car or to cover the needs of a large building. SOFCs use [83] a solid ceramic electrolyte using metallic oxides which is usually an yttria stabilized zirconia or (YSZ). As regards fuel, a variety can be used including hydrocarbon, hydrogen, carbon monoxide, methane, ammonia, alcohols, natural gas and solid carbons. Fuel diffuses through the anode to the anode/electrolyte (**Figure 11**) interface and it reacts with the oxygen ions, releasing electrons that are transported through an external circuit, producing electricity.

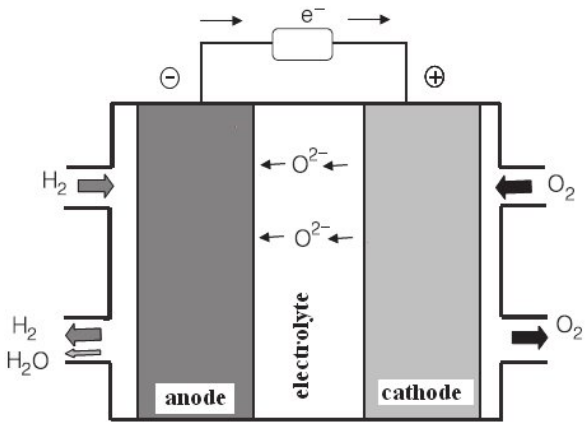

Figure 11. Schematic representation of a typical SOFC [93].

The advantages of this fuel cell are that: it is tolerant to CO in comparison with other fuel cells that are poisoned, and it is flexible since it can directly function with more than one special fuel. These characteristics make SOFC usable on portable applications or small-scale structures. On the other hand, SOFC suffer from quick twist and turns of heat as it strains its materials a lot because of the high temperature operations. The reactions of this fuel cell are shown below by **eq. 41**, **eq. 42**, **eq. 43**:

$$\text{Anode: } H_2 + O^{2-} \rightarrow H_2O + 2e^- \quad (41)$$

$$\text{Cathode: } CO + O^{2-} \rightarrow CO_2 + 2e^- \quad (42)$$

$$\text{Overall: } H_2 + CO + O_2 \rightarrow H_2O + CO_2 \quad (43)$$

2.3.3.5 Molten Carbon Fuel Cell (MCFC)

MCFCs are among the first fuel cells that were commercialized using a variety of fuels such as methane or higher hydrocarbons fuels extracted from biomass or natural gas [94]. They belong in the same category with SOFCs working on high temperatures, around 650°C using a liquid electrolyte of lithium and potassium $(Li/K)_2CO_3$ or lithium and sodium $(Li/Na)_2CO_3$ carbonate. The

catalysts on the anode and cathode taking advantage of the temperatures, using non-precious materials. As a result, MCFCs reduce considerably the cost of production by avoiding the use of expensive materials. The fuel used, ranging from natural gas, anaerobic digested gas, coal gas, biogas, to hydrogen, is fed on the anode reacting with ions of CO_3^{2-} that pass the electrolyte from the cathode, producing water and carbon dioxide. The characteristic reactions are shown below, in **Figure 12** and they are described by **eq. 44**, **eq. 45**, **eq. 46**:

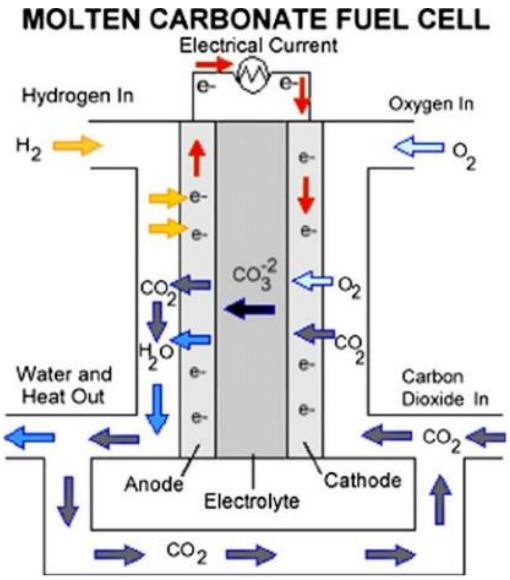

Figure 12. Schematic representation of a molten carbonate fuel cell [95].

$$\text{Anode: } CO_3^{2-} + H_2 \rightarrow H_2O + CO_2 + 2e^- \quad (44)$$

$$\text{Cathode: } CO_2 + \tfrac{1}{2}O_2 + 2e^- \rightarrow CO_3^{2-} \quad (45)$$

$$\text{Overall: } H_{2(g)} + \tfrac{1}{2}O_{2(g)} + CO_2 \rightarrow H_2O_{(g)} + CO_2 \quad (46)$$

The major advantages of MCFC are that it can use a lot of different fuels via the internal reforming operation converting them into hydrogen. Also, this fuel cell is resistant to poisoning by some substances that appear in the reaction such as CO or CO_2. The efficiency can reach up to 60% for simple use of electricity or it can maximize up to 85% when it is used for co-generation of heat and electricity. On the other hand, the main drawback is the durability of the fuel cell since it operates in such high temperatures that the electrolyte is apt to corrosion problems due to its nature.

2.3.3.6 Direct Alcohol Fuel Cell

Direct alcohols fuel cells [96] are distinct from the fuel cells referred. They can generate electricity by feeding the system directly with fuel without the need of converting it firstly into hydrogen (internal reforming method), however the operation is similar to that of a proton exchange membrane fuel cell. They are considered as future fuel cells, since some of their

advantages such as low temperature operations, low fuel consumption in combination with high energy production makes them ideal on specific applications especially in automotive industry. This type of fuel cells will be analyzed in the next chapter. The alcohols that are mainly used to feed the alcohol fuel cells are methanol, ethanol, propanol, glycerol and ethylene glycol.

The fuel cells that were examined above represent the evolution of the first fuel cell, whose working principle is the direct supply of hydrogen. Hydrogen is the most active fuel for fuel cells, since its oxidation rate is about four times greater than any other one-carbon compound, which oxides in turn, faster than hydrocarbons by about the same extent. Nonetheless, its use is accompanied with two great problems. It is the most common element and despite of the fact that it is abundant, it doesn't naturally exist as a gas on Earth. The production of hydrogen is possible either from water splitting (electrolysis) or from hydrocarbons. In the first case, is called “green hydrogen” because it is produced from renewable sources (biomass, solar, wind) but up until now, the process has been very expensive. There are more “colours” of hydrogen such as grey, that identifies hydrogen that comes from the reformation of methanol and partial oxidation; brown hydrogen, produced from coal and, yellow hydrogen when the source is nuclear power. The second problem that arose is storage. Specifically, because hydrogen is a small molecule, it can leak rapidly, especially when it is held in a compressed state. Additionally, it has low ignition energy and consequently it can cause explosions.

For the purpose of dealing with the above problems, a new approach is being followed that relies on the indirect storage of hydrogen in other fuels. For instance, one efficient technique of storage is in alcohols, such as methanol and ethanol, which is discussed and analyzed in the following chapter.

2.2.4 Other electrochemical devices

2.2.4.1 Electrochemical Sensors

A sensor is a device that responds to a physical stimulus (movement, light, concentration etc.) and it transmits it to electrical impulse as a technique of measuring any alterations in the material’s fundamental properties. It provides continuous information about its environment. Electrochemical sensors are employed widely across a wide range of application fields and have become increasingly popular as potent analytical tools, particularly in the pharmaceutical and biomedical, science and food technologies, as well as environmental applications [97]. They are divided into three categories; potentiometric, amperometric and conductometric. A typical electrochemical sensor consists of a

sensing electrode, a counter electrode which are separated by a thin electrolytic layer and a reference electrode as shown in **Figure 13**.

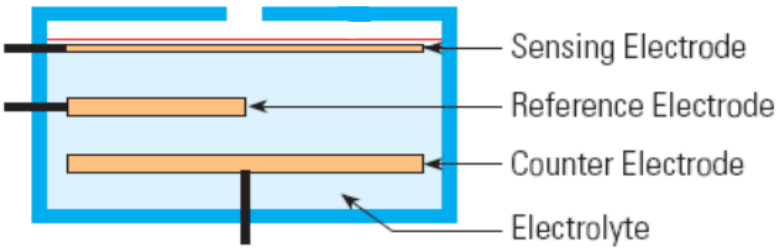

Figure 13. Schematic representation of an electrochemical sensor [98].

Alongside the sensing electrode, where stable potential acts on, the reference electrode is inserted in the electrolyte. Firstly, the sample reacts with the sensing electrode and then reaches the counter electrode to generate a strong enough electrical signal. Most electrochemical sensors use an electrode surface as the reaction's location. The electrode will either oxidize or reduce the sample. The reactions of the sample molecules with the sensing electrode and counter electrode are simultaneously monitored. The concentration of the sample is typically directly correlated with the measurement outcome. The sensor may target the sample depending on the amount of voltage given to the sensing electrode [98].

CHAPTER III

3. Direct Alcohol Fuel Cells

3.1 DAFC and sustainability

The simultaneous growing global energy demand and the extensive use of internal combustion engines that function with fossil fuels have caused many problems to our planet. Fossil fuels are unsustainable energy sources due to their negative environmental impact while their gradual depletion poses significant risks and challenges. Among the potential, long-term solutions for the substitution of fossil fuels to meet the demands of sustainable development, biofuels gained traction over the recent years. A prevailing method for the implementation of this idea is the development of fuel cells. Specifically, as mentioned in the previous chapter, hydrogen is the most effective fuel for fuel cells. Nevertheless, its widespread use as a fuel is limited due to the lack of efficient systems for its storage as well as its high production cost. Hydrogen storage should involve the least possible chemical transformations in order to minimize the inherent energy losses associated with multistep chemical reactions. For instance, producing hydrogen from natural gas is a process that involves many steps. First, natural gas that contains hydrogen, CO_2, CO, CH_4 and other by-products, is steam reformed via conventional reformers. Consequently, a second step needs to be taken involving water gas shift, which includes partial oxidation and pressure swing adsorption, where carbon dioxide and other impurities are removed from the gas stream, leaving pure hydrogen. Apart from the multistep procedure, natural gas steam reforming requires high temperatures. All these issues that negatively affect efficiency and cost, have led to the development of alternative technologies to produce high purity hydrogen such as indirect storage of hydrogen in other fuels, especially in alcohols such as methanol and ethanol. Notwithstanding the fact that hydrogen can be produced from a variety of feedstocks, including fossil fuels such as natural gas, oil, and coal, it is preferable to use ‘green’ hydrogen, which is a product of biofuels, such as biomass, by steam reforming, owing to the catalysts' limited tolerance for CO concentration.

Methanol and ethanol are the two main alcohols produced from biomass and utilized in direct alcohol fuel cells. Methanol is an interesting hydrogen source because in ambient conditions it is in liquid form, which eases storage and transportation [99, 100]. Also, it has high H/C (4:1) ratio. Due to the lack of C-C bonds it has a low reforming temperature (200-300^{o}C) and low risk of coking [101]. Finally, even though methanol is toxic, it is biodegradable that is major advantage.

Hydrogen can be produced from methanol through several processes. However, the most effective is steam reforming because it provides higher concentration and yield of hydrogen compared to partial oxidation, combined reforming, and/or methanol decomposition [102].

On the other hand, ethanol is also considered to be one of the most promising alternative fuels because of its low toxicity, as well as its renewable, sustainable and biodegradable nature. Furthermore, bio-ethanol's price is gradually falling due to the development of fermentation technologies. Ethanol has even lower toxicity levels than methanol, it is easy to transport, while it has comparatively high hydrogen content. Its utilization results in a nearly closed carbon dioxide cycle that significantly reduces net emissions to the atmosphere. Besides that, ethanol is also sulphur-free and as a result, it doesn't cause damages to the metallic surface of catalysts enhancing in this way their longevity [103]. Since hydrogen is obtained from both ethanol and water, the ethanol steam reforming optimizes the hydrogen yield [104]. Ethanol can be put straight into the reformer to create hydrogen without the need for extra steam and the steam reformer can be connected to water gas shift reactor without the need of additional heat exchanger due to the temperature rate at which the steam reformer operates at (350-500^{o}C).

Nissan employed alcohol fuelling to power the first biofuel-powered automobile, applying all these technological advancements for the first time. In 2016, Nissan presented its first fuel cell vehicle [105, 106], operating with a mix of, water blended ethanol bio-fuel, achieving an efficiency around 55%, using a safer, eco-friendly fuel with short-time tank refill. In this vehicle, as it's shown in **Figure 14**, a SOFC stack with external reforming converts bioethanol into hydrogen on the reformer and after that, it flows on the fuel cell, generating electricity which can charge the battery.

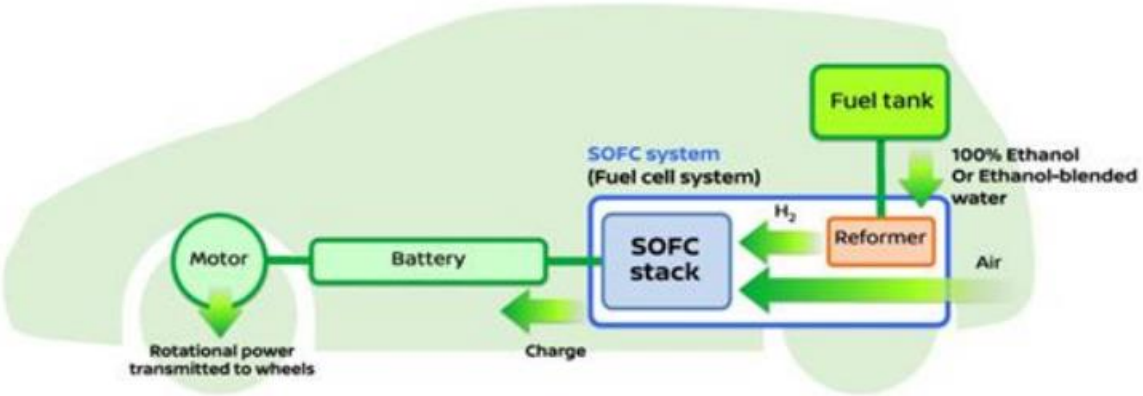

Figure 14. Representation of a SOFC vehicle [105].

More specifically the operation of the fuel cell is shown in **Figure 15**. Ethanol is reformed into hydrogen through the main reaction in **eq. 47**,

$$C_2H_5OH + H_2O \rightarrow 6H_2 + 2CO_2 \quad (47)$$

where the hydrogen that is produced from the reformer enters the fuel cell reacting with the air coming from the cathode. The heat produced from the reaction on the fuel cell is captured and returns facilitating the reform process, saving a large amount of wasted energy.

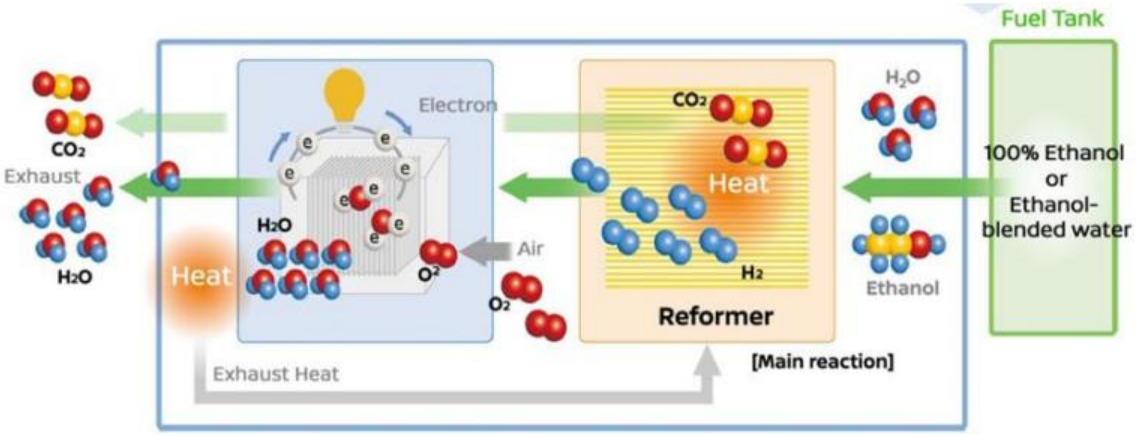

Figure 15. Operation of external reform of SOFC [105].

3.2 Reforming of Hydrocarbons

Direct alcohol fuel cells, typically function using two approaches, internal and external reforming (**Figure 16a, 16b**). The concept behind this idea is the direct feed of the fuel cells with biofuels that are reformed through a reformer. The development of reforming hydrocarbons in hydrogen fall in one of the following processes: steam reforming; dry reforming; autothermal reforming (combination of steam reforming and partial oxidation); and partial oxidation. Sometimes there's a combination of two or more methods. Partial oxidation requires the least quantity of hydrocarbons, and it doesn't involve a catalyst, although it has a low H_2/CO ratio. Autothermal reforming on the other hand operates at lower temperatures than partial oxidation but it demands air/oxygen. Steam reforming is a highly industrial method, there's no need of oxygen input and it has the lowest operation temperatures. Moreover, it has the highest H_2/CO ratio yet, it has the highest greenhouse gas emissions from all the aforementioned methods [107]. Steam and dry reforming are endothermic reactions, meaning that additional heat is needed for their operation, while partial oxidation is exothermic, thus produces heat.

3.2.1 Steam Reforming

Hydrogen is the first fuel that comes in mind when referring to fuel cells. Since we have mentioned that the storage of hydrogen is difficult, scientists search for bio-fuel conversion of mostly liquid and solid alcohols like ethanol and methanol, but there are also non-green fuels such as biodiesel and glycerol coming from biodiesel [108], as well as hydrocarbons such as methane. The most widely used method to produce hydrogen today is by using natural gas as a fuel,

representing approximately 50% of the total hydrogen production globally [109]. Considering though, the quest for the elimination of fossil fuels, there are many biofuels that can also be converted into Hydrogen via steam reforming. The process of catalytic steam reforming refers to the reforming of a biofuel into CO, CO_2 and H_2O in the presence of a catalyst. It starts from the point that syngas has been produced from biomass through an endothermic reaction where heat energy is required to reach the equilibrium of the reaction. The produced syngas reacts with a steam in high temperature of 700-1100^o Celsius and pressure of approximately 3-25 bar where hydrogen and CO are produced. Because CO is not desirable, a second reaction, called water gas shifting, follows where CO reacts with water and produces CO_2 and Hydrogen. The most preferred catalysts are noble metal catalysts such as Rh/Al_2CO_3 or Ni/Al_2CO_3 for ethanol while for methanol, copper-based catalysts are on the top of list [110],[111].

3.2.2 Dry Reforming

Dry reforming (DR) is a process which converts hydrocarbon fuels, mainly methane (CH_4), into hydrogen and carbon monoxide using CO_2 [112], [113]. The main application of this operation is the same as steam reforming and partial oxidation, i.e., the reformation of fuels into hydrogen for various applications. However, the fact that gas emissions such as carbon dioxide can be used to produce hydrogen makes dry reforming an eco-friendlier operation. Dry reforming is still in research stage and thus there are not many applications except from methane reforming. The main problem of this method is carbon formation which reduces deactivation, although formation is on the same level with steam reforming, but H to C ratio in dry reforming is making the problem more difficult to overcome. The conversion of alcohol fuels into hydrogen comes from their reaction with CO_2 producing CO and H_2 which in turn is followed by a water gas shift reaction to reform the remaining carbon monoxide. It is a highly endothermic reaction, requiring a lot of thermal energy (heat). According to researches, the ideal temperatures for the dry reforming of ethanol is 1200-1300^o C, [114] at pressures of 0.1 – 2 MPa. The catalysts used are mostly Ni-based but Cu, Rh and Co-based catalysts are also used.

3.2.3 Autothermal Reforming

The autothermal reforming process is a combination of partial oxidation (POX) and steam reforming (SR). It consumes less energy than steam reforming and partial oxidation since it combines, the exothermic reaction of the latter with the endothermic of the former aiming at reaching thermal equilibrium. The aim of this process is high yield hydrogen production but also, low carbon monoxide emissions. Taking these features into consideration, catalysts are the key to

achieve this. Usually there is a preference in noble metal catalysts such as Rh, Pt, Pd and Ru. The disadvantages are that materials are expensive, pushing the researchers to find less expensive catalysts, such as non-noble metals i.e. Ni and Co [115]. Moreover, coke deposition and long-term stability are two other features that are searched for. Autothermal reforming is usually used in smaller scale hydrogen production devices [116]. Its superiority compared to SR and POX, relates to quick start-up times compared to SR and higher hydrogen productivity compared to POX.

3.2.4 Partial Oxidation

Partial oxidation refers to the reaction of a hydrocarbon or alcohol fuel with pure oxygen producing hydrogen and carbon monoxide. The features that characterize this process are, quicker reaction, and startup rates, compared to steam and autothermal reforming. Direct conversion of a fuel in this way is an exothermic reaction making it more attractive since no external heat is required. Also, the variability in fuels' utilization is another benefit that makes this type of reforming attractive. This process is divided into two subcategories, direct and indirect partial oxidation[117, 118], [119]. In the first case, reforming process is proceeded directly with one step for example, the reaction of methane is described from **eq. 48**:

$$C_2H_2OH + \frac{1}{2}O_2 + 3H_2 \tag{48}$$

On the other hand, in the indirect method, some part of the fuel is reformed into carbon dioxide and water, and syngas. Then, it is reformed via steam reforming and water gas shifting. It is not clear in the studies in which way methanol and ethanol are reformed but according to some studies, the reactions follow the indirect way. Catalysts that are usually used are supported transition metals such as Ni, Co and Fe, noble metals, and perovskite oxides. Oxidation of the fuel separates oxidation in two categories, depending on the temperature of the reaction: catalytic (CPOX) and thermal (TPOX) partial oxidation, where the first operates at low temperatures 700 – 900^o Celsius, while the second at higher than 1200^{o}C. POX reaction is highly affected by the carbon to oxygen ratio which operates better in low temperatures, so for this reason SOFC systems can integrate this kind of reaction as a reforming method.

3.3 Internal Reforming

As mentioned above, most fuel cells need to convert hydrocarbon primary in fuel hydrogen-rich gas required for electrochemical reactions. One possible way to achieve the conversion is the indirect fuel converting system such as an external steam reformer or a partial oxidation reactor. Nevertheless, for the steam reformer to operate, heat is needed to drive the process. This heat is

provided by the exhaust gases of anode and cathode. These gases are directed into a burner with excess fuel where the combustion takes place. The heat from the burner is used to preheat both fuel and steam and provide the heat that the reformer requires. However, there is another more efficient and favorable way to provide the appropriate amount of heat, that is by carrying out the reforming in the cell stack, known as internal reforming. Internal reforming eliminates the need for a separate fuel reformer making the design of the system more efficient. Additionally, there is a high reduction in the need for cell cooling, which is often accomplished by flowing extra air through the cathode. Moreover, internal reforming also minimizes the volume and the weight of the whole system since it eliminates the need for water gas shift and preferential oxidation reactors to purify the fuel after the external reformer [120].

Internal reforming in a fuel cell can be accomplished in two ways: i) indirect or integrated and ii) direct reforming. In the first method, the reformer section and the fuel cell anode are physically apart but they are thermally very close to one another. In the second method, alcohol is directly fed to anode where the reforming takes place. It is applied mostly on solid oxide fuel cells and molten carbonate fuel cells.

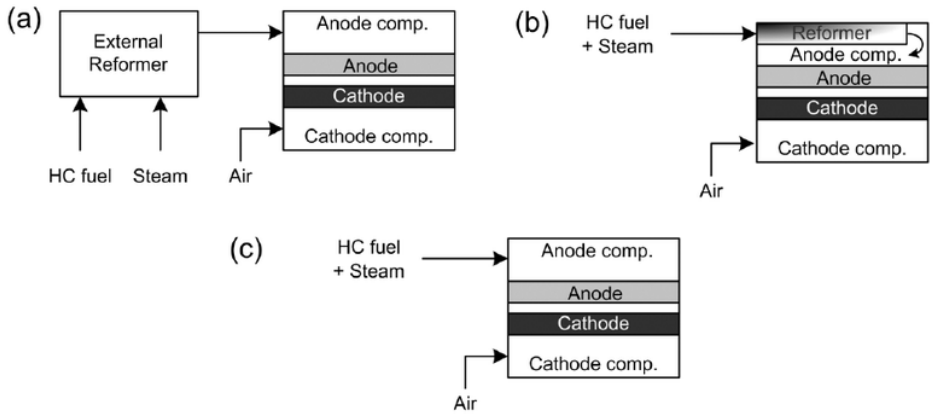

Figure 16. Schematic representation of a) external reforming b) indirect internal reforming and c) direct internal reforming [121].

In **direct internal reforming** (DIR) (**Figure 16c**) reforming catalysts are loaded in the anode gas channel directly. The electrochemical oxidation of hydrogen in fuel cells can provide some of the steam and heat needed for the reforming reaction, so there's no requirement for extra fuel to be burned to drive the reaction. Additionally, because hydrogen is still being consumed, the equilibrium of the reforming reaction may be further shifted to the right, enhancing fuel conversion, resulting in a more uniform distribution load of hydrogen and providing inherent dynamic stability. Nevertheless, an anode material with strong catalytic characteristics for power production and steam reformation is required when direct internal reforming is utilized. For

example, when in solid oxide fuel cells, the anode is made of nickel/zirconia cermet, which has the appropriate attributes for both steam reforming and power generation, there is no need for extra catalyst, and it can provide substantial activity. The main issue related to this method is the carbon deposition on the anode of the cell and the consequent electrocatalyst deactivation, which affects cell performance and longevity. It was attempted to raise the steam to carbon ratio to reduce the formation of carbon, but this had the unintended consequence of diminishing the electrical efficiency of the cells by diluting the fuel with steam. Therefore, cutting-edge anode materials that permit direct internal reforming at low steam to carbon ratios may provide important advantages. Another problem, mostly affecting high-temperature solid oxide fuel cells, is brought by the endothermic nature of the reforming reaction, which results in significant cooling effects and temperature gradients and, as a result, places a ceiling on the permitted amount of internal reforming [122], [123].

The **indirect internal reforming** (**Figure 16b**) approach involves conversion of the fuel by reformers positioned in close thermal contact with the fuel cells stack [124]. A reforming catalyst is used to carry out the reforming process, and it is positioned in an indirect reforming unit within the fuel cell assembly that are separate from the anode electrode but in close thermal contact. In this way, the heat that is produced during the exothermic electrochemical reaction is efficiently consumed from the endothermic steam reforming procedure. Because the catalysts are devoid of electrolyte vapor contamination, longer catalyst life is anticipated. The reformed gas then is directed to the anode electrodes for the electrochemical reaction to occur and hydrogen is produced [125, 126]. The advantage of this approach is that because the reforming catalysts are not poisoned by electrolyte vapor, a longer catalyst life is anticipated. Also, the anode electrode is protected by the carbon deposition and there's a good heat transfer between the fuel cell and the reformer. A well-known drawback of this method is the potential imbalance between the rates of endothermic and exothermic reactions, which causes a significant local temperature drop, especially close to the entrance of the internal reformer, that inevitably leads to mechanical failure because of thermally induced stresses [127].

3.4 External Reforming

It was previously mentioned that internal reforming is a more efficient operation for hydrogen production, however there is a drawback, taking in consideration the results of several studies performed on this kind of reforming [128]. These studies showed that carbon formation on the anode can cause deactivation and deterioration. At the same time, the large temperature

difference between fuel and fuel stack can causes mechanicals stresses. To avoid these problems, external reforming is the operation when pre-processing steps occur in two reactors separately. The most common fuel cells for external reforming are SOFCs and MCFCs, used as power generators combining the energy from fuel cell and from gas turbines. Because of the high operation temperatures (700-900°C) the advantage of this reforming is the co-generation of electricity and heat and as a result, the increase of the overall efficiency, as heat can be used for water heating or other applications increasing overall efficiency. The process of external reforming is shown in **Figure 17.**

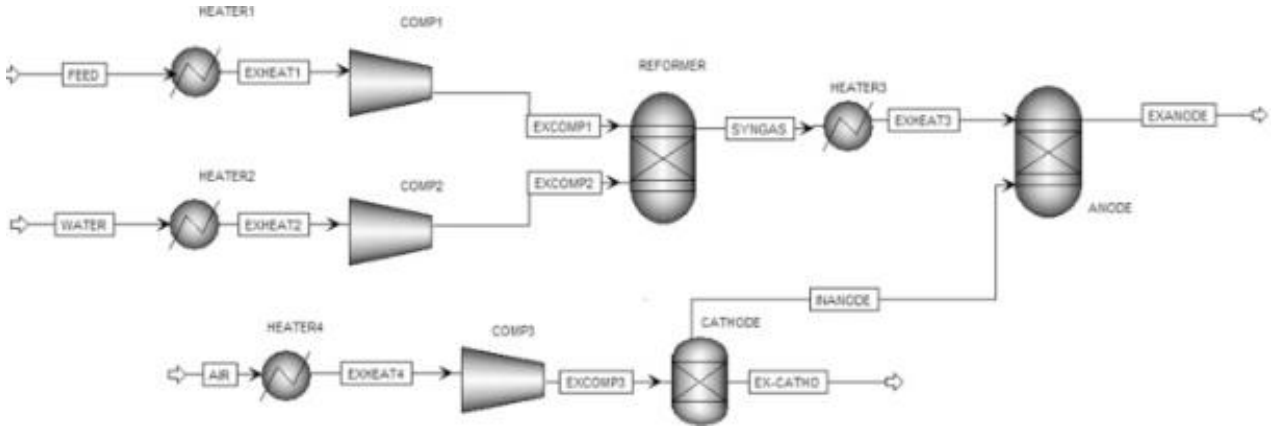

Figure 17. Schematic representation of external biofuel reformer feeding a SOFC system [128].

Biofuel and water enter in separate ways in order to increase the temperature and after that they get pressurized by the compressor, reaching the appropriate temperature and pressure. After reforming into syngas which is a mixture of H_2, CO, CO_2, H_2O and unconverted fuel, the syngas enters the anode of the fuel cell. Moreover, fuel and CO can be converted into hydrogen via steam reforming and water gas shifting respectively. On the anode, air passes through the heater and the compressor entering the anode of the fuel cell stack and reacting with the hydrogen.

3.5 Direct Alcohol Fuel Cells

Pure hydrogen or hydrogen in a high percentage of purity; is more efficient, it produces higher current densities, and has a better overall performance on fuel cells. The main problem with hydrogen is the difficulty regarding its storage and distribution since there are not enough distribution networks in the cities. Direct alcohol fuel cells were invented in order to overcome the barriers of hydrogen storage and transportation. In contrast with conventional fuel cells, DAFC have higher volumetric energy density, they have simple operation and, liquid fuels are preferable than gaseous due to safety concerns such as flammability of the fuel.

More research for direct feed utilization has been made for liquid fuels since they can be stored and transported more easily. Also, as regards safety concerns, alcohol is less flammable than hydrogen in high pressure. The fuels that have been studied for usage are methanol, ethanol, ethylene glycol and glycerol. Methanol has gained most of the interest and progress, as it's a liquid fuel, it is not expensive, and it can be stored and transported easily. It has high volumetric energy (15.9 MJL^{-1}) in STP conditions. However, there are some issues with methanol that need more research such as low activity, the poisoning of the anode to carbon monoxide production, as well as the depolarization loss on the cathode due to crossover of methanol through the Nafion membrane. These issues along with the fact of the toxicity in the products of methanol, such as formic acid and formaldehyde, as well as the fact that it is not a renewable fuel pushed the scientific community to search for other fuels. Ethanol seems to be promising since it can be easily produced through the fermentation of sugar in large quantities and at low cost, there is also an already existing transportation network since it is used as a blended fuel in vehicles. This fuel also produces toxic emissions, acetic acid, and acetaldehyde due to the incomplete electrooxidation reaction, but it is less toxic than those of methanol. Studies have also been made on the other fuels, ethylene glycol and glycerol but, they are still at research stage.

As regards fuel cells, PEMFC have shown the larger research activity and progress throughout the years because of the variety of applications, on portable devices, vehicles, but also in stationary power sources. These fuel cells operate with proton exchange membranes, the most common is Nafion membrane, providing sufficient chemical stability. The operation of PEMFC requires a reformer, internal or external, to operate since only hydrogen is applied. The reactions of DA PEMFC are shown below in **eq. 49**, **eq. 50** and **eq. 51**:

$$\text{Anode: } C_nH_{2n+1}OH + (2n-1)H_2O \rightarrow nCO_2 + 6nH^+ + 6ne^- \quad (49)$$

$$\text{Cathode: } O_2 + 4H^+ + 4e^- \rightarrow 2H_2O \quad (50)$$

$$\text{Overall: } 2C_nH_{2n+1}OH + 3nO_2 \rightarrow 2nCO_2 + (2n+1)H_2O \quad (51)$$

Some features that need further research are the use of expensive materials such as platinum electrodes; the low temperature operation which slows down the kinetics and as a result electrocatalysts can accelerate reactions' rates. Alkaline fuel cells (AFC) were also studied for alcohol feeding. They were developed from 1960 to 1980 but they weren't preferred due to the quick progress of PEMFC. Apart from that, AAFC have some advantages that could give them the green light to operate. They are less corrosive in alkaline environment; the kinetics are faster in this medium of electrolyte and faster oxygen reduction reactions which enables them to use less

expensive materials such as non-noble metal catalysts which could be silver catalysts and perovskite oxides and low cost electrocatalysts. The key feature of these catalysts is the tolerance on methanol crossover and also, they are more active on the reaction of oxygen to hydroxide. As a matter of fact, AEMFC in ethanol feed can achieve the same performances as those of Direct Methanol PEMFC, at lower cost and more simple structure. SOFC is another popular fuel cell that is researched for direct feed utilization. These stacks operate at temperatures higher than 600^{o}C which makes them capable of reaching efficiency of up to 80% when they are used for co-generation of electricity and heat. This is the main application of SOFC, since they are usually used for stationary applications such as power plants. There are SOFCs stacks that operate in lower than 600^{o}C temperatures, where they can use less expensive metallic interconnects and sealing. The time of start-up is quicker with less heat exchange as well as the time of turning off the system. SOFCs can operate with direct feed of alcohol on the anode without any pre-reforming method however with this way there is also coking deposit on the anode. Another problem with this type of fuel cell is the performance of alcohols in comparison with hydrogen. According to the bibliography, there is less performance due to the complication of the reactions, to disrupt the alcohol fuel.

3.5.1 Direct Ethanol Proton Exchange Membrane Fuel Cells

Proton exchange membrane fuel cells also referred to as polymer electrolyte membrane fuel cells stand out among other types of fuel cells due to the many characteristics that define their working principle. Proton exchange fuel cells operate at low temperature rates (usually < 90^{o}C) so they have a quick start up and response in load changes and operating conditions. They are quite tolerant in CO_2 so the atmospheric air from the cathode can be used instead of pure oxygen. Also, they provide high density current in excess of 1.0 W/cm^2, high electrical power densities of more than 1 kA/cm^2 and potential difference [129]. The working range of pressure is low (1-2 bars) and so they ensure safe operation while they have efficiency of more than 50%. Great tolerance is also observed at the pressure difference of reactants. Moreover, these types of fuel cells are compact and durable while they have simple mechanical design. Because of these characteristics, PEMFCs have gained lot of attention over the last years in academic, industrial, and governmental organizations, especially for mobile and portable applications such as automobiles, other forms of transport and many small devices. Publications per year about PEMFCs are given in **Figure 18.**

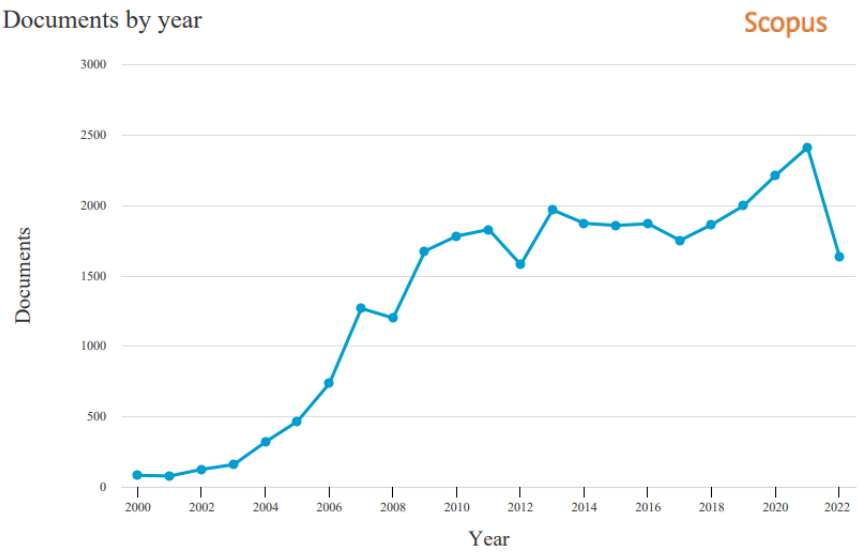

Figure 18. Researches that have been conducted over PEMFCs per year (Copyright © 2022 Elsevier B.V. All rights reserved, Scopus® is a registered trademark of Elsevier B.V.).

In general, PEMFCs utilize polymer electrolyte membranes (PEM) in order to conduct ions (H^+) and they act like solid electrolytes. The proton exchange membrane is essential to the functioning of the fuel cell because in addition to serving as a hydrogen ion carrier, it also serves as an electrical insulator and a layer that separates the reactants between the anode and cathode. The membrane must adhere to particular specifications. Firstly, there's a need for high ionic conductivity, low fuel permeability and high gas separation capacity. Moreover, it is crucial for the membrane to have electrochemical, morphological, and dimensional stability and good thermal and hydrolytic stability. In both dry and hydrated phases, there is also a demand for materials with strong mechanical properties. Despite the different PEM structures, perfluorinated membranes are currently most commonly utilized in PEMFCs. The most common membrane for PEMFCs is Nafion membranes which are polytetrafluoroethylene (widely known as PTFE or Teflon) [130]. Nafion membranes were first developed by DuPont and their main characteristics are, high proton conductivity, chemical stability, and long life (more than 60.000 hours). They are also distinguished for their high thermal stability and chemical resistance to Cl_2, H_2 and O_2. Nevertheless, Nafion membranes have disadvantages such as low performance in anhydrous conditions and at high temperatures (>80^{o}C). Due to these problems, research has been made in developing other membranes like polybenzimidazole (PBI) and sulfonated poly(sulfone) that are distinguished for their high thermal and oxidation stability. However, no other membrane could compete with the performance and durability ratio of Nafion membranes and so they still retain their leading position for PEMFCs especially dopped with various inorganic and organic fillers in order to improve their performance [131].

3.5.1.1 Working Principle, Setup, Performance

Recently, proton exchange membrane direct alcohol fuel cells have attracted much attention and especially direct ethanol fuel cells, since hydrogen is an impractical solution. Among all the possible fuels that can be used for either internal or external reforming in fuel cells, methanol was the most favourite because of its high electrochemical activity. However, methanol is toxic to humans and the sluggish kinetics still represent serious problems. During the attempts to identify fuels for fuel cells, ethanol caught researchers' attention. Ethanol's (EtOH) energy density is approximately 26.8 MJ/kg.

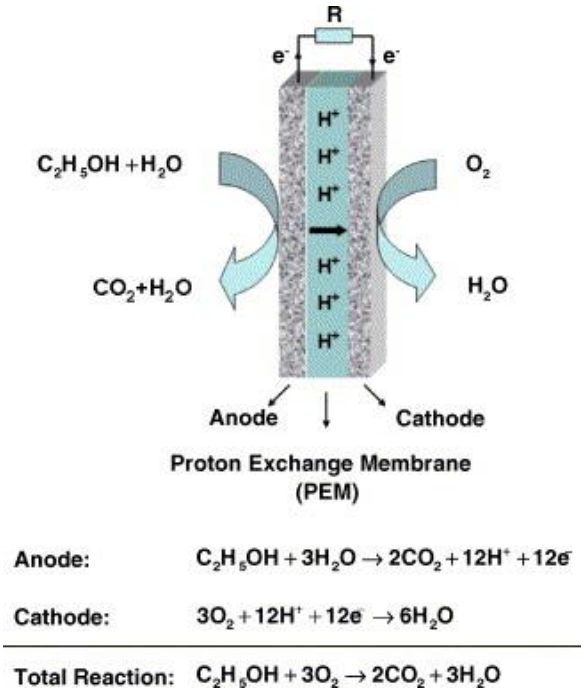

Figure 19. Working principle of a direct ethanol fuel cell [132].

The working principle of a direct ethanol fuel cell is presented in **Figure 19**. More specifically, the aqueous ethanol solution is fed to the anode where the complete oxidation to CO_2 and water takes place with the aid of electrocatalysts. Then, protons are passing to the cathode through the electrolyte and the electrons flow in a close circuit and they meet the cathode. At this stage the protons and the electrons react with the oxidant, which is air or pure oxygen, in order to produce water. Every ethanol molecule produces 12 e^- but the oxidation process also produces many by-products and intermediates and the reactions are described below by **eq.52**, **eq.53**, **eq.54**.

Anode: $C_2H_5OH + 3H_2O \rightarrow 2CO_2 + 12H^+ + 12e^-$, E_a= + 0.19 [133] (52)

Cathode: $3O_2 + 12H^+ + 12e^- \rightarrow 6H_2O$ (53)

Overall reaction: $C_2H_5OH + 3O_2 \rightarrow 2CO_2 + 3H_2O$ (54)

3.5.1.2 Challenges

The fundamental issue in the procedure is the difficulty of breaking the C-C bond, which is particularly challenging in low temperatures. The desired procedure that leads to complete ethanol oxidation implies C-C bond cleavage by forming CO which is eventually oxidized to CO_2 owing to high energy conversion. There are two major pathways that can occur from ethanol's oxidation reaction. In the first one, C_1, the C-C bond is broken, resulting in the production of C_1 fragments. These fragments are oxidized in CO and in the last step in CO_2. In the C_2 pathway the C-C bond does not break and ethanol undergoes sequential oxidation reactions to acetaldehyde (CH_3CHO) and acetic acid (CH_3COOH). Complete ethanol oxidation to CO_2 involves a complex network of reactions with over 128 different types of possible C_2 and 21 different types of C1 intermediates [133, 134].

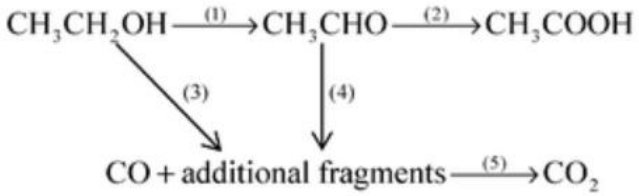

Figure 20. Ethanol's oxidation possible pathways [99].

In **Figure 20** the general scheme of ethanol's oxidation is shown. More specifically, in the reaction (1) ethanol is oxidized to acetaldehyde transferring two electrons and acetaldehyde, in turn; it can be oxidized in acetic acid transferring two additional electrons. Acetic acid's oxidation is very difficult and so it can be considered as the final product of the whole reaction especially on platinum electrodes because it is very stable. Even if acetic acid's oxidation takes place there are only four extra electrons produced and so the overall energy is lower than the energy in complete oxidation. The reaction described above belongs to the C_2 pathway. On the other hand, reactions (3), (4) represent pathways that allow the transfer of 12 electrons in total. In both processes, the molecule's C-C bond cleavage is involved, releasing adsorbed CO and other fragments. These extra fragments are most likely subsequently oxidized to produce adsorbed CO molecules. The last transfer of an oxygen atom to the adsorbed CO molecule is necessary for the conversion of the adsorbed CO to CO_2 and the finalization of the reaction that describes the C_1 pathway.

Because the cleavage of the C-C bond is a mechanism that is not yet understood and aims to overcoming this problem, the most widely accepted procedure used is, ethanol's oxidation following the C_2 pathway, which is called partial oxidation even though it produces only 4 electrons. Therefore,

the design of efficient electrocatalysts to selectively enhance C1 pathway is highly desirable for the development of direct ethanol fuel cell technology, although there is also a struggle with ethanol's oxidation reaction sluggish kinetics on the anode electrocatalyst that must be solved at the same time. The majority of the studies performed have demonstrated that, platinum-based electrode materials, which have strong catalytic activities towards ethanol oxidation, are the most advantageous for achieving complete oxidation [135]. Even though ethanol oxidation at Pt electrodes is being studied, various issues arise, including auto-inhibition or poisoning phenomena using pure platinum electrodes. Thus, in order to improve the electrocatalytic activity, platinum is modified by adding other metals, a procedure that will be analysed in the next chapter [136].

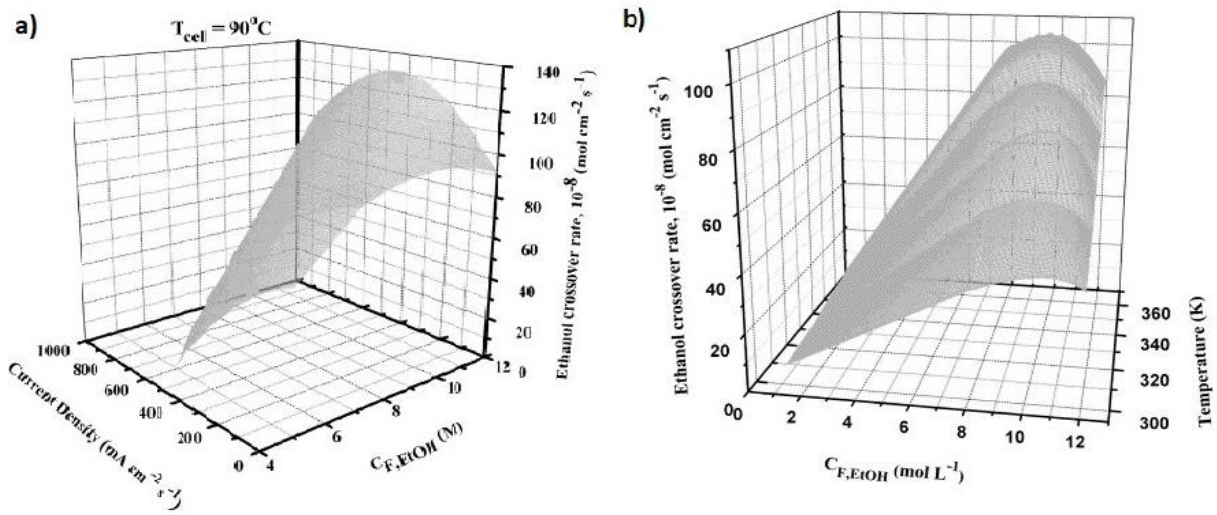

Figure 21. a) Effect of both current density and ethanol concentration feed on ethanol's crossover rate b) Ethanol crossover rate as a function of a range of ethanol feed concentrations and cell operating temperatures [137].

Regarding the various fuel supply and management concepts, direct ethanol fuel cells can be divided into passive and active. Active systems need external mechanism to feed the cell with fuel and oxidant and fits for large fuel cells but it has higher cost and lower energy density. On the other hand, passive systems take advantage of natural forces diffusion, convection (air breathing) and evaporation in order to operate without the need of any additional energy consumption. Both systems face the problem of ethanol crossover when the cell operates with high density concentrations, which is another important challenge for the development of direct alcohol fuel. The term fuel crossover describes the unintended movement of fuel (fuel molecules, not fuel ions) from the anode to the cathode through the electrolyte membrane by an external or natural force, generating heat, which is an undesired phenomenon. As a matter of fact, ethanol is recognized for having a lower rate of crossover due to its lower permeability through Nafion membrane and slower electrochemical oxidation kinetics.

Decreased cathode potential and cathode depolarization are two drawbacks of ethanol crossover. This phenomenon also has an impact on the fuel cells' efficiency that is decreased [138]. Consequently, permeated ethanol and intermediates may poison the cathode catalyst affecting the cell's performance. Additionally, it wastes fuel while the device is operating [139]. In general, ethanol crossover is affected and actually increased by temperature, current density and feed concentration. It can be seen in **Figure 21a** that the crossover rate depends on both current density and feed concentration. Above a certain concentration (8mol/L) a volcano behaviour is observed due to the swelling of the membrane [137].

Figure 21b shows the crossover rate as a function of different feed concentrations and cell operation temperatures. The main approach to solve this problem is through the feed of diluted ethanol solution. Although this causes energy losses in direct ethanol fuel cell system the efficiency of ethanol at the anode catalyst may cause polarization of the cell voltage. Moreover, diluted fuel solution feed leads to greater gradient of water concentration between the cathode and anode sides and consequently, more water passes through the membrane to the cathode. This, along with the water produced by oxygen reduction, increases the risk of flooding and so it leads to an increase in oxygen resistance and fuel cell performance. As a result, a new issue -the issue of water management- is emerging.

Water management in direct ethanol fuel cells, is about removing the water from the cathode and replenish the water loss from crossover in the anode. Nonetheless, this issue may be resolved easily by removing the cathode water, transferring it to the anode where it is needed. This procedure is called back diffusion. Researchers found more alternatives, for reducing ethanol crossover, such as modifying the electrolyte membrane, enhancing anode catalyst activity and inserting the microporous layer at the anode structure. These solutions concern mainly active systems while only a few studies on passive systems have been reported despite their importance.

3.5.2 Direct Ethanol Anion Exchange Membrane (Alkaline) Fuel Cells

Over the last decade, there is a growing interest about AEMFC because of their perspectives to operate with high performances. According to **Figure 22** between 2000 and 2009 there hasn't been any significant interest as there are less than 100 research articles, however between 2010 and 2017 we can see a fast-growing research activity about AEMFCs.

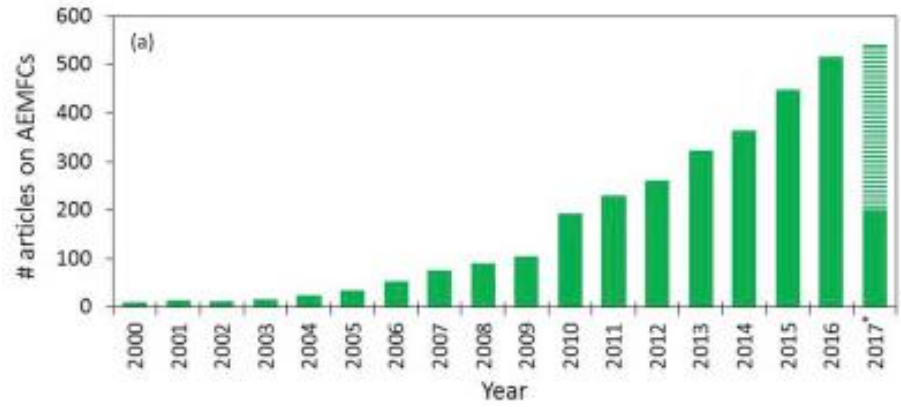

Figure 22. a) Research that has been conducted on AEMFCs, b) representation of cell voltage versus current density [140].

Although AEMFC have similar structure with PEMFC, their fundamental difference is the use of an anion exchange membrane operation in a high pH environment with a solid polymer membrane. It usually operates at temperatures between 60 – 80^{o}C, the peak power can reach a high amount of 1.8 W/cm^{2} at ambient pressure [141] utilizing ETFE-based, radiation-grafted anion exchange membrane using hydrogen feeding on the anode and air on the cathode. Peak performance, according to research is affected by the catalyst material. As a result, on the cathode, it is shown that non-PGM catalysts such as silver, some metal oxides and nickel can reach the highest yield value. While on the cathode, carbon supported Ni-Cu, Pt or nickel decorated Pd catalysts are appropriate for hydrogen feeding. Besides the catalysts, the characteristics of the MEA that showed better performance are the usage of ionomer on the membrane with good conductivity of more than 40 μS/cm, and thickness less than 30 μm at room temperature. Hydrogen as it was mentioned in the previous chapter requires expensive materials, storage is difficult for continuous use, and it is not eco-friendly. DAFCs are characterized by higher volumetric density in comparison with hydrogen.

The fact that research focuses on anion exchange membranes, knowing that PEMFCs offer a good package of performance, is attributed to challenges that have to be faced. These challenges that in an alkaline media are managed in a better way, refer to the crossover of the fuel, where ethanol flows from the anode to the cathode through the membrane without reacting, resulting in performance losses as the chemical reaction is imperfect. Another challenge that in an alkaline media [142-144] fuel cells operate better is related to water management, which plays a primary role in ionic conductivity. The membrane of the MEA is the main part that distinguishes fuel cells into categories such as, liquid, or solid electrolyte, acid, or alkaline environment. It is observed that AEMFCs have a problem with ORR kinetics as they are very sluggish. In the 1960s, they were widely

used in spacecraft missions such as the APOLLO using a liquid potassium hydroxide electrolyte and although it enhanced performance and kinetics, carbonate formation limiting hydroxide OH^- diffusion on the membrane and pore blocking of the electrode, were sufficient problems to interrupt their further development. Therefore, the conclusion was that a solid electrolyte, instead of a liquid electrolyte, enhances the overall performance through the avoidance of carbonation and leakiness, representing problems that can occur during mechanical failures.

For the AEMFC to be satisfactory in terms of performance, certain criteria should be met. Beginning with low ethanol permeability throughout the membrane because the higher it gets as the reactions become incomplete, high ionic conductivity of over 100 x 10^{-3} S/cm is also essential; low-cost materials which is the main reason of research in an alkaline environment; as well as thin layer between anode and cathode between 50–80 μm. Moreover, mechanical, and long-term chemical and thermal stability are characteristics that AEM must provide during the operation. Anion exchange membranes fall into two main categories: (a) polyelectrolyte membranes where, ionic groups based on quaternary ammonium are connected on the chain of polymer while anions are connected with the ionic function groups to keep electroneutrality on the electrolyte, and (b) alkali-doped membrane which is based on the interaction of the cations of alkali with electronegative atom. The most commonly used solid electrolyte for alkaline fuel cell consists of quaternized ammonium membrane, developed by Tokuyama A201, which can achieve high amounts of released energy, of 58 mW/cm^2 at ambient conditions. Another form of membrane is alkali doped polybenzimidazole (PBI) membranes, usually dopped with KOH or NAOH [145]. An added base increases EOR kinetics because of the extra anions extracted from NaOH as it is shown by **eq. 55**:

$$12NaOH \rightarrow 12Na + 12OH^- \quad (55)$$

In general, the performance in an alkaline environment is relatively low, making a change in the pH value to change the conductivity of the electrolyte. The pH is increased by adding a base on the ethanol leading to faster kinetics, increasing conductivity and resulting in higher performance of the stack. Polyvinyl alcohol (PVA) membrane has also been studied and it is regarded as an excellent fill-forming material. This group of membranes involves low-cost material and preparation, and it is also nontoxic.

3.5.2.1 Working Principle, Setup, Performance

A typical AEMFC [146] consists of an anion exchange membrane in the middle, a catalyst layer on the anode and cathode, and a diffusion layer on the anode and cathode (**Figure 23)**. Catalyst layers usually include a mix of catalysts and ionomers that provide triple-phase boundaries. The main task of diffusion layers is to support catalysts' layer and to conduct electricity. A diffusion layer consists of two parts, a backing layer that is made of carbon cloth or carbon paper and a microporous layer (MPL).

On the anode, ethanol flows through the diffusion layer and it continues on the catalyst layer mixed with base NaOH or KOH, or pure ethanol, where oxygen reduction occurs EOR as seen in **eq. 56**:

$$\text{Anode:}\quad C_2H_5OH + 12OH^- \rightarrow 2CO_2 + 9H_2O + 12e^- \quad E_a = -0.74\ V \tag{56}$$

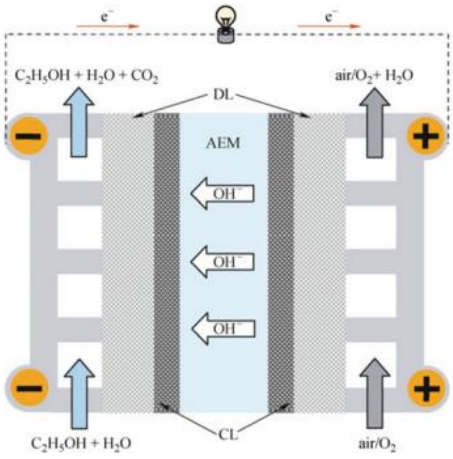

Figure 23. Representation of anion exchange membrane direct ethanol fuel cell [146].

On the cathode, pure oxygen or air reacts with the water that is obtained from the fuel in addition to the water that is produced from the anode reaction and passes through the electrolyte, in combination with the electrons that flow in the circuit, producing the demanded anions. The produced anions pass through the membrane from the cathode to the anode to react with the ethanol according to **eq. 57**, **eq. 58**:

$$\text{Cathode:}\quad O_2 + 2H_2O + 4e^- \rightarrow 4OH^- \quad E_c = 0.4\ V \tag{57}$$

$$\text{Overall reaction: } C_2H_5OH + 3O_2 \rightarrow 2CO_2 + 3H_2O \quad E=1.14\ V \tag{58}$$

Besides these products, ethanol also produces some toxic elements -acetic acid (acetate) and acetaldehyde – because of the oxidation reaction that are expressed by **eq. 59**:

$$C_2H_5OH + 5OH^- \rightarrow CH_3COO^- + 4e^- + 4H_2O \tag{59}$$

In fact, the product of the overall reaction contains more acetic acid rather than carbon dioxide, hence the reaction of the ethanol is shown below by **eq. 60**:

$$C_2H_5OH + O_2 + OH^- \rightarrow CH_3COO^- + 2H_2O \quad (60)$$

Multiple studies have shown [146] that between Pt based and Pd based catalysts, the second option results in higher performances. Also, alkali doped membrane offers good performances and conductivity values. According to the research on Pd/C and PdNi/C catalysts on the anode while on the cathode there was a FeCo catalyst, the results showed an OCV of 0.89 V and 0.79 V respectively in each occasion while the current density was 90 mW/cm^2 and 67 mW/cm^2 at 60^o Celsius. In another occasion of alkaline doped membrane, [147] containing PtRu/C on the anode and Pt/C on the cathode results showed a current density of 49.2 and 60.95 mW/cm^2 at temperatures of 75^{o}C and 80^{o}C respectively.

3.5.2.3 Challenges

AEMFC faces some challenges that are based on the idea of the ethanol feeding, ethanol crossover, conductivity on the membrane, durability, and stability that all contribute to the total performance and efficiency of the stack. Ethanol crossover occurs when ethanol fuel passes through the membrane unexpectedly, as it is an unwanted phenomenon which reduces the efficiency of the fuel stack; it can poison the cathode catalyst due to products that contribute to the oxidation of the catalyst. There are several reasons for its occurrence such as, current density, ethanol concentration on the fuel, the thickness of CL and the temperature. Ionic conductivity affects the performance of the fuel cell, it usually rises through the augmentation of the ionomer concentration, reaching to the maximum value of conductivity and after that point it starts decreasing. Increasing the ion exchange capacity and the temperature enhances performance. Furthermore, it was mentioned before that conductivity raises its value by adding a base KOH or NaOH on the ethanol solution and on the membrane. Regarding the membrane conductivity, it depends on the dipping time of the membrane to the added base, thus too much time can hurt the membrane and reduce conductivity.

3.5.2.2 AEMFC vs PEMFC differences

Although acid and alkaline fuel cells have the same structure but different exchange membrane, there are more differences that distinguish the operation of these two types of fuel cells. Beginning with the exchange membrane, instead of protons exchanging on the membrane there is anion exchange on the membrane. Another difference is that they have opposite directions (**Figure 24**) as regards the ions and anions exchanging. While ions move from anode to

cathode at PEMFC, anions in contrast, move from cathode to anode. The final difference refers to water production; on AEMFC water is produced in double portion in comparison with PEMFC while it is also a reactant on the cathode. It's worth mentioning that except from anion production, there are also other products of the reaction such as HCO_3^-, CO_3^-, however anion OH^- is the main product of the reaction.

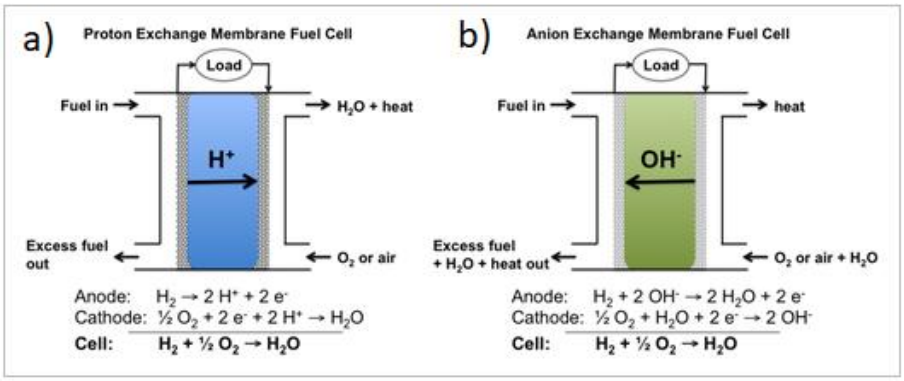

Figure 24. Schematic representation of a) PEMFC, b) AEMFC, of hydrogen feed [148].

The interest in alkaline media electrolyte instead of acid electrolyte was the result of the fact that reaction kinetics, both ethanol oxidation reaction (EOR) and oxygen reduction reaction (ORR), are faster. An important feature to highlight is production cost; fast kinetics are capable to complete the demanded reactions and therefore there is no need of precious materials on the catalyst surface. Regarding the fuel sector, there is flexibility on the alkaline environment, so it allows the use of hydrogen and alcohol fuels like ethanol and methanol, with reforming or with direct feeding. Efficient water management, quicker ORR, and extended research for more materials about membrane on the alkaline environment are among the challenges that need further research.

3.5.3 Direct Alcohol Solid Oxide Fuel Cells

Solid oxide fuel cells (SOFCs) are advanced electrochemical reactors that present significant advantages over traditional energy conversion systems -and even new technology systems- and they are therefore the subject of extensive research activity, as shown in **Figure 25a**. They are employed in the industrial sector, offering at the same time a realistic prospect of becoming commercially viable [149]. High efficiency electrochemical energy generation is offered by these fuel cells without any environment degradation [142, 150]. They provide high efficiency (up to 65%), fuel adaptability and low NO_x and SO_x emissions. Furthermore, they operate at elevated temperatures (700-1000^{o}C) which in essence eliminates the need of external reformer, and thus extra expenses, for the fuel to be reformed and feed the cell while and it also improves the tolerance of the fuel cell in fuel impurities. Investigations on solid oxide fuel cells have taken place

using a variety of configurations, including tubular and planar geometries. **Figure 25b** illustrates the design of the tubular geometry cell. Additionally, pressurized solid oxide fuel cells may be utilized for replacing combustors in gas and steam turbines. These hybrid systems have an efficiency of approximately 70% [151].

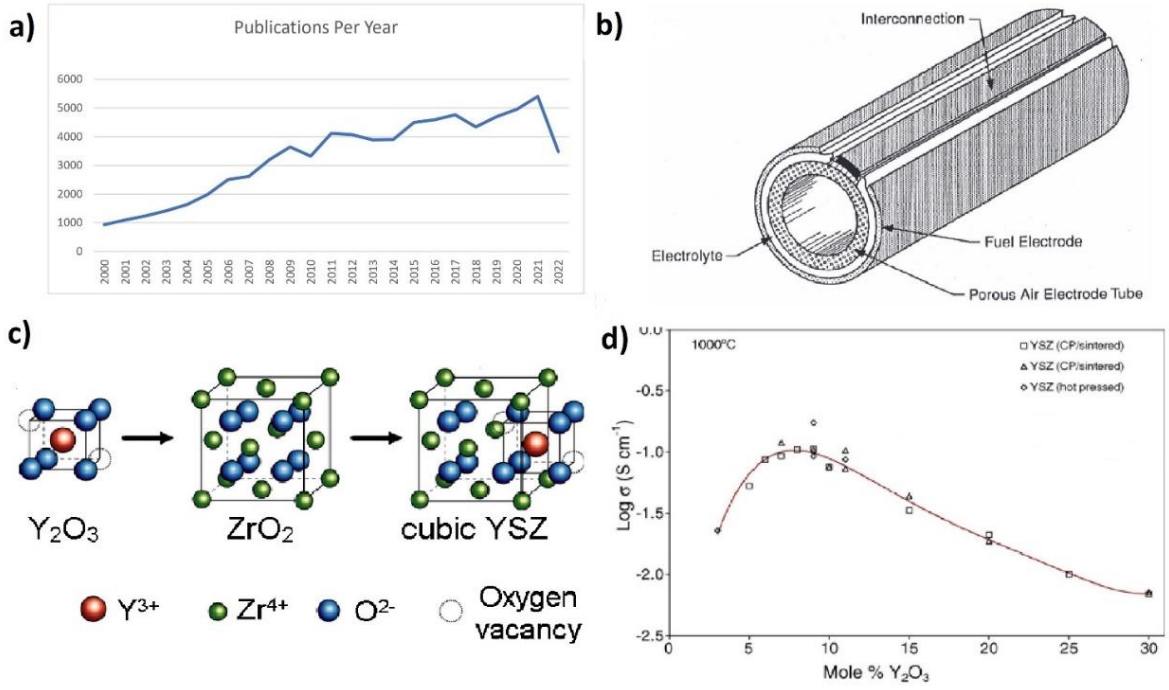

Figure 25. a) Publications per year for Solid oxide fuel cells according to Dimensions database b) Tubular solid oxide fuel cell design [150] c) Yttria stabilized zirconia representation on a molecular level [152] d) Conductivity of yttria stabilized zirconia in air at 1000°C [153].

A new trend that has gained a lot of momentum and rendered SOFCs pole of attraction over the last decades, is the solid oxide fuel cell combined heat and power systems which can raise overall system efficiency by approximately 80%. More specifically, these systems, in residential use, take advantage of the high range produced heat to produce hot water achieved by simple heat exchangers. Also, in a stationary system the heat can be used for instance to gasify coal.

In solid oxide fuel cells, the most common electrolyte is yttria-stabilized zirconia (YSZ) which is an oxygen ion conductor (O^{2-}). Yttria-stabilized zirconia (YSZ) is a structural ceramic material in which the yttrium oxide (Y_2O_3) addition stabilizes the cubic crystal structure of zirconium dioxide (ZrO_2) at ambient temperature as shown in **Figure 25c**. YSZ is characterized by some prominent features such as thermal shock resistance and high temperature tolerance, which is quite useful in SOFCs since the temperatures are elevated and it undergoes thermal cycles from room temperature to operation temperature and vice versa. It has also good chemical stability in both oxidising and reducing atmospheres and outstanding mechanical properties. Moreover, it is abundant, quite

inexpensive, and robust while it is easy to manufacture. Pure zirconia may change forms in a variety of temperatures. For instance, it has a monoclinic structure at ambient temperature, a tetragonal structure at around 1170^{o}C, and a cubic structure at about 2370^{o}C. Yttria, has a high solubility in zirconia, stabilizes it at cubic fluorite phase from room temperature to its melting point (2680^{o}C) while at the same time it increases the oxygen ions vacancies making the mixture highly ionic conductive [154]. In YSZ, Y_2O_3 typically makes about 8 mol% of the total because in higher concentrations the ionic conductivity is significantly decreased as shown in **Figure 25d**. In tubular SOFCs, zirconia is doped with about 10% yttria. YSZ is chemically inert toward other components that are used in solid oxide fuel cells [153]. For optimal fuel cell performance, the YSZ electrolyte must be completely porous-free, to prevent gases from passing through it from one side to the other while at the same time it must be uniformly thin in order to reduce ohmic losses, high oxygen ion conductivity and as close to zero as possible electron transport rate. The anode in SOFCs, in contrast to the electrolyte, must have porous structure and be electrically conducting [155].

The vast majority of SOFCs use nickel as anode material, mixed with the electrolyte material to create a cermet, due to its low cost and the thermal expansion coefficient that provides. The preferable nickel percentage content is around 30% because this is the threshold for the electrical conductivity needed, as under this concentration the electrical conductivity is the same as the electrolytes. Moreover, above this concentration the thermal coefficient of nickel/yttria-stabilized zirconia increases linearly with the nickel content and so there's a major thermal mismatch with the electrolyte. Thus, there is high likelihood for the electrolyte to crack or, for the anode to delaminate during manufacture, operation, and temperature cycling. Cathode must have the same features as anode in solid oxide fuel cells. Due to the high temperatures, the choices are limited to noble metals or electronically conducting oxides. Electronically conducting oxides are the only materials utilized in practice since noble metals are not financially feasible. In addition, in this case, the material must have thermal expansion coefficient comparable to that of the solid electrolyte and should not display any signs of propensity to react with the electrolyte. Many doped oxides have been studied, but the one that stands out is the Strontium-doped lanthanum manganite (LSM) for zirconia based SOFCs [156].

3.5.3.1 Working Principle

A solid oxide fuel cell (SOFC) consists of the anode where fuel enters with water, the cathode using the oxygen air, the electrolyte, and the interconnect. When there is tubular design of SOFC another part is important, the cell-to-cell connector. According to the research on direct ethanol operation, in most of the cases of ethanol fuel, an internal reformer that converts ethanol

to hydrogen before it enters on the fuel stack is used. The reactions of the direct ethanol fuel are shown below by **eq. 61**, **eq. 62**:

$$\text{Anode: } C_2H_5OH + 3H_2O \rightarrow 6H_2 + 2CO_2 \quad (61)$$

$$\text{Cathode: } 0.5O_2 + 2e^- \rightarrow O^{2-} \quad (62)$$

Direct ethanol is not as efficient as hydrogen however, with internal reforming SOFC performance shows much better values. Ethanol is reformed partially on the anode using a small amount of water to enable the reaction. Water plays a key role in the reforming process as it controls the activity of the reaction where maximum output voltage can go up to 1.5 V. The reactions in this case, after the steam reforming and water gas shifting where hydrogen and carbon monoxide exist, are shown below by **eq. 63**, **eq. 64**, **eq. 65**, **eq. 66**:

$$\text{Anode: } H_2 + O^{2-} \rightarrow H_2O + 2e^- \quad (63)$$

$$CO + O^{2-} \rightarrow CO_2 + 2e^- \quad (64)$$

$$\text{Cathode: } O_2 + 4e^- \rightarrow 2O^{2-} \quad (65)$$

$$\text{Overall: } H_2 + CO + O_2 \rightarrow H_2O + CO_2 + \Delta E \quad (66)$$

In this case of internal reforming an anode that is coke forming resistant, with high electronic and ionic conductivity is needed. The main material is Yttria, which satisfies all these requirements. However, when hydrogen is the fuel, it seems that it cannot withstand ethanol feeding. In fact Steil et al [157], reported that after 4.5 hours of operation with dry ethanol, the fuel cell collapsed, and the performance in this switching of fuel dropped from 1.15 V on hydrogen to 0.95 V on ethanol. The solution on this coke deposing is the modification of Yttria anode by adding extra materials such as Pt and Sn, which are responsible for forming Ni-M bimetallic catalyst.

Regarding stability, S.D Nobrega et al [157], reported that on a voltage of 0.7 V using hydrogen and ethanol as fuels, after 1.5 hour there was stability where, ethanol's current density was slightly better at 0.067 A/cm^2 than hydrogen at 0.059 A/cm^2. Another important fact is that on this experiment the stability occurred for more than 100 hours on ethanol feeding, offering a good heading that no carbon formation existed on the Ni catalyst and thus ethanol can be fully converted successfully.

3.5.2.2 Challenges

As any other electrochemical device, direct ethanol solid oxide fuel cells face some challenges regarding the components, materials and reactions that take place. One of the most common problems is the coking formation on Ni-based anode. This type of anode materials are vulnerable to coking as Ni-based cermets are highly active for catalytic fuel cracking reactions,

hastening the thermal decomposition of hydrocarbons, which results in high accumulation of coke on the anode surface [158]. In order to solve this problem research has been conducted on Cu-based cerments and perovskite -a material that has the same crystal structure as the mineral calcium titanium oxide- oxides [159]. Because Cu has poor catalytic activity on hydrocarbons and the carbon does not deposit on anode surface, Ni-Cu mixed materials in specific percentage contents are also recommended for anode in SOFCs. The non-nickel anodes, however, have issues with low electrocatalytic activity, limited chemical stability due to the ease of interfacial interactions with other cell components, and a high cost of manufacturing, which prevents their use in more advanced applications [160]. Two strategies can be followed to prevent coke formation: one by thermodynamics and one by reactions kinetics. From a thermodynamical perspective carbon formation cannot be prevented [161, 162]. In this respect, the addition of O atoms to the hydrocarbon fuel is advantageous to reduce carbon formation, and the presence of an O atom in the molecular structure of ethanol is advantageous for this goal. Moreover, the addition of water in steam form in fuel gas increases the O/C and H/C ratio and as a result it mediates the coke formation. When the proper amount of water is used, this method can boost the fuel's efficiency, because of the fuel steam reforming, but if the added steam is higher or lower than what is needed, the efficiency of the fuel cell will drop because of the fuel dilution. This can be tackled by using anode materials with the capability of water storage, since water is one of the products of the oxidation reaction. The coke formation is also affected by the reaction kinetics. Thus, from a kinetic viewpoint, the way to avoid coke formation is either to reduce the carbon deposition rate or increase the carbon removal rate. For instance, alloying Ni with less active fragments, such as Fe and Cu, can supress the carbon formation rate. However, this diminishes the overall electrocatalytic activity and as a result the efficiency of the cell [163]. In contrast, increasing the rate of carbon removal by altering the catalyst's surface is another way to suppress coke production. Recent research showed that Ni-based alloy electrocatalysts have better tolerance to carbon. One strong suggestion over this method is the utilization of proton-conducting perovskite oxides such as $BaZr_{0.4}Ce_{0.4}Y_{0.2}O_3$ (BZCY). These perovskites can naturally take the protons from the dissociation of water's electrons and capture the water molecules, which helps to reduce the carbon deposition [164]. Liu et al have developed and reported Ni with $BaZr_{0.1}Ce_{0.7}Y_{0.2-x}Yb_xO_{3-\delta}$ (BZCYYb) anodes with a high water storage capability that have excellent coking and S tolerance for SOFCs that operate with hydrocarbons [165]. However, there is no report on the practical applications of these perovskites in SOFCs so far.

CHAPTER IV

4. Low Temperature Direct Ethanol Fuel Cells in Acidic Media

4.1 Introduction

Direct ethanol fuel cells, among other fuel cells, have developed significantly over the past 20 years thanks to their exceptional qualities and ecologically friendly operation. In general, ethanol can undergo oxidation in either an acidic or an alkaline environment, leading to two distinct pathways. This chapter will present an overview of the literature on low-temperature direct ethanol fuel cells operating in an acidic medium. Anode, cathode, and electrolyte materials will be reviewed. To determine the ideal combination using the information available in the literature to date, the findings of multiple research groups will be analysed and compared.

In the direct ethanol fuel cells analysed in this thesis, ethanol is oxidized in acidic medium. More specifically, the oxidation occurs in low pH environment (pH<5.0) and since the H^+ concentration is fairly high in acidic DEFCs, the cation transition occurs more favourably than in a basic medium [166]. PEMs are therefore more suited for low pH values. In acidic type fuel cells, water is produced at the cathode, and it is consumed at the anode during oxidation reaction [167]. The anode compartment's ethanol concentration tends to decline, requiring replenishment, while the cathode compartment's water concentration rises, necessitating removal to avoid flooding and issues with fuel cross-over. Additionally, proton exchange membrane fuel cells offer flexibility in terms of using solid electrolytes and thus preventing electrolyte leakage [168]. Ethanol's electrochemical oxidation is a gradual process that involves numerous parallel channels and a complicated mechanism. Acetaldehyde and acetic acid are the products of partial oxidation created when ethanol is oxidized through the so-called C_2 pathway, whereas CO and CH_x fragments that can be further oxidized to CO_2 are the reaction intermediates that are created when there is C-C bond cleavage (C_1 pathway). Nevertheless, due to the poor activity of catalysts usually the EOR process cannot occur completely making the C_2 pathway most common [133, 134]. Inferior conversion efficiency and incomplete oxidation represent the main obstacles in DE PEMFCs commercialization. Also, one of the most significant problems that DE PEMFCs face is the CO poisoning. Platinum anode is poisoned by adsorbed CO, which is generated from the dissociation of ethanol, strongly binds with active sites, blocking the catalytically active surface area and thus the reactivity of catalyst reduces [169]. Hence, it is crucial to design electrocatalysts that are highly active, have good CO-tolerance and are stable in order to achieve better efficiency and avoidance of the aforementioned serious problems.

The complete ethanol anodic oxidation, oxygen reduction and overall reaction of DEFC could be described by **eq. 67**, **eq. 68**, **eq. 69**:

$$\text{Anode reaction: } CH_3CH_2OH + 3H_2O \rightarrow 2CO_2 + 12H^+ + 12e^-,\ E^- = 0.084\ \text{V versus SHE} \quad (67)$$

$$\text{Cathode reaction: } 3O_2 + 12H^+ + 12e^- \rightarrow 6H_2O,\ E^+ = 1.229\ \text{V versus SHE} \quad (68)$$

$$\text{Overall reaction: } CH_3CH_2OH + 3O_2 \rightarrow 2CO_2 + 3H_2O,\ E_{emf} = 1.145\ \text{V} \quad (69)$$

Here, E^- and E^+ respectively denote anodic and cathodic reaction potentials and E_{emf} donates standard electromotive force ($E^+ - E^-$). SHE denotes the standard hydrogen electrode.

4.2 Electrocatalysts for DE PEMFCs

4.2.1 Anode materials

On the anode of direct ethanol fuel cells ethanol's oxidation occurs and thus, the metals that are used for anode electrocatalysts must serve this purpose. Electrocatalysts should facilitate ethanol's oxidation reaction (EOR) and at the same time reduce the values of the oxidation onset potential [132]. High electronic and catalytic activity, are some additional characteristics that are desired in electrocatalysts. Pt catalysts is the main material used for anode and cathode providing the best performances, while it has been shown to be the sole active and stable noble metal for oxidizing alcohol, especially in acidic media [170]. However, taking into consideration the high cost of noble metals, research has been made on bimetallic, trimetallic or ternary catalysts. To effectively use these metals, they have to be well dispersed to small particles on conductive carbon supports. Doping the Pt catalyst is a method used to reduce the cost and decrease the CO poisoning effect of the catalyst aiming to the reduction of Pt usage combined with other materials such as Sn, Ni, Rh and Ru.

Pd and Ir based catalysts are also used and belong to the noble metal category, and they own similar performances. Also, monometallic, bimetallic or trimetallic alloys are usually used with the above materials or even with Fe and Mo. The traditional approaches of impregnation, co-precipitation, and ion exchange do not provide enough metal surface area or good metal particle distribution. An alternative technique that uses prefabricated metal colloids and subsequent deposition on the support material has been studied to circumvent the aforementioned drawbacks. Catalysts' main operation is, breaking the C-C bond of the ethanol, and the high concentration of the converted CO_2 in comparison with the other products of ethanol, acetic acid and acetaldehyde. C-C bond cleavage increases fuel utilization and fuel cell efficiency. In addition to the features mentioned above, a good catalyst must also satisfy the requirement of high electric

conductivity which is achieved by using carbon as a support which has high electric conductivity and a significant impact on the activity of supported catalysts, altering the electronic structure of the catalyst in addition to particle shape, size, and distribution and thus, it is the most commonly used supporting material with a suitable surface as Tsiakaras et al. mentioned [132] in their review in 2005.

4.2.1.1 Platinum-Based

Pt monometallic

Platinum (Pt) is the most commonly used metal on electrocatalysts, due to its ability to drive the ethanol oxidation reaction (EOR). It has been proven that the bigger catalytic surface area enhances the catalytic activity, and thus mostly carbon-based materials are used as efficient supports on EOR applications. Pure Pt is readily poisoned by CO-like intermediates of ethanol electro-oxidation. However, the combination of Pt with other metals can enhance the electrocatalytic activity towards EOR and suppress the poisoning. Therefore, one of the main aims of research is to create efficient electrocatalysts that could carry out ethanol oxidation at lower potentials. The main focus of Pt poisoning mitigation has been the addition of co-catalysts to platinum, particularly ruthenium and tin. The most investigated anode materials found in literature are PtSn and PtRu based. In the existence of Ru, Sn oxides, the oxidation of the firmly adsorbed oxygen-containing species is promoted by providing oxygen atoms at a nearby site at a lower potential than that provided by pure Pt. According to the inherent mechanism, Pt's electronic structure is altered by Ru, Sn, which has an impact on how oxygen-containing species bind to it [171],[172]. Since the early 2000s, many experimental studies have been devoted to anode-electrocatalysts for EOR either on the three-electrode method or in an electrochemical single cell. However, it should be noted that when employing acidic fuel cells, there are fewer types of catalysts accessible due to the low pH environment [173].

Perez et al. [174], performed an experiment on commercial Pt/C catalysts with different Pt content 20, 30, 40 and 60 wt.%. The measurements were taken with Nafion membrane, Pt loading of the catalysts layers was 1.0 mg/cm^2 and 0.1 mol/l $HClO_4$ with Vulcan XC-72R support. Direct ethanol single cell tests were carried out by feeding 1 mol/l aqueous ethanol solution at the anode and at the cathode oxygen at 3 atm pressure at 90^{o}C with different Pt particle size. The current densities increased in the order 60 wt.% Pt/C < 40 wt.% Pt/C < 20 wt.% Pt/C < 30 wt.% Pt/C. The performance of the cells with 20 wt.% and 30 wt.% Pt/C was similar, while the cell with 40 wt.%

and 60 wt.% Pt/C showed a lower performance. These results were also confirmed by Tayal et al. [175], experimented on monometallic carbon supported Pt/C -on a 40 wt.% of Pt and 60 wt.% carbon- catalyst which showed low amounts of current density around 5.9 mA/cm^2 and the ethanol oxidation started around 650 mV. In general, the catalyst support material has a significant impact on the performance and longevity of PEMFCs [176].

Out of the Pt monometallic catalysts investigated, the one with 20% Pt loading had the better performance while the catalysts with higher loading percentage had lower performances. Although 30% Pt catalyst had higher current density the negative effect on ORR was also the highest, decreasing the overall cell performance.

4.2.1.2 Platinum Bimetallic (Binary) Alloys

It has been seen, according to extensive research that Pt alone is not as a capable oxidant as when it is doped with metals, and as it was mentioned above because of the high cost of Pt, most binary and ternary catalysts are researched [136]. Most research on bimetallic catalysts has been made on carbon supported PtSn/C and PtRe/C where they show the best performance providing a current density of catalyst. Except from Sn and Re more metals have been researched such as Co, Rh, Pd and Ni since the cost of these metals is much lower than Pt.

Pt-Ru, Pt-Sn, Pt-W

Tsiakaras et al. [177], performed a single fuel cell test in order to compare anode materials for direct ethanol fuel cells with pure Pt and Pt alloyed with Ru, W, Sn as anode catalyst at standard temperature around 100^{o}C. Nafion® 115 membrane was used with Vulcan XC-72R carbon support (carrier) with BET area of 250 m^2/g while the active single cell area is 9 cm^2. The cathode material used was pure Pt/C at 20 wt.% Pt with 1.0 mg/cm^2 metal loading and feeding of non-humidified oxygen at flow rate of 120 ml/min at 0.2 Pa pressure. Anode was fed with ethanol solution 1 M at flow rate 1 ml/min. Pt_1Ru_1/C appears to have the most negative potential at about 0.53 V and peak potential at 0.23 V, lower than single Pt/C. The rates of peak potentials of Pt_1Pd_1/C, Pt_1Sn_1/C, Pt_1W_1/C were respectively 0.65 V, 0.71 V and 0.75 V. As it is obvious from the results (**Figure 26**), the positive peak current of ethanol on PtW is close to this of PtSn but it appears at higher positive potential. PtSn/C presents higher positive peak current density and as a result higher activity to ethanol electro-oxidation. The first oxidation peak corresponds mainly to the formation of CO_2 for ethanol whereas the second oxidation peak is caused by other products as acetic acid and

acetaldehyde for ethanol [178]. PtRu has the lowest overpotential and thus, it is also a promising catalyst.

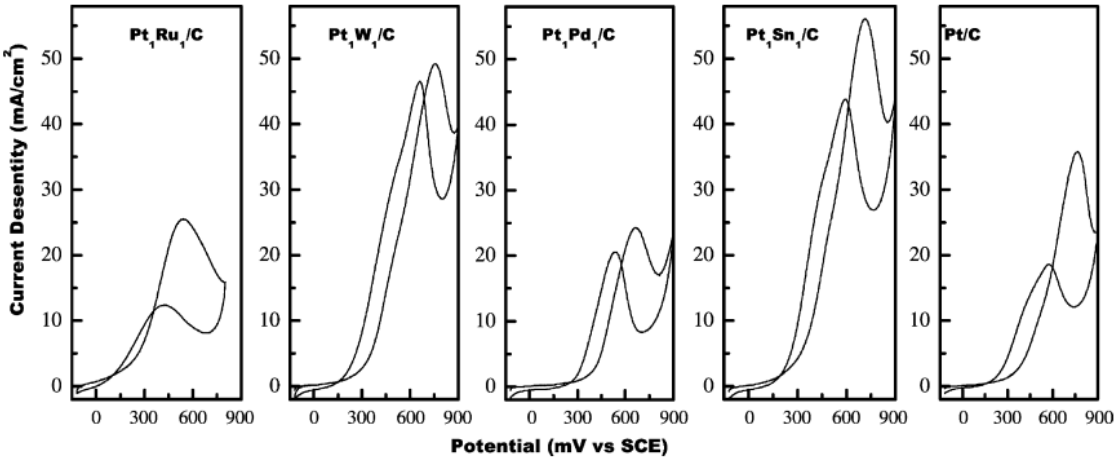

Figure 26. Cyclic voltammetry spectra of carbon-supported bimetallic catalysts at 25 ◦C. Electrolyte is 0.5 M H_2SO_4 solution containing 1.0 M ethanol. The scan rate was 10 mV/s [177].

The table below (**table 1**) shows the results from the single cell test for every tested catalyst for open circuit voltage, power density and current density at 30 and 60mA/cm^2. This further shows that Sn has a high compatibility as a good bimetallic catalyst for ethanol oxidation when paired with Pt in low pH environment and since CO_{ads} species have a significant impact on the catalysts' surfaces active site, Sn functions more as a resistance improvement against surface active site poisoning.

Table 1: Summary of performance of single fuel cell tests adopting different catalysts (90°C) [177].

		At 30 mA/cm^2		At 60 mA/cm^2			
Anode catalysts	Open circuit voltage (mV)	Output voltage (mv)	Corresponding power density (mA/cm^2)	Output voltage (mV)	Corresponding power density (mA/cm^2)	Maximum power density (mW/cm^2)	Current density at maximum power density (mA/cm^2)
Pt/C	547	275	8.25	177	10.62	10.85	75.1
Pt_1Pd_1/C	500	285	8.55	193	11.58	11.97	75.1
Pt_1W_1/C	540	312	9.36	232	13.92	15.88	86.4
Pt_1Ru_1/C	677	461	13.83	368	22.08	28.54	120.3
Pt_1Sn_1/C	811	662	19.86	576	34.56	52.22	135.55
$Pt_1Ru_1W_1/C$	698	503	15.09	425	25.50	38.54	142.2
$Pt_1Ru_1Mo_1/C$	720	486	14.58	389	23.34	31.19	120.5

The test identifies that Pt_1Sn_1/C is the most suitable catalyst from those four bimetallic (Pt_1Sn_1/C > Pt_1Ru_1/C > Pt_1W_1/C > Pt_1Pd_1/C > Pt/C), as shown in **Figure 27**. Overall, the impact of Sn, Ru, and W in addition to Pt were substantial on the Pt-based electrocatalysts' ability to catalyse the oxidation of ethanol. The PtRu electrocatalyst had the lowest overpotential and the PtSn electrocatalyst had the

maximum current density. At lower overpotential values than Pt, Sn, Ru, and W can undoubtedly generate oxygen-containing species. The oxidation of adsorbed CO-like intermediates requires these oxygen-containing (OH_{ads}) surface species. This so-called bifunctional process explains in part why Sn, Ru, and W have a greater impact on the electro-oxidation of ethanol. Higher Sn concentration aids in the creation of OH_{ads} at lower temperatures and speeds up the whole process. This conclusion combined with the electrochemical results above make Pt_1Sn_1 exceptional for temperatures around 90^0C, and Pt_3Sn_2 for temperatures around 60^oC.

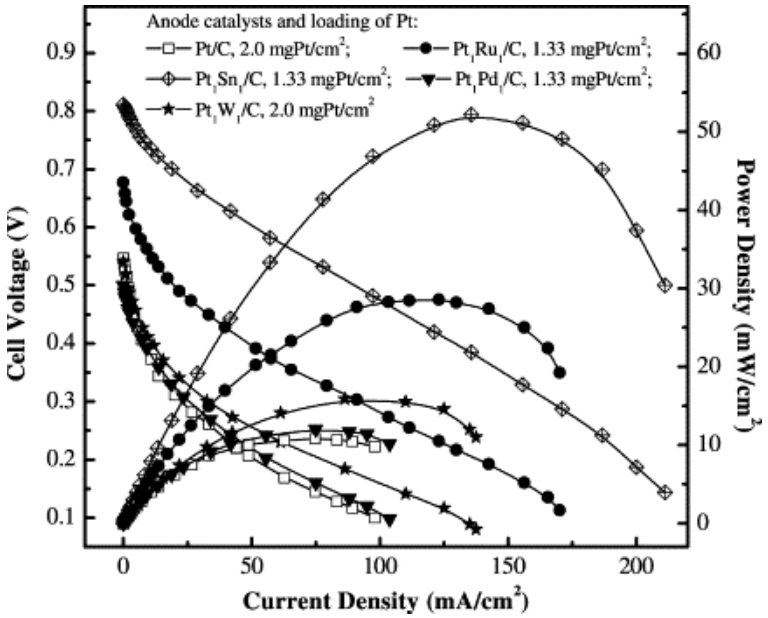

Figure 27. Performances of single direct ethanol fuel cell with different PtSn/C catalysts as anode catalysts at 90°C. Anode is PtSn/C with different Pt/Sn atomic ratio (1.33mg_{Pt}/cm^2). Solid electrolyte is Nafion®-115 membrane. Ethanol aqueous solution is 1.0 mol/l and its flow rate is 1.0 ml/min; cathode contains Pt/C (Johnson Matthey Co.) with 1.0 mg_{Pt}/cm2 [177].

Pt-Sn based catalysts

Tsiakaras et al. [179], fabricated Pt and Pt_xSn_y nanocomposites deposited on Vulcan XC-72R support, as anode electrocatalysts with Nafion-115 membrane and Pt/C 20 wt.% with 1.0 mg/cm^2 metal loading as cathode electrocatalyst. Non-humidified oxygen was fed to the cathode while 1mol/l ethanol solution at flow rate of 1 mol/min was fed to the anode. According to the results, pure Pt with 20 wt.% content and metal loading 2.0 mg/cm^2 anode catalyst had a low open-circuit voltage of 0.55 V at 90^oC, while significant drop was observed when the current density was 30mA/cm^2 with power density was 8.1 mW/cm^2. This pattern was indicative of a robust activation control in low current densities, which is characteristic of an ethanol oxidation reaction.

Pure Pt/C anode achieved power density of 10.8 mW/cm^2, at 75 mA/cm^2. It was proved that all Pt_xSn_y catalysts with metal loading of 1.3 mg/cm^2 had open circuit voltage (OCV) above 0.7 V at 90^{o}C. Pt_4Sn_1/C and Pt_3Sn_1/C had power densities of 34.6 mW/cm^2 and 43 mW/cm^2, respectively, at 130 mA/cm^2. Also, Pt_2Sn_1/C had 0.81 V OCV which was as high as Pt_1Sn_1/C. The maximum power density achieved was 61.2 mW/cm^2 at 146 mA/cm^2 current density. When Sn content increased at 40 wt % i.e. when Pt_3Sn_2/C was employed as anode, OCV value was 0.82 V and the cell voltage was 0.68 V (30 mA/cm^2) and 0.59 V (60 mA/cm^2), with peak power density of 55.8 mW/cm^2 at 135.6 mA/cm^2. Also, a peak was observed at Sn 33 wt.% and corresponding atomic ratio PtSn is (2:1). As a result, at 90^{o}C, Pt_2Sn_1/C was demonstrated to be a more suitable anode catalyst for direct ethanol fuel cell. Oliveira Neto et al. in 2007 Neto, et al. [180] demonstrated that the presence of Sn contributed to the development of a more selective catalyst for ethanol oxidation and increased the CO-tolerance of the Pt. In a more recent research, Atbas et al. [181] worked on bimetallic PtSn electrocatalysts at 9:1, 7:3, and 5:5 Pt:Sn atomic ratios, with 10 wt.% Pt content on carbon support. 0.5 M H_2SO_4 was used as an electrolyte and the anode was fed with 1 M EtOH solution. In fact, for the CO oxidation reaction the potential was close to 0.66 V for 10 wt.%Pt-Sn (9:1)/C catalyst, 0.65 V for 10 wt.%Pt-Sn (7:3)/C catalyst and 0.58 V for 10 wt.%Pt-Sn (5:5)/C catalyst. As a matter of fact, 10 wt.%Pt-Sn (7:3)/C catalyst had the lowest onset potential for CO oxidation and the highest anodic current during EOR.

Only high carbon dioxide yields enabled the achievement of practical DEFC efficiency because it provided 12 electrons per each ethanol molecule which was the higher rate than any other EOR product [182]. However, almost exclusively acetaldehyde and acetic acid were produced when ethanol was electro-oxidized on Pt-Sn bimetallic catalysts, which resulted in a lower efficiency for the generation of electrical energy [183]. Platinum active sites were reduced or alcohols were less effectively adsorbed onto the Pt surface when the Sn content was too high [184]. After extensive research on the appropriate Pt:Sn ratio, the optimal ratio at 90^{o}C was found to be 2:1 Pt_2Sn_1 (33 wt.% Sn).

Pt-Ru based catalysts

During the examination of the ethanol oxidation, Schmidt et al. [185] observed that Ru partly inhibited the development of chemisorbed species derived from dissolved ethanol. The selectivity for the formation of ethanol was observed to be higher than that for single Pt because this promoted the oxidation route through weakly adsorbed compounds [186]. Calegaro et al. [187] proved that Ru content of less than 20 wt.% had no effect on ethanol oxidation current and

the maximum enhancement was observed at about 37-40% Ru concentration. This probably happened due to the two opposite phenomena occurring in the presence of Ru; the promotion of CO oxidation and the ethanol adsorption inhibition, which appeared to have unfavourable effects. Optimum atomic ratio Pt:Ru was proven to be 3:2. Lima et al. in 2008 [188], fabricated Pt, PtRu and PtRh composites deposited on Vulcan XC-72R, as anode electrocatalysts with Nafion membrane and 20 wt.% content and 6.0 mg/cm^2 loading. The anode was fed with 0.5 M EtOH solution and 0.1 M $HClO_4$ solution used as electrolyte. The electrochemical results showed that materials containing Ru had lower overpotential, which suggests that CO oxidation occurred more rapidly. This was accounted on the availability of O or OH groups for the coupling with CO species absorbed upon Pt loading, leading to the creation of CO_2. As a result of the presence of Ru, which boosted electrocatalytic activity, a substantial amount of double layer charging current was also found. Additionally, it was established that Ru resulted in low overpotential on CO_2 production and other oxygenated intermediates, which promotes higher current densities but poor reaction efficiency. In general, the measurements showed that Pt_3Ru_2 had the best performance (37-40% Ru content), while for over 40% Ru the current decreased.

Pt-Rh based catalysts

An identical experiment was conducted by Lima et al. [188]. The authors concluded that Rh on bimetallic PtRh alloy was connected to an inherent electrocatalytic characteristic rather than to the primarily supplying oxygen for CO bonding. Electrochemical results showed that PtRh exhibited superior ethanol oxidation catalytic performance over pure Pt while it had also better performance than PtRu at lower overpotential.

Rhodium addition generally leads to easier C-C bond breakage and increased CO_2 generation, but it has no effect on raising the barrier to CO oxidation. Rh is detrimental to the electrocatalytic activity of the binary electrodes even if the generation of CO_2 is proportionately larger in the presence of Rh. This is seen by the fact that the currents of ethanol oxidation consistently fall with increasing levels of Rh most likely as a result of the sluggish kinetics of ethanol's adsorption on Rh. Silva-Junior et al. [189], investigated binary PtRh catalysts with Nafion membrane and 0.1 mol/dm^3 EtOH solution and 0.1 mol/dm^3 HCl_4 over Vulcan XC-72R support, with 60 wt.% Pt metal loading. The results showed that $Pt_{91}Rh_{09}$/C had an ethanol oxidation peak at 0.35 V and reached first peak current density at 0.82 V followed by a reduction up to 1.03 V and after that the power density grew at 1.25 V. On the other hand, $Pt_{28}Rh_{72}$/C had a peak at 0.7 V and less intense current density. As a conclusion, researchers observed that for 33 wt.% or richer content of Rh, no detectable activation current appeared.

Later, in 2017 Wang et al. [190], synthesized a PtRu nanostructured catalyst with TiO_2-C hybrid support material. The investigated catalysts were Pt/TiO_2-C, Rh/TiO_2-C, Pt/C, Pt_9Rh/C and Pt_9Ru/TiO_2-C, with 20 wt.% Pt metal loading and 200 mg TiO_2-C powders as support materials. Experiment was carried out in 0.1 mol/l $HClO_4$ and 1.0 mol/l C_2H_5OH. In **Figure 28a**, it becomes clear that Rh/TiO_2-C has extremely low EOR activity. The peak current densities for Pt_9Ru/TiO_2-C, Pt_9Rh/C, Pt/TiO_2-C and Pt/C were 1039.5, 427.2, 261.3, and 125.1 mA/mg_{Pt}, respectively. As seen, Pt_9Ru/TiO_2-C clearly exhibited the highest catalytic activity for ethanol oxidation. Also, it was proven that Pt_9Ru/TiO_2-C had the most negative EOR potential indicating that it had greater dynamic activity than the other materials. Furthermore, Pt_9Ru/TiO_2-C had higher activity than Pt_9Rh/C which means that TiO_2-C provided better catalyst support for EOR than pure C. The findings suggest that Rh and TiO_2 may encourage relatively low oxidation of CO-like intermediates and assist the breaking of the C-C bond in ethanol. All things considered, Pt_9Rh/TiO_2-C provides an appealing anode material for highly efficient direct ethanol fuel cells. The research proved that $Pt_{91}Rh_{09}$ had better performance but still worse than PtRu performance. Moreover, Pt_9Rh/TiO_2 catalyst seems appealing for anode material and had better activity than PtRh.

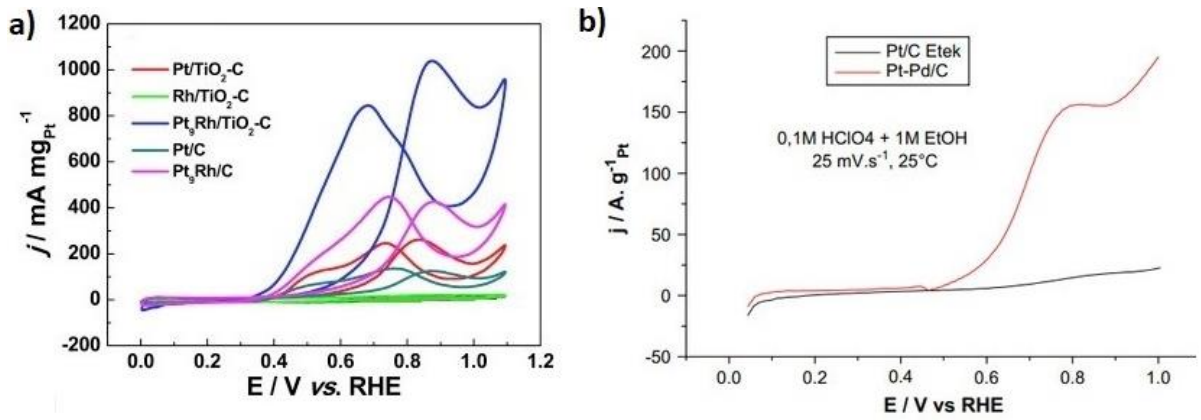

Figure 28. a) The linear scan curves of the as-prepared catalysts in N_2-purged 0.1 mol/L HClO4 and 1.0 mol/L C_2H_5OH aqueous solution at 25°C, scan rate 2 mV/s [190] b) Comparison of the anode characteristics for the oxidation of 1 M ethanol in 0.1 M $HClO_4$ on PtPd/C and Pt/C electrodes at 25°C and scan rate of 25 mV/s [191].

Pt-Ni based catalysts

The activity of Pt electrocatalysts is reported to increase with the inclusion of Ni as the second or third ingredient. The reduction of EOR's potential is the main benefit while also it increases the current density [192].

Altarawneh et al. [193] synthesized a PtNi alloy with 30% mass metal and 0.4 mg/cm^2 metal loading at 80^{o}C and made a comparison with pure Pt/C electrocatalyst. The membrane used was Nafion 115 and Vulcan XC-72R as support. The electrolyte was H_2SO_4 at 1.0 M and the anode fed with 1 M ethanol at flow rate of 0.2 ml/min. The electrochemical results showed that the currents at the PtNi/C anodes were not as high as Pt/C at potentials up to 0.45 V, but were considerably lower at greater potentials and also had similar onset potentials for ethanol oxidation, with slightly higher currents at PtNi/C up to 0.4 V. Investigators concluded that the selectivity for complete EOR to CO_2 - for breaking the C-C bond of ethanol to produce CO_2- was significantly better on PtNi catalysts and this led to a higher number of exchanged electrons, resulted in an improvement of the overall process efficiency [184]. Furthermore, they noticed that according to in situ infrared spectroscopy, the toxic effects of CO_{ad} was much lower at PtNi/C compared to Pt/C. Chelaghmia et al. [178], also carried out a three-electrode experiment on PtNi catalysts with 0.1 M H_2SO_4 and 1 M of ethanol and concluded to the fact that the current density of the two oxidation peaks recorded on Pt–Ni/C are higher than that on the Pt/C (1.5 times higher) as shown in **Figure 29a.** The presence of Ni makes it easier for newly chemisorbed species to oxidize and acts as an anti-poison site by accelerating CO oxidation at lower potentials.

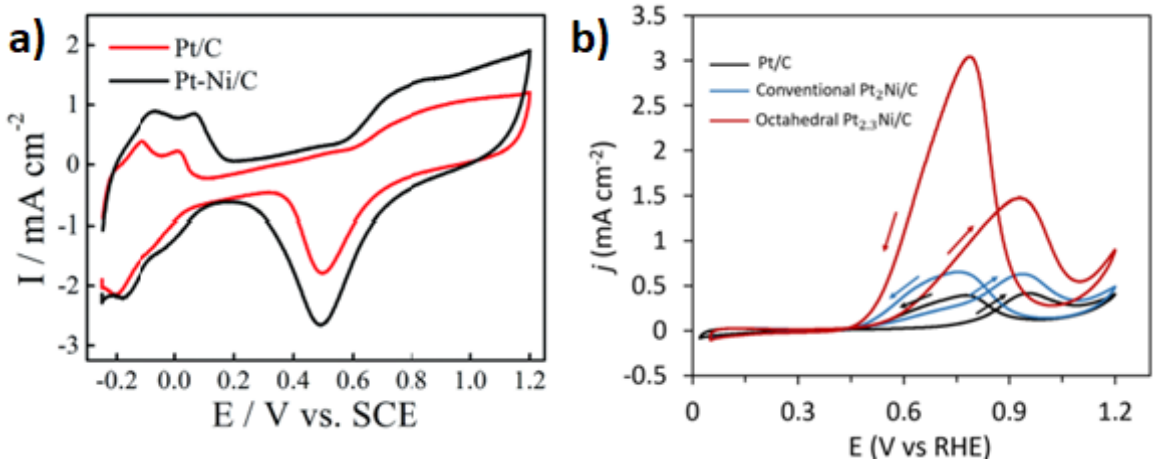

Figure 29. a) CVs of Pt–Ni/C and Pt/C electrocatalysts in 0.1 M H_2SO_4 solution at a scan rate of 50 mV/s and 298 K. The inset is the CV of smooth Pt electrode in 1.0 M H_2SO_4 solution [178] b) CVs of the Pt/C (black line), conventional Pt_2Ni/C (blue line), and octahedral $Pt_{2.3}Ni/C$ electrocatalyst (red line) in an Ar-saturated 0.2 M ethanol + 0.1 M $HClO_4$ solution at a scan rate of 50 mV/s [178].

Sulaiman et al. [194], fabricated PtNi nanocatalysts with atomic ratios 2:1 (conventional) and 2.3:1 (octahedral) (Pt:Ni) and compared them with pure Pt/C catalyst. The electrochemical

results came from a three-electrode experiment with 0.1 M $HClO_4$ electrolyte, 0.2 M C_2H_5OH ethanol supply and 18 wt.% Pt metal loading. As it is obvious from **Figure 29b,** all catalysts have a similar forward peak current potential around 0.9 V. The peak current density of octahedral $Pt_{2.3}Ni/C$ (1.46 mA/cm^2) was 2.4 and 3.7 times higher than that of conventional Pt_2Ni/C (0.62 mA/cm^2) and Pt/C (0.39 mA/cm^2), suggesting that both the octahedral form and alloying action would enhance the electrocatalytic action towards the EOR. $Pt_{2.3}Ni/C$ showed the best catalytic activity compared to the other electrocatalyst and due to its increased affinity for C_2 reaction pathways, it severely decreased the challenge of CO-poisoning.

Pt-Pd based catalysts

Kadirgan et al. [191], fabricated PtPd nano-sized alloys and used Pt/C (20% ETEK) for comparison. Electrocatalysts were prepared at 1:1 atomic ratio and 30% total metal in weight of catalyst, while Vulcan XC-72R was used as support, 0.1 M $HClO_4$ as electrolyte and 1.0 M of ethanol solution as anode feed. According to the measurements, PtPt/C showed improvement in CO-tolerance and oxidation current densities of ethanol on Pt–Pd/C two or threefold compared to that of pure Pt (Pt/C ETEK). Pt/C electrode is shown in **Figure 28b**. The greater electrochemical surface area and the synergistic interaction between Pt and Pd were considered to be responsible for the significant increment in the catalytic activity for ethanol oxidation compared to Pt/C. These effects may be interpreted as electronic effects where the presence of Pd resulted in a change in the electronic density of state of platinum, weakening the CO-Pt bond or increasing the overall reaction rate by reducing electrode poisoning.

Another research on PtPd electrocatalysts was made by Zheng et al. [195], who fabricated PtPd nanocubes (NCs) deposited on reduced graphene oxide (RGO) support, with atomic ratio 1:5 (Pt_1Pd_5). The electrolyte used was 0.5 M H_2SO_4 with 0.5 M EtOH. The RGO-supported alloy hybrid showed superior EOR activity with specific activity of 2.31 mA/cm^2 at 0.6 V, which was comparable to (or better than) the state-of-the-art Pt-based EOR catalysts as seen in **Table 2** in acid solution. Moreover, these catalysts had high CO-tolerance without current decay during steady-state polarization at 0.6 V. With just 8.9% loss of electrochemical surface area (ECSA) after 10,000 cycles of voltametric testing, their longevity was impressive.

Table 2. Comparison of EOR performance in acidic media for RGO-supported PtPd NCs with recently reported literature [195]

Samples	Electrolyte	Scan rate (mV/s)	Specific activity (mA/cm^2)	Mass activity
PtPd NPs	0.5 M H_2SO_4 + 0.5 M C_2H_5OH	50	1.12	0.49 A/mg_{Pt}
Pt_1Pd_5 NC/RGO	0.5 M H_2SO_4 + 0.5 M C_2H_5OH	50	2.31	1.08 A/mg_{Pt}

Liu et al. [196], investigated PtPd alloy foam films with Nafion membrane, in 0.5 M H_2SO_4 electrolyte and 0.5 M C_2H_5OH ethanol supply. The results indicate that all PtPd alloy foams show increased catalytic activity towards ethanol oxidation when compared to the pure porous Pt film electrode, as shown in **Figure 30**. Pt_1Pd_1 performed the best among the foam electrodes, offering peak current densities (about 0.3 V) and sustained current densities (around 0.1V) that were almost 2.5 times greater than those on the porous Pt film.

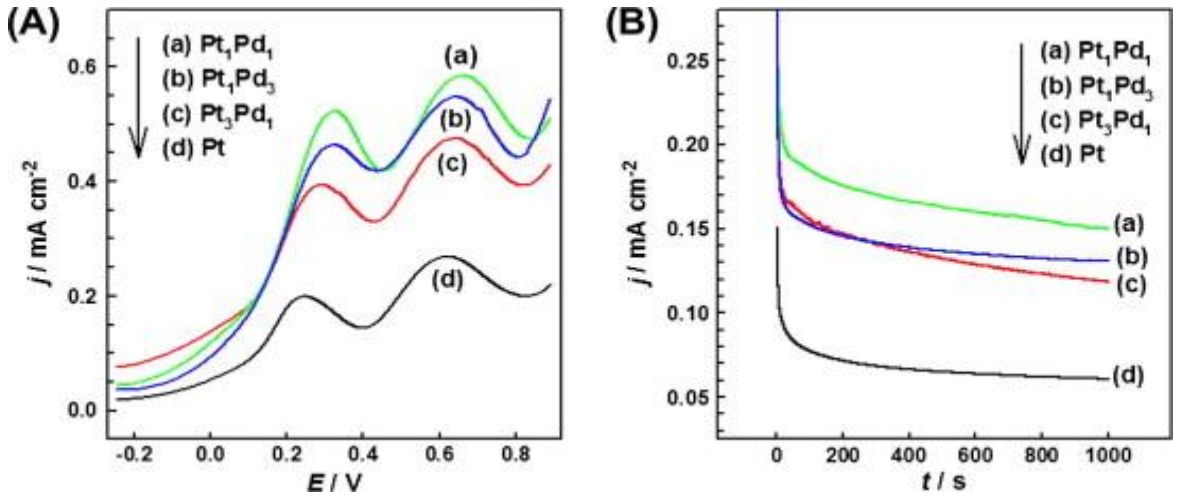

Figure 30. a) Linear sweep voltammetry (from the third cycle of CVs) at 50 mV s^{-1} and b) chronoamperometric curves at 0.1 V for the prepared foam films as denoted in 0.5 M H_2SO_4 + 0.5 M ethanol [196].

4.2.1.3 Platinum Trimetallic (Ternary) Alloys

Pt-Ru based catalysts

The leaching of the less noble metal from the alloy surface is one of the main issues with bimetallic platinum alloy-based catalysts in an acidic environment. The insertion of another metallic element can eliminate a situation like this [197]. It has been proved that Pt catalysts with Ru addition provide a good performance on ethanol oxidation however; further research shows that the addition of another metal to PtRu/C catalysts offers better results, facilitating the breaking

of the C-C bond. In 2003, Tsiakaras et al. [198], studied the effect of ethanol oxidation on many Pt based catalysts, binary and ternary. Trimetallic Pt-based catalysts were, PtRuMo/C and PtRuW/C at 90 °C using as solid electrolyte Nafion 115 membrane, providing on the anode 1.0 mol/l of ethanol aqueous solution while the catalyst used on cathode was Pt/C of 1 mgPt/cm^2. For PtRuW/C, an OCV of 698 mV was achieved, using a current density at 60 mA/cm^2, the output voltage (OV) was 425 mV, and the maximum power density reached was 38.54 mW/cm^2 at 142 mA/cm^2 with OV at 680 mV. As for PtRuMo, it was achieved an OCV of 720 mV, with an OV of 389 mV at current density 60 mA/cm^2, while the maximum power density reached was 31.10 mW/cm^2 at 120.5 mA/cm^2 providing an OV of 570 mV. According to the results, both W and Mo enhanced the cell performance. However, PtRuW showed better activity than PtRuMo. Tanaka et al. [199], using a co-shuttering method that puts an Au layer on Pt based bimetallic and ternary catalysts, proved that PtRuW/C achieved higher performance than bi-metallic catalysts, achieving a stabilization at around 30 minutes of operation and on the 35% of the starting value. In 2006, Guanchun Li and Pickup [200], investigated the effect of Pb on a PtRu/C catalyst, at low potential of 0.5 V PtRuPb/C the highest catalytic activity was achieved, which was similar and a bit lower to PtSn/C, comparing with PtRu, PtPb and Pt catalyst. On higher potential over 0.5 V the performance of PtRuPb/C was poor, around 2 mA/cm^2 at 0.8 V. An important fact is that this catalyst showed the highest current density 0.7 mA/cm^2 at 30 minutes of operation, compared with PtM-(M=Sn, Ru, Pb) and Pt catalysts. Spinacé et al. [201] also hosted an experiment of ethanol electro-oxidation by PtSn/C, PtRh/C, and PtSnRh/C catalysts containing 20 wt.% metal loading. They observed an increase in catalytic activity in the ternary catalyst PtSnRh/C with atomic ratio 50:40:10 which demonstrated that the addition of Rh as a third element enhanced the catalytic activity of ethanol oxidation. E.M.Cunha et al. [202] prepared a PtRuSn catalyst using the Pechini method, which refers to the decomposition of polymeric precursor (DPP), prepared a PtRuSn catalyst. The temperature of the carbon treatment was 400°C under N_2. The results showed that this method is very capable of easily and successfully preparing catalysts. The addition of Ru and Sn increased ethanol oxidation and the onset potential was measured at 0.2 V, while the highest performance ~~was~~ measured was 48 mA/mg$_{Pt}$ at 1.0 V. $Pt_{0.8}Ru_{0.1}Sn_{0.1}$ proved to have the highest electrocatalytic activity compared with other ratios of the same catalyst and also PtSn, PtRu and Pt in hydrogen atmosphere.

Jarupuk et al. [203] constructed a PtRuSn catalyst in a nonionic surfactant's lyotropic liquid phase in an aqueous environment. Gonzalo García et al. [204] investigated PtRuMo/C catalysts. The results showed

that active sites are replaced in a fast way, such that more acetaldehyde and acetic acid was produced, which were responsible for higher ethanol oxidation. The loading of PtRu was 30% supported on Vulcan XC 72R, using the colloidal method, and Mo's load on the PtRu was, 0, 1 and 3 wt.%. The catalytic activity, comparing the 3 different Mo loadings, was respectively: 0% similar to 1% < 3%. Nobuyoshi Nakagawa et al. [205], followed an impregnation method to prepare a PtRuRh/C using the nitrates of Pt, Ru and Rh and exposed it to a mixed H_2 15% and N_2 85% environment, generating an overall current three times higher than PtRu/C and Pt/C. Furthermore, the durability and the onset potential of PtRuRh were also higher than the other two catalysts. The addition of Rh to PtRu had an obvious positive impact on ethanol oxidation, that was proved by comparing the current densities at 1 V. It appeared to be 1.5 times higher than PtRu and pure Pt. At very low potentials (< 0.3 V), PtRuMo/C catalysts displayed a high CO tolerance, and there was little to no CO poisoning of the Pt and Ru surfaces. Additionally, Antolini et al. [206] reported that hydrogen spillover effect was responsible for the high ethanol oxidation on PtRuNi.

In 2020, Choudhary et al. [207] conducted a research on Pt electrocatalysts doped with rhenium (Re) on functionalized multi-walled carbon nanotubes (f-MWCNT) for the electrooxidation of ethanol in a single DEFC and a half cell in acidic medium. Carbon nanotubes (CNTs) as an electrocatalyst support material have recently attracted significant attention in low-temperature fuel cell applications due to their unique properties, such as crystalline structures with high electrical conductivity, excellent chemical and electrochemical stability, and large specific surface area, when compared to conventional carbon black powder [207]. In this experiment (carried out at 80°C) Nafion 117 used as polymer electrolyte membrane. CVs measurements were recorded in 2 M ethanol mixed with 0.5 M $HClO_4$ and electrocatalysts loading at 1 mg/cm^2 and they are displayed in **Table 3**.

Table 3. Summary of electrocatalytic performance of electrocatalysts towards ethanol electrooxidation (E_f: forward oxidation peak potential, I_f: forward current density, E_b: backward oxidation peak potential, I_b: backward current density) [207].

Electrocatalysts	Onset potential (V)	E_f (V)	I_f (mA/cm^2)	E_b (V)	I_b (mA/cm^2)
Pt-Ru (1:1)/f-MWCNT	0.30	0.794	48.76	0.610	35.665
Pt-Re(1:1)/f-MWCNT	0.28	0.798	23.60	0.598	16.234
Pt-Ru-Re(1:1:1)/f-MWCNT	0.15	0.8082	65.460	0.5128	41.791
Pt-Ru-Re(1:1:0.5)/f-MWCNT	0.10	0.7814	83.34	0.5592	65.53
Pt-Ru-Re(1:1:0.25)/f-MWCNT	0.25	0.7849	57.94	0.570	38.96

In the trimetallic electrocatalyst Pt-Ru-Re (1:1:0.5)/f-MWCNT, the addition of rhenium (Re) dramatically lowered the onset potential by 0.2 V and raised the current density at 83.34mA/cm^2 which was the highest peak. Due to the synergistic effects of components and the good conductive f-MWCNT support, Pt-RuRe (1:1:0.5)/f-MWCNT electrocatalysts had the highest electrocatalytic activity among produced electrocatalysts. The single cell experiment was hosted with 0.5 M H_2SO_4 and the anode was fed with 2 M ethanol at flow rate of 1.2 ml/min, with 40 wt.% Pt on the catalysts and 1.0 mg/cm^2 metal loading. The cathode was fed with humidified oxygen at flow rate of 60 ml/min. The results (**Table 4**)**,** indicate that when using trimetallic Pt-RuRe (1:1:0.5)/f-MWCNT electrocatalysts as anode, it improves the DEFC cell performance compared to bimetallic Pt-Re (1:1)/f-MWCNT, Pt-Ru (1:1)/f-MWCNT and other trimetallic Pt-Ru-Re(1:1:0.25)/f-MWCNT and Pt-Ru-Re(1:1:1)/f-MWCNT electrocatalysts. Pt-Ru-Re (1:1:0.5)/f-MWCNT had the maximum power density of 9.52 mW/cm^2 at a current density of 38.4 mA/cm^2. The appropriate amount of Re increased significantly the cells' performance, activity, and durability while the higher percentage stopped intermediates from being further oxidized, which had a negative impact on how well the cell was functioning. Further information provided for temperature operation of DEFC at 80^{o}C, showed that Pt-Ru-Re (1:1:0.5)/f-MWCNT achieved OCV 0.744 V, maximum power density of 23.2 mW/cm^2 and current density at maximum power density of 83.34 mA/cm^2.

Table 4. Summary of performance of different anode electrocatalysts in single cell DEFC tests for 2 M ethanol at a cell temperature of 30^{o}C [207]

Anode electrocatalyst	OCV (V)	Maximum power Density (mW/cm^2)	Current density at maximum power density (mA/cm^2)
Pt-Re (1:1)/f-MWCNT	0.542	4.74	22.56
Pt-Ru (1:1)/f-MWCNT	0.683	7.48	30.40
Pt-Ru-Re (1:1:1)/f-MWCNT	0.70	8.8	35.20
Pt-Ru-Re (1:1:0.5)/f-MWCNT	0.708	9.52	38.40
Pt-Ru-Re (1:1:0.25)/f-MWCNT	0.688	8.13	33.60

Pt-Sn based catalysts

Spinacé et al. [208] prepared PtSnNi/C of 50:40:10 atomic ratio using an alcohol reduction method [209]. The performance of this catalyst was higher than PtSn/C for values between 0.1-0.9 V, while stability was also higher than PtSn/C throughout the potential range, which was attributed to the presence of tin and SnO_2. Beyhan et al. [210] used the Bönnemann method to observe PtSnNi/C. The addition of Ni aided on the break of C-C bond while it also changed the lattice of the total catalyst which favored higher activity and current density values. PtSnNi/C and PtSn/C performed giving a much higher current density than PtNi/C and Pt/C and ethanol oxidation begun at around

0.2 V. The OCV was 760 mV, while the current density of 159.6 mA/cm^2 with a power density of 47 mW/cm^2. Almeida et al. [211], confirmed that Ni addition on the catalyst is beneficial for ethanol oxidation comparing many PtSnM catalysts such as, M=Ni, Ru, Rh, Pd, W using the decomposition of polymeric precursor method. Among all the catalysts, PtSnNi achieved promising overall performance. It had the highest mass activity current at 3.5 A/g_{Pt} while for the others it was under 0.8 A/$g_{Pt,}$ and the highest power density at 46 mW/cm^2 while, besides $Pt_{82}Sn_{09}Ni_{11}$, PtSn was greater than all the other ternary metals as it is shown in **Figure 31a**. On the other hand, PtSnRu presented the highest lifetime of 35 h, which was probably caused due to Ru oxides formations, while PtSnNi lasted 25h. The worst durability was on PtSnW which lasted 10 min.

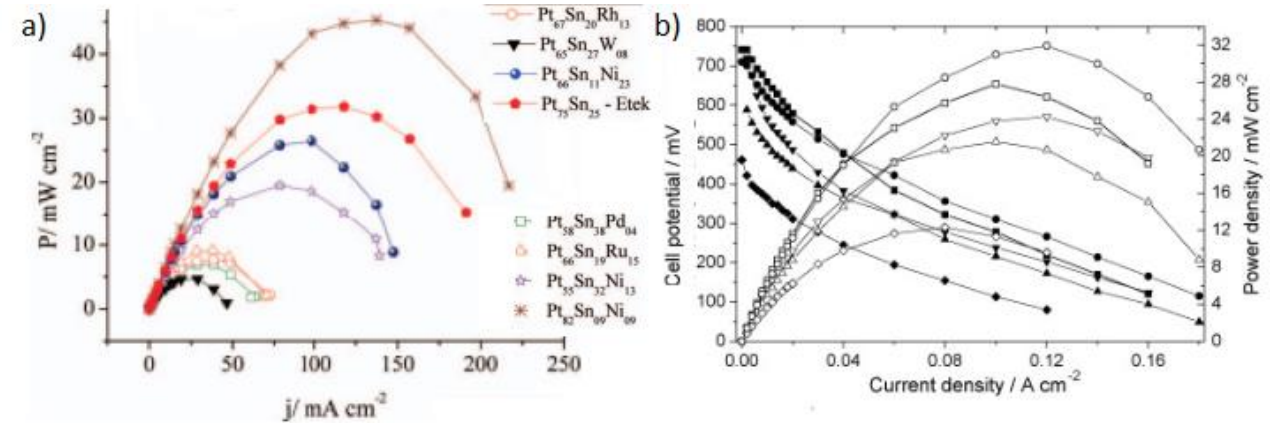

Figure 31. a) Power density vs Current density [211], at T_{PEMFC} = 80°C, for PtSnM (M=Pd,Ru,Ni,Rh,W) in different atomic ratios, at 1 M ethanol, O_2 pressure at 3 bar, cathode: Pt_3Sn E-TEK 2 mg_{Pt} cm^{-2}, electrolyte: Nafion 117 membrane. b) Representation of polarization curves [212], for different atomic ratios of PtSn and PtSnRu. Preparation of catalyst was at 110°C, pressure 3 atm O_2, 1 M of Ethanol Solution. Cathode catalyst was Pt/C. (□) PtSn/C 1:1, (Δ) PtSnRu 1:1;1, (○) PtSnRu 1:1:0.3, (∇) PtRu/C E-TEK 1:1, (◊) Pt/C E-TEK [211, 212].

Rousseau et al. [212] studied the effect of Ru on PtSn using the Bönnemann method. Stability was at a very good level as it remained steady at around 0.6V for 230 min. The addition of Ru offered higher performance and activity values than pure PtSn, while the remarkable point is that production of acetic acid increased opposite to CO_2 and AAI where the formation decreased. Antolini et al. [213] employed the method of formic acid to reduce metallic precursors. In three examinations at room temperature, 40°C and 90°C, PtSnRu/C (1:1:0.3) achieved the highest activity and this result was attributed to the reaction of Sn with Ru oxides as well as to the small particle sizes. The results of different ratios of PtSnRu and PtSn are shown in **Figure 31b**.

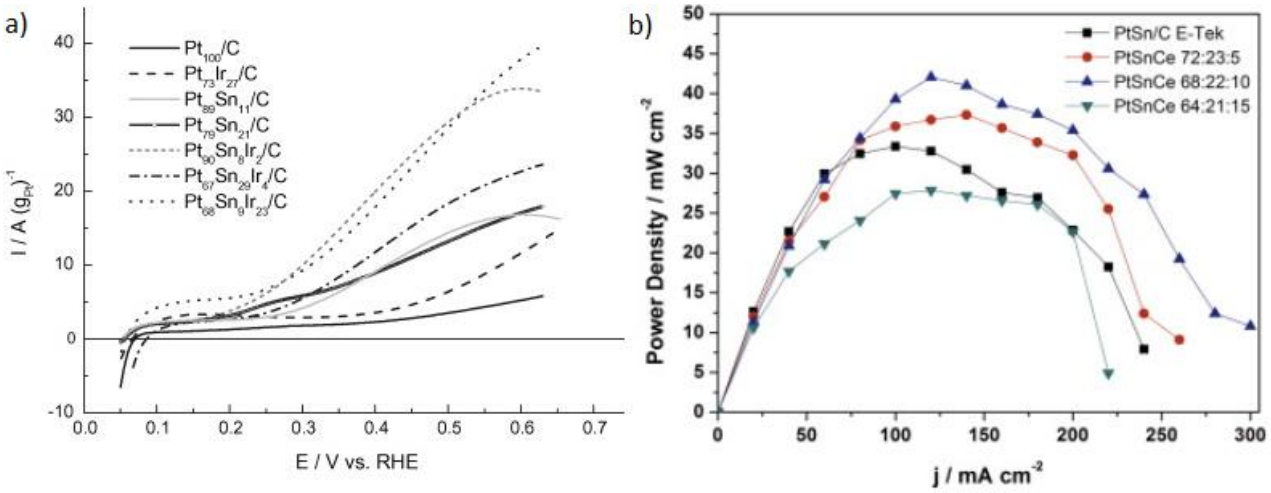

Figure 32. a) Presentation of cyclic voltammetry normalized by Pt loading, (dot line) $Pt_{68}Sn_9Ir_{23}$, (grey dashed line) $Pt_{90}Sn_8Ir_2$, only anodic curve, for different ratios of PtSnIr and PtSn on 40% of metal loading on, 0.5mol/dm^3 H_2SO_4, 1 mol/dm^3 Ethanol electrolyte at 20 mV/s. b) Power density curve of PtSnCe and PtSn using 2 wt.% metal loading, and 20 wt.%, 1mg$_{Pt}$/cm^2 cathode Pt/C E-TEK, electrolyte: Nafion® 117 membrane, 2 M ethanol supply and 2 mL/s flux [214, 215].

In 2007, Ribeiro et al [214], investigated the effect of PtSnIr/C catalyst. The addition of Ir to this catalyst resulted in better electrocatalytic activity than Pt/C. **Figure 32a** shows the onset potentials for different PtSnIr catalysts, where the best performances were achieved at small ratios of Sn 8–9 %, while the different values of Ir ratio didn't show much effect on the performance. Ribeiro et al. [216] studied the effect of PtSnW following the Pechini method which refers to the decomposition of precursor (DPP). Operation temperature was at 90°C where the onset potential started around 0.2 V, and a legand effect seems to be the main cause for this activation potential. Elson A.de Souza et al. [217] studied the PtSnRh/C catalyst in different ratios. The oxidation onset potential was lower than PtSn and higher than PtRh, PtRh< PtSnRh< PtSn. The best ratio of Rh ratio proved to be a $Pt_{0.8}Sn_{0.8}Rh_{0.2}$ performing a peak potential at 1.0 V around 70 mA/cm^2. CO_2 was produced mostly on PtSnRh, which seems to be the result of the addition of Rh which promoted C-C breaking bond giving an anodic route to CO formation, while Sn assisted the ethanol oxidation. Comparing the ratio of CO_2/CH_3COOH vs potential, PtSnRh showed a value of 0 to 0.3 on a scale of 0 to 0.9 V, where the peak ratio was 0.3 at around 0.7 V. Corradini et al. [218] showed that PtSnPr/C accelerated mass activity and stability, compared to the PtPr catalyst. The increase of these values was due to either the increased active area or specific activity. Souza et al. [215] using a polymeric precursor preparation proved that, Ce addition on PtSn had a remarkable performance and CO absorption. The best ratio was PtSnCe (68:22:10) where CO presence was reduced by 50% compared to PtSn, while it also fully oxidized CO at around 0.6 V. Peak power density reached the 43 mW/cm^2 (**Figure 32b**). This catalyst was producing 4 electrons and mostly acetic acid in comparison with the common catalysts that produce 2 electrons and mostly acetaldehyde. Juliana M.Jacob et al. [219] using a formic acid preparation for PtSnCe, showed that

ethanol oxidation occurred in two separate ways depending on the Ce/Sn factor which fell between 0.2 and 0.9.

J. Ribeiro and M. Ribeiro [220] constructed and compared PtSnTa. The addition of Ta increased the ethanol oxidation values more than pure Pt as Ta gave more oxygen that promotes EOR, which further supported the creation of new active sites that enhanced catalytic activity. PtSnTa lasted about 5 min on the high current value around 18 A/g_{Pt} while in the it steadily dropped at 6 $A/g_{Pt.}$ in the next 2 h. The onset potential reached 1.17 V at 2 M of ethanol and 0.5 M H_2SO_4 which is a good value compared with the ethanol oxidation potential around 1.15 V, while the peak power density was about 27 mW/cm^2. J.Perez et al. [221], observed that PtSnLa/C, which belongs to the rare Earth materials, prepared with polyol method had similar characteristics with PtSn/C. The CO oxidation was better than Pt/C which implying that La promoted oxidation procedure. Comparing power densities, PtSnLa didn't achieve a high value of 10 mW/cm^2 but it was higher than pure Pt. Catalytic activity was also higher than Pt after 2800 s, Pt/C current reached close to zero, while PtSnLa remained steady at 0.5 mA/cm^2. The products were mostly AA and AL and a bare amount of CO_2. EungjeLee et al. [222] synthesized PtSnMo on 60% of carbon support. Cyclic voltammetry showed that $PtSnM_{0.6}$ had the highest mass activity of 80 A/g_{Pt} while the onset potential was at 0.2 V compared to the $PtSnMo_{0.4}$, PtSn and Pt. Regarding the stability, $PtSnMo_{0.6}$ had a significantly better single cell performance on applied potential of 0.5 V in 0.5 M of H_2SO_4 and 1 M of ethanol at temperatures of 65°C and 90°C, while the peak power density reached the highest value of all catalysts at 25.7 W/cm^2 at 90°C. RubénRizo et al. [223] tested a PtSnCo nanocube with atomic ratio (48:51:1). Ethanol oxidation PtSnCo started at a low potential of 0.3 V that was lower than that of the PtSn nanocube. Chronoamperometry measurements showed that it can handle CO poisoning, where at 0.5 V of applied potential, there was an in initial drop in the first 300 s which remained steady at a current density of 30 mA/mg_{Pt}, a value that was superior compared to the Pt's current density.

4.2.1.4 Platinum oxide-based catalysts

An unconventional proposal on anode catalysts for direct ethanol fuel cells in acidic medium was made by Suffredini et al. Suffredini, et al. [224], introducing for the first time deposition of lead oxide-based catalyst on carbon powder. The anodes employed in this study contained Pt, Ru, Ir and Pd and carbon with 10% of catalyst loading, all compared to Pt/C commercial catalyst. Nafion was used as membrane, H_2SO_4 as support electrolyte 0.5 mol/l and ethanol feed at 1.0 mol/l. The alloys had the following mass ratios: Pt:Ru (50:50), Pt:Ir (50:50), Pt:Pb (50:50), Pt:Ru:Ir (50:25:25), Pt:Ru:Pb (50:25:25). Electrochemical results showed that, in the presence of ethanol, current densities were higher for Pt-PbO_x/C, Pt-(RuO_2-IrO_2)/C (178mV) and Pt-(RuO_2-PbO_x)/C (155 mV) which indicated good performance to

promote EOR, while Pt-(IrO_2-PbO_x)/C (467 mV) had the lowest value. Furthermore, it was observed that EOR has onset potentials around 150-200mV in all catalysts except for Pt-(IrO_2-PbO_x) whose onset potential reached 500mV. Therefore, it appeared that IrO_2 and PbO_x do not operate effectively combined, as evidenced by the non-synergic behaviour of the catalytic activity for ethanol oxidation. The catalysts Pt-(RuO_2-PbO_x), Pt-(RuO_2-IrO_2), Pt-PbO_x/C, Pt-RuO_2/C and Pt-IrO_2 exhibited significantly enhanced catalytic activity for the ethanol oxidation (determined by increased current activity and decreased positive reaction onset potentials) relative to the observations on a Pt commercial catalyst. In fact, the preparation of materials with high catalytic activity for direct ethanol fuel cell systems with the addition the metallic oxides to Pt, proved to be a highly intriguing method. Hence, the use of this lead oxides combination (PbO_x) highlights the necessity of their use in the research on alcohols' oxidation, as the catalyst containing lead oxide demonstrated the greatest performance among the binary catalysts. The final rating for EOR catalytic activity was: Pt-(RuO_2-PbO_x)/C ≥ Pt-(RuO_2-IrO_2)/C > Pt-PbO_x/C > Pt-IrO_2/C > Pt-RuO_2/C > Pt-(IrO_2-PbO_x)/C > Pt/C. It has been shown by Li et al. [225] that, using ternary PtRhSnO_2/C electrocatalysts with atomic ratio Pt:Rh:Sn=3:1:4, created by depositing Pt and Rh atoms on carbon-supported tin oxide nanoparticles, may cause EtOH to be immediately converted into CO_2 in an acidic medium. Furthermore, according to Comignani et al. Comignani, et al. [226], on the investigation of NiO oxide, the results of CO stripping studies showed that the removal of CO on Pt-NiO/C electrodes is substantially simpler than that on Pt/C catalyst, indicating that the bifunctional process is facilitated by the proximity of Pt and NiO particles.

Zignani et al. [227] investigated the behavior of metal oxides TiO_2 and SnO_2, on the PtRu catalyst. TiO_2 at a 50% percent loading on the PtRu showed three times higher electrochemical ethanol oxidation than pure PtRu. Almeida et al. [228], recently reported that the use of iron oxides, as support, exhibit exceptional activity during the oxidation of ethanol, indicating that transition metal oxides might be a feasible substitute for oxidizing fuels. The measurements showed that γ-Fe_2O_3-C had exceptional effect on Pt an PtSn catalysts. These oxides are inexpensive in comparison to other metal oxides, and they have high surface, electropositivity and porosity which are excellent physiochemical properties [228].

The best performances have been given by Pt-(RuO_2-PbO_x)/C and PtRhSnO_2/C (with atomic ratio Pt:Rh:Sn=3:1:4), while TiO_2 and γ-Fe_2O_3-C also had significant impact on the catalyst's activity towards ethanol oxidation. For the second catalyst it was proven that the capacity to cleave the C-C bond in ethanol at room temperature as well as the lowest positive reaction initiation potential are two of its main characteristics. A reduction in activity was caused by both an excessively low and high tin concentration.

4.2.1.5 Other PGM-based catalysts

Ir-Sn based catalysts

Pt and Ir have comparable features including sharing the same period and block (6d) of the periodic table, the same fcc crystal structure, and similar masses and atomic sizes. Iridium, however, costs around 60% less than platinum, making it a suitable substitute for Pt as a catalyst in fuel cells and is also resistant to decomposition in acidic media [229]. Cao et al. [230] fabricated Ir_3Sn/C and Ir/C catalysts comparing their electrocatalytic activities with Pt/C and Pt_3Sn/C in a single cell test at 90°C. 1 M ethanol was prepared and Nafion 115 was used as polymer electrolyte membrane. Anode contained 20 wt.% Ir/C, Ir_3Sn/C, Pt_3Sn/C or Pt/C electrocatalyst while the metal loading was of 1.5 mg/cm^2 and fed with 1 M EtOH solution. Cathode contained 40 wt.% Pt/ C electrocatalyst with a Pt loading of 1.0 mg/cm^2 and was fed with dry oxygen of 0.2 MPa. **Figure 33a** depicts that, when Ir/C was used as the anode catalyst for DEFC, the OCV is around 0.77 V, which is significantly higher than the OCV when Pt/C was used as the anode catalyst and showed that Ir/C has better catalytic activity. Tin was added to Ir/C to accelerate the OCV to around 0.82 V, which was about the same as that of Pt_3Sn/C. Additionally, it was observed that the Ir_3Sn/C cell performed better than the Pt_3Sn/C cell when the current is low, namely in the activation area. Although the performance of Pt_3Sn/C started to outperform Ir_3Sn/C when the current value was increased, the two catalysts' overall performances were equivalent.

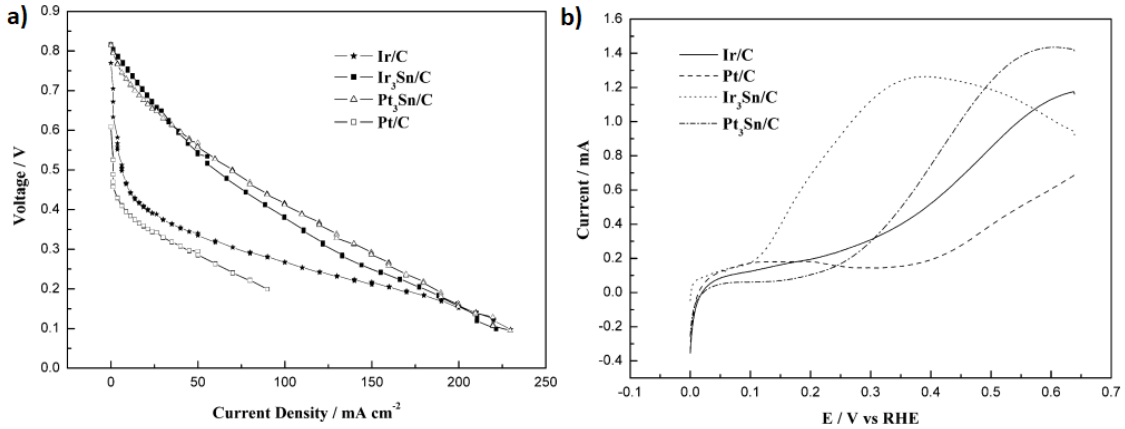

Figure 33. a) Polarization curves of a direct ethanol fuel cell employing Ir/C, Ir_3Sn/C, Pt_3Sn/C and Pt/C as the anode catalyst, respectively. Anode fuel feeding: 1 M ethanol at 1 ml/min, cell temperature 90°C, $P_{cathode}$= 2 bar, 1.5 mg/cm^2 precious metal loading of anode catalysts, 1 mg/cm^2 Pt cathode catalyst (Pt/C-40% from Johnson Matthey). The currents in this Figure were normalized to the geometric area of the single cell b) Linear sweep voltammograms of ethanol oxidation on Ir/C, Pt/C, Ir_3Sn/C and Pt_3Sn/C catalysts in 0.5 M H_2SO_4 with 1 M ethanol at room temperature with a scan rate of 10 mV/s [231].

Furthermore, Ir_3Sn/C is most active towards ethanol oxidation as shown in **Figure 33b**. Measurements revealed that Ir-based catalysts had stronger anodic catalytic activity than Pt-based catalysts, at low potential regions. Ir_3Sn/C demonstrated overall performance that was equivalent to Pt_3Sn/C, making it a suitable substitute for the anode catalyst in direct ethanol fuel cells.

Ir-Pb based catalysts

In a recent report, Zhang et al. [232], reported a new class of porous Ir_3Pb nanodendrites (NDs) alloyed with Au traces. The carbon supported samples were denoted as ND-$Ir_3PbAu_{0.01}$/C, ND-$Ir_3PbAu_{0.05}$/C and ND-$Ir_3PbAu_{0.1}$/C, respectively. The compared electrocatalysts were ND-$Ir_3PbAu_{0.05}$/C, ND-Ir_3Pb/C, NP-Ir_3Pb/C, Ir/C and Pt/C-JM. The results showed that compared to Ir/C, Pt/C-JM, and other previously reported EOR electrocatalysts, the porous Ir_3Pb-NDs performed as a very effective EOR catalyst with improved catalytic activity, CO_2 selectivity, and durability. Interestingly, alloying with Au considerably improved the electrocatalytic performance of porous Ir_3Pb NDs for the EOR, particularly the CO_2 selectivity and durability with the best performance achieved by ND-$Ir_3PbAu_{0.05}$/C.

In conclusion, Ir is a very promising alternative metal for non-platinum materials with performances higher that Pt while the bimetallic Ir_3Sn/C has shown similar performance with Pt_3Sn/C but it was more active towards ethanol oxidation. Furthermore, porous Ir_3Pb-NDs also improved catalytic activity, CO_2 selectivity, and durability with best performance achieved by ND-$Ir_3PbAu_{0.05}$/C.

Ir-Ru based catalysts

Du et al. [233], investigated carbon supported Ir-Ru nanoparticles. $Ir_{67}Ru_{33}$/C, $Ir_{77}Ru_{23}$/C, $Ir_{91}Ru_9$/C were compared with pure Ir/C and Pt/C (ETEK, 20%) catalysts in an electrolyte containing 0.5 M H_2SO_4 and 0.5 M ethanol. The results showed that $Ir_{77}Ru_{23}$/C had superior performance towards EOR at a constant voltage of 0.2 V as shown in **Figure 34**.

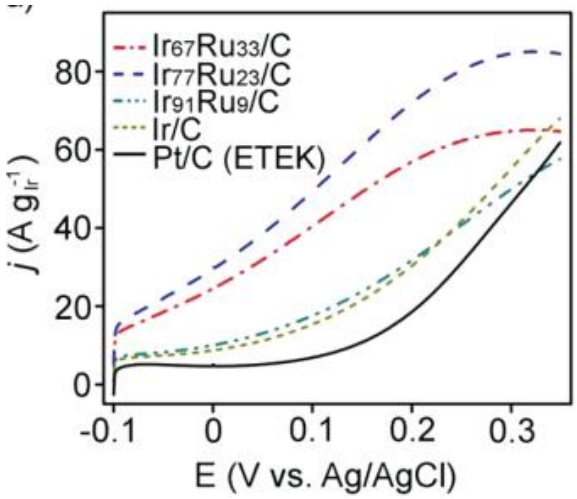

Figure 34. Polarization curves and of Ir−Ru/C in comparison with Ir/C and Pt/C (ETEK) at a potential of 0.2 V in 0.5 M H2SO4 and 0.5 M ethanol solutions [233].

Furthermore, $Ir_{77}Ru_{23}$/C had a higher current density, indicating better electroactivity of $Ir_{77}Ru_{23}$/C towards dissociation of ethanol compared to Pt/C. Du et al. also concluded that C–C bond breaking was easier (lower reaction barrier) over the Ir–Ru alloy surface, supporting their experimental results that alloying Ru with Ir leads to a better and promising catalyst for DEFC application.

4.2.1.6 Non-Precious Catalysts

In the direction of reducing the cost of electrocatalysts used in DE-PEMFCs, significant efforts have been made to prepare effective non-precious-metal-based suitable anodic catalysts. Yang et al. [234] introduced metal-organic frameworks (MOFs), that possess various pore sizes and surface areas. At the same time, by modifying their surface properties with a range of organic compounds, the channel surface provided special functionalities as well as unique catalytic sites for chemical reactions. The MOF material N,N'-bis(2-hydroxyethyl)dithiooxamidatocopper(II) [$(HOC_2H_4)_2$dtoaCu] is a two-dimensional framework composed of dimeric Cu units and bridging ligands $(HOC_2H_4)_2dtoa^{2-}$ and it appeared to be a good proton and electron conductor. Yang and his colleagues evaluated [$(HOC_2H_4)_2$dtoaCu] catalytic activity in acidic media by cyclic voltammetry. The electrolyte solution was 0.5 M H_2SO_4. The measurements, presented in **Figure 35**, proved that, when ethanol was added to the electrolyte, the positive scan revealed a significant increase in the oxidative current density occurring at peak I and peak II.

To determine the oxidation products, gas chromatography analysis was conducted which revealed that only 6.8% acetaldehyde was detected as an oxidation product within 20 minutes while no acetic acid was found. These results, proved that the catalytic electrooxidation of ethanol by the oxidized [$(HOC_2H_4)_2$dtoaCu] species is responsible for the increase in the oxidative current of peak I while at the same time, at peak II a considerable amount of acetaldehyde was detected. The material's ability to electrooxidize ethanol proved to depend on ethanol's concentration. The current density at peaks I and II raised consistently as the ethanol content increased. According to the results of this experiment, even if ethanol only partially oxidized to acetaldehyde under the given circumstances, the performance in terms of oxidation potential and current density was comparable to Pt-based catalysts and they are very promising with the addition of an oxide.

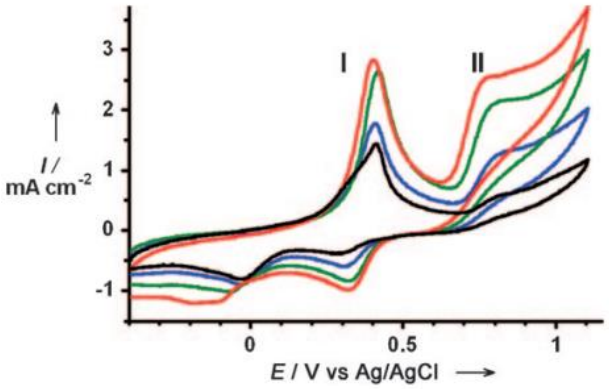

Figure 35. Cyclic voltammograms of a glassy carbon electrode coated with $[(HOC_2H_4)_2dtoaCu]$ in 0.5 M H_2SO_4 containing different concentrations of ethanol (black 0.0, blue 0.5, green 1.0, red 2.0 M ethanol). Sweep rate=100 mV/s [234].

In a very recent study, Rohani et al. [235] modified a glassy carbon electrode by cobalt nanoparticles stuck to the activated carbon (CoNP/AC/GCE) for ethanol oxidation. Anode was fed with 0.2 mM EtOH and the electrolyte used was 0.05 M H_2SO_4. As perceived from curve i (**Figure 36a**), the unmodified electrode did not show any electrochemical activity in the ethanol-free solution at the applied potential range. However, as curve ii shows, the modified electrode in the sulfuric acid electrolyte represented respectively the redox peak at 560 and 240 mV which were related to the oxidation and reduction of the cobalt existing at the modified electrode. The anodic potential changed to more positive values as the scan rate rose, in line with the anode peak current (**Figure 36b**). The selectivity for the oxidation of ethanol was improved, and the overpotential of ethanol electrooxidation on the surface of the modified electrode was greatly reduced. The results validated the usefulness of the modified electrode CoNP/AC/GCE as a straightforward and inexpensive tool for the DE-PEMFCs.

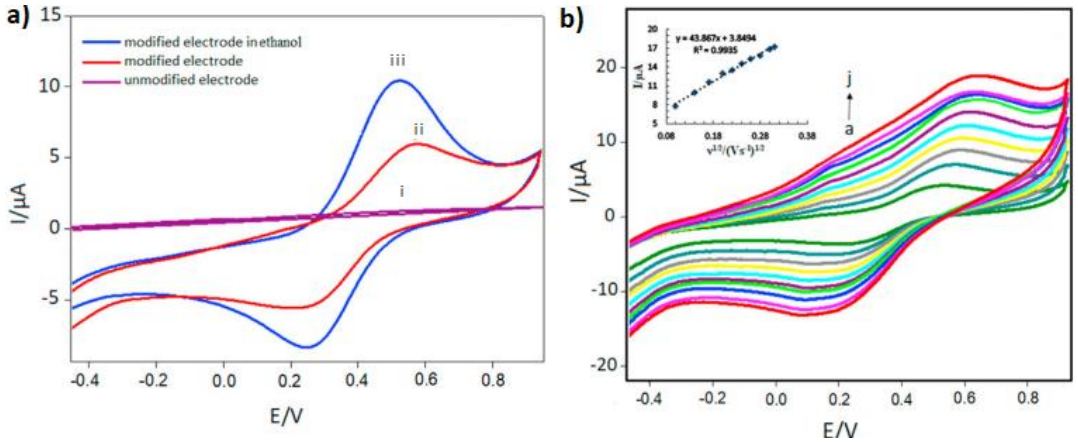

Figure 36. a) cyclic voltammograms of (i) unmodified glassy carbon electrode in electrolyte solution and 0.1 mM of ethanol, (ii) modified glassy carbon electrode in electrolyte solution, (iii) modified glassy carbon electrode in electrolyte solution and 0.1 mM of ethanol. All in potential scan rate of 30 mV/s b) cyclic voltammograms of CoNP/AC/GCE in sulfuric acid solution (0.05 M) containing 0.2 mM of ethanol at different scan rates (10-90 mV/s) [235].

4.2.2 Cathode materials

The performance of the fuel cell is strongly affected on the cathode by the oxygen reduction reaction, measuring the ethanol crossover rate and the parasitic current density. Parasitic current density occurs due to ethanol crossover from the anode to the cathode and results in performance losses. Particularly, ethanol and oxygen share the same active sites when crossover occurs, and as a result, ethanol is oxidized on the active sites that oxygen would be reduced if it was alone. The presence of ethanol on the cathode leads to the increase of the total overpotential named as ideal overpotential which is the subtotal of the overpotential of the ORR plus the overpotential due to ethanol crossover and EOR.

Over the last decades, DE-PEMFC that use Pt based catalysts are mostly used [236]. Moreover, other materials such as Pt-free catalysts have been studied in order to avoid the use of noble metals in the future. Tsiakaras et al. [198] investigated the efficiency of a commercial 20 wt.% Pt/C, catalyst on the cathode while PtRu was in the anode which was compared with a model-based parametric analysis that took place in 2008 [163] using a Nafion 115 membrane. The results of the model showed that between values ranging from 0.25 mol/L to 4 mol/L of ethanol feeding, the best performance was at 1 mol/L, providing a maximum current density around 19 mW/cm^2 while, the maximum power density loss was only 8.24%. Antolini et al. [237] studied the behavior of a PtCo/C (3:1) catalyst compared with a typical Pt/C, on a variable overpotential from 0.1 V to 0.9 V at 60^{o}C and 90^{o}C using O_2 at 3 atm pressure. The focus was between 0.7 V – 0.9 V where both catalysts showed almost the same performance, around 0.18 A/cm^2. However, it was observed that measuring the current density in terms of specific activity (SA), in A/mg$_{Pt}$ – while its numerical value is in A/cm^2 -, some differences appeared on the performance. As shown in **Figure 37b**, PtCo/C performed better throughout all temperatures between 60°C and 100°C, with the best performance at 100°C, where the maximum power density was 16 mW/cm^2 and the current density was 0.135 A/cm^2 (**Figure 37a**).

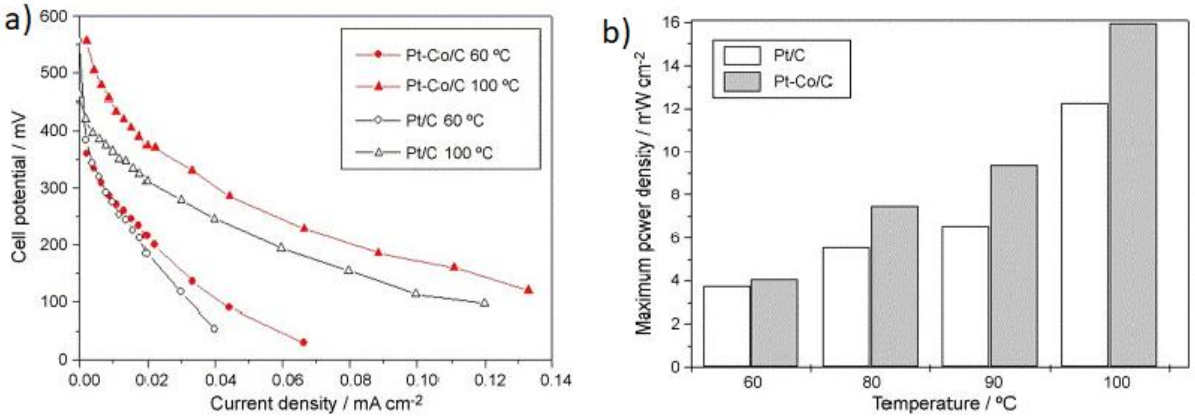

Figure 37. a) Polarization curves for single PEMFC showing ORR, for Pt/C and PtCo/C as cathode catalysts at 1 mg_{Pt}/cm_2 loading, at 60°C, at 3a tm O_2, at 1 mol/L ethanol solution, anode catalyst Pt/C 20 wt.% and loading of 1 mg_{Pt}/cm2. b) Power density of Pt/C and PtCo/C diagram at temperatures 60°C, 80°C, 90°C, 100°C [237].

Lopes et al. [238] prepared a PtPd/C cathode catalyst, proving that the binary PtPd offers better oxygen reduction than pure Pt. In the absence of ethanol, the activity of PtPd was slightly better than that of Pt, producing a power density of 7 mW/cm^2 while oxygen reduction began at 60°C and 90°C and onset potential of 0.44 V and 0.48 V respectively (**Figure 38b**)**.** The improvement at 90°C is attributed to the durability of the catalyst on ethanol poisoning while at 60°C the performance difference is less as ethanol crossover is not strong enough. Esfandiari et al. [239] showed that addition of Ag to commercial Pt/C enhanced the performance of the ORR. Different ratios of PtAg/C were compared with Pt/C and the trials proved to be Ag@Pt/C (1:3), had an ECSA of 67.9 m^2/g_{Pt} with an OCV at 712 mV vs Ag/AgCl reference electrode higher than that of Pt/C, while CV diagrams showed that adsorption of hydrogen peaked at -0.2 V to 0 V. The overall performance of the fuel cell was higher than Ag@Pt/C (1:3) catalyst on the cathode with 470 mW/cm^2. Ma et al. [240] synthesized carbon based catalysts, C/Fe-TMPP and C/Fe-Pc and tested them on 2 M of ethanol and 0.5 M H_2SO_4 at 80°C, on PtRu/C anode catalyst. Power density indicated higher power densities for both catalysts compared to commercial Pt/C, 10.9 mW/cm^2 for C/Fe-TMPP at 0.6 V and 6.7 mW/cm^2 for C/Fe-Pc at 0.35 V. Yu-ChenWei et al. [241] used Co as additive to Pd/C with atomic ratio, PdCo/C (3:1) and metal loading at 19.4%.

Luigi Osmieri et al. [242] tested the effect of Fe-N/C on carbon support materials. Four supports were used for the experiment, MWCNT, MPS, AB and CNS. In the occasion of MPS, two catalysts were prepared, Fe-N/MPC1 and Fe-N/MPC2, where the difference between them was that Fe-N/MPC2, was taken under pyrolysis treatment for a second time. All the catalysts had a C loading of over 91.9%. The four carbon-based were compared with each other and with Pt/C anodic and cathodic scan. Despite the fact that the anodic scan of Pt had higher onset potential, the cathodic scan presented a better reduction curve as it can be seen in **Figure 38a**, from a Linear sweep voltammetry (LSV), with 0.5 M H_2SO_4 solution. Pt/C on cathodic scan had an onset potential at 0.87 V while from all the others catalysts Fe-N/MPC2 achieved an onset potential at 0.82 V which had 0.1 V higher than Fe-N/CNT. Salomé et al. [243], showed that carbon supported PdSn, when it was heat treated , showed increased ethanol tolerance. Three PdSn catalysts were compared depending on the duration of heat treatment. For PdSn-2H and PdSn-2H heat treatment took respectively 2 and 3 hours. Polarization curves in the absence and presence of ethanol are depicted

in **Figure 38c.** Both catalysts performed better in the absence of ethanol as ethanol was taking the active site where oxygen could be placed and reduced.

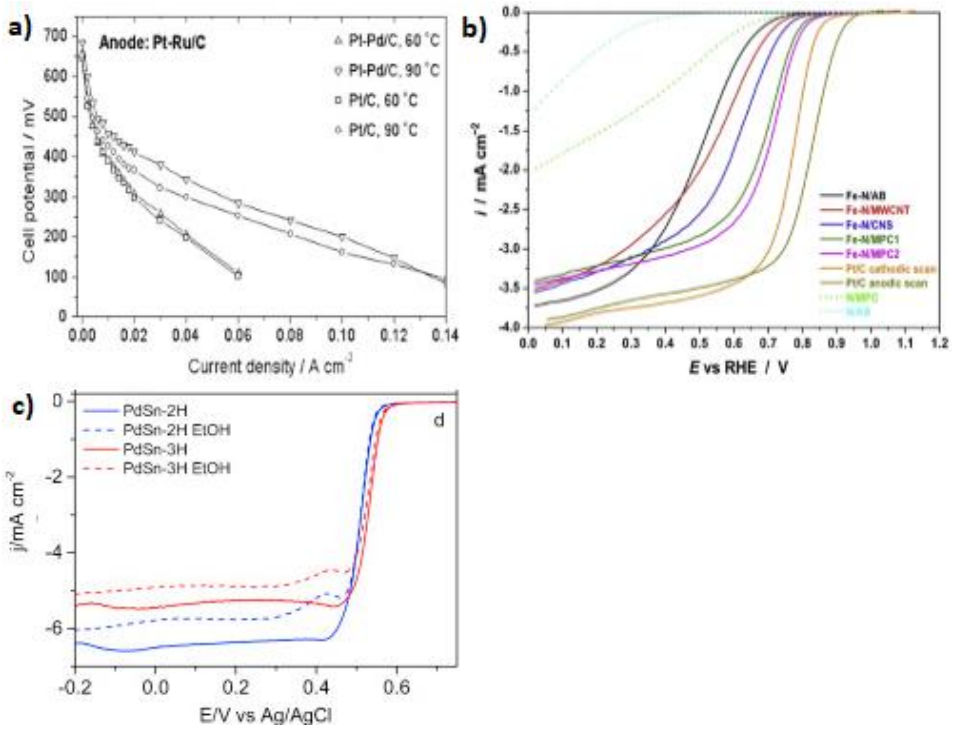

Figure 38. a) Linear sweep voltammetry, 0.5 M H_2SO_4, five carbon based Fe-N/C and one Pt/C 20% loading (anodic and cathodic), at 900 rpm and O_2 with RH=100%. b) Linear sweep voltammetry using 1 M ethanol, for Pt/C and PtPd/C cathode catalysts, on Pt-Ru/C anode 1 mg/cm_2, 1 atm pressure O_2 and 60°C, 3 atm O_2 at 90°C. c) Polarization curves of ORR, without ethanol (solid lines), 0.5 M ethanol (dashed lines), in 0.5 M $HClO_4$, with scan 5 mV/s and 1600 rpm rotation disk [243].

Oxygen reduction at 0.5 M ethanol (dashed lines), was better for PdSn-2H, at an onset potential of 0.56 V, producing a final current of -6 mA/cm^2. Chandran et al. [244] observed that PtSn supported on carbon nanotubes (PCNT) showed an onset potential at 0.7 V at a potential measurement range of 0-0.7 V, producing a final current at -3.8 A/cm^2. Wang et al. [245], constructed an ultra-thin nanowire PtPdCu /NW catalyst, where the best ratio was (36:41:23) used as both anode and cathode catalyst. PtPdCu with Pt loading at 1.2 mg_{Pt} /cm^2, was capable at both EOR and ORR reactions, and on a single cell experiment it performed 21.7 mW/cm^2, almost 4 times better than commercial Pt. PtPdCu increased the surfaces' active sites and reduced CO poisoning resulting in improved values of power and current density.

4.3 Electrolyte Materials

The performance and efficiency of direct ethanol fuel cells largely depend on the electrolyte membranes, which are the key components of a fuel cell. The two tasks performed by the polymeric membrane in PEM fuel cells are the following: electrical insulator that prevents electrons from flowing through the membrane as well as a charge carrier for protons to separate the reactant gases [246]. The primary requirement for superior electrolyte membranes applied in DEFCs are high proton or ionic conductivity, low ethanol permeability, low electron conductivity, oxidation prevention, low fuel crossover, long-term chemical and thermal stability, high mechanical stability, and water management.

Additionally, the material for electrolyte membranes must be readily available, inexpensive to produce, and able to make films that are as thin as possible (50–80 μm), biodegradable and non-hazardous [247]. At this point, Nafion (perfluorinated sulfonic acid electrolyte membrane) is extensively employed in PEMFCs since the 1970s because of its good chemical and electrochemical characteristics, mechanical stability, strong proton conductivity, and the fact that it is not only showing a doubling of the membrane's specific conductivity but also a four-orders-of-magnitude increase in its lifespan (104-105 hours) [246]. Nonetheless, defects of the Nafion membrane are caused by expensive manufacturing, cathode poisoning, cathode oxidation, fuel wastage and highly permeable fuels inside the membranes, which result in swelling issues and fuel loss. Consequently, PEMFC's performance is negatively affected. Performance degradation of the membrane at temperatures of over 80^{o}C is one of the key causes because the membrane's dehydration has a negative impact on its mechanical stability and proton conductivity. Therefore, making significant improvements to or discovering a different membrane for FCs use is essential [248]. Jablonski et al. [249] examined the oxygen penetration through Nafion-117 membranes and how it affected the efficiency of DE-PEMFCs in open circuit. In the absence of an electric current, oxygen passed through the Nafion-117 membrane from the cathode compartment to the anode. Thus, acetaldehyde and acetic acid were created as a result of the ethanol's oxidation. Therefore, efficiency declines. A few years later, Battirola et al. [250] tried to enhance the DE-PEMCs' functionality by avoiding the ethanol crossover effect using Nafion-117 membranes doped with Pt and Pt-Ru nanoparticles. Tests were performed in DEFCs at 90^{o}C and showed that Pt doped and PtRu doped Nafion membranes improved power density 38% and 56% respectively, as illustrated in **Figure 39**, highlighting the activating role of Ru in this application. Matos et al. [251], developed a Nafion 115-titania (NT) composite electrolyte membrane. The results showed that ethanol

absorption of composites was significantly decreased for high volume fractions of titania (>10 vol%), although the proton conductivity at high temperatures was only marginally titania-dependent. Due to these results, it was proven that the performance of DEFCs using Nafion-Titania 15 wt.% (NT15) and Nafion-Titania 20 wt.% (NT20) composites was lower than the one obtained for Nafion-115 (N115). The inorganic particles helped reduce the ethanol uptake while the proton conductivity at high temperatures was not significantly altered.

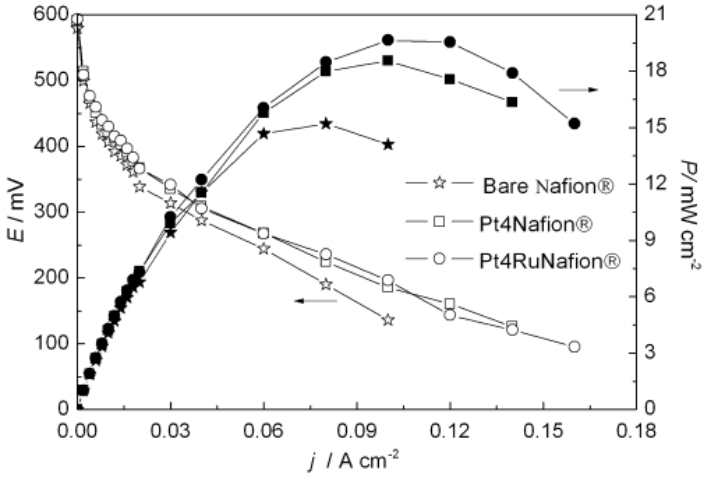

Figure 39. Power density and potential vs. current density for unitary DEFC at 110°C, 2 atm O_2 pressure, 1 mol/l of ethanol solution, Pt/C 30% wt. E-TEK as anode and cathode with Pt loading 2 mg/cm^2. MEA prepared with Nafion 117 membranes doped or non-doped with different amounts of platinum and ruthenium. Filled symbols: power densities. Open symbols: potential [250].

Besides the improvements made on Nafion membranes, they still suffer from high costs and low stability, stimulating further research activity for new types of membranes. Another widely used material for PEM-DEFCs is the sulfonated poly(ether ether ketone) (SPEEK). These membranes show tunable proton conductivity as well as superior chemical and thermal stability [252].

Maab et al. [253], modified sulfonated poly(ether ether ketone) (SPEEK) membranes for direct ethanol fuel cells. The tested membranes were coated with carbo molecular sieves (CMS) and SPEEK/polyimide (PI) homogeneous blends. Maab and colleagues, proved that both hybrid membranes led to significant decreases in ethanol crossover compared to simple Nafion 117 membrane. In the DEFC experiments, the SPEEK/PI mixes outperformed CMS-coated SPEEK membranes. The SPEEK/PI membranes performed significantly better than Nafion-117 membranes, especially in DEFC studies carried out at 90°C, primarily due to the efficient decrease of ethanol crossing.

According to **Figure 40a**, at 90°C, the DEFC performance of the 180 nm SPEEK membranes covered with CMS is comparable to that of Nafion 117. When 10% of the experimental error is taken into account, the polarization curves for both CMS-coated SPEEK membranes and Nafion 117 are

comparable. They are all easily distinguished from the standard SPEEK membrane. When power density is considered, the membrane with a thicker CMS layer performs significantly better. Nonetheless, considering all the measurements combined with **Figure 40b**, SPEEK/PI blends had better performance than CMS-coated SPEEK membranes in the DEFC tests.

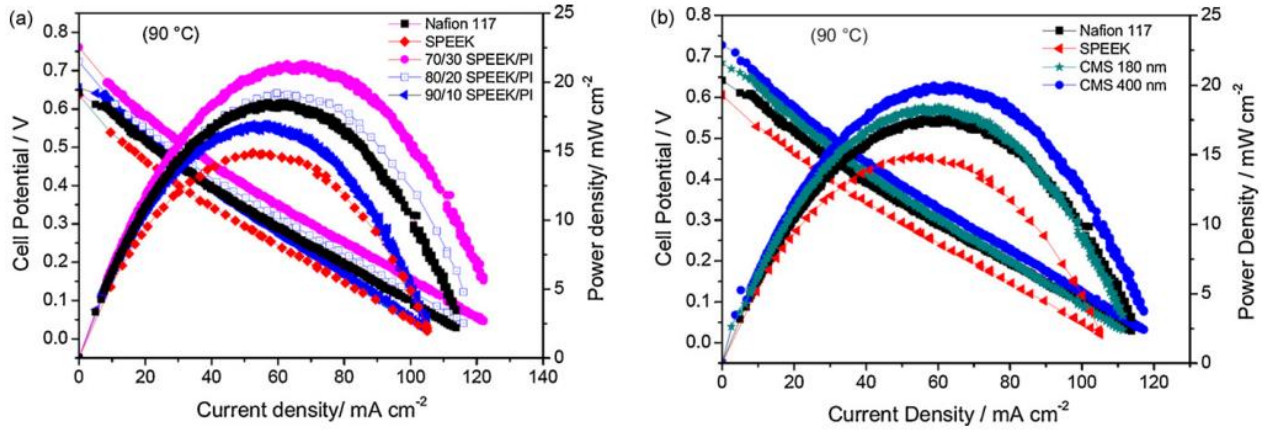

Figure 40. Polarization and power density curves at operating temperature of 90°C: a) Nafion 117®, plain SPEEK and 90/10, 80/20, 70/30 SPEEK/PI blends and b) Nafion 117®, plain SPEEK and CMS-coated SPEEK [253].

Fu et al. [254], introduced a series of hybrid proton-conducting membranes with an interpenetrating polymer network (IPN). The glutaraldehyde cross-linked PVA was interpenetrated with a copolymer of 2-acrylamido-2-methyl-propanesulfonic acid and 2-hydroxy-ethyl methacrylate cross-linked by poly(ethylene glycol) dimethacrylate. The membranes showed reduced fuel permeability and less swelling in ethanol solutions at high fuel concentrations. Fu and his colleagues concluded that, low ethanol permeability also suggested that membranes were appropriate for DEFC applications, and a high fuel concentration may be employed to decrease fuel crossover and optimize the anode kinetics, leading to gains in the fuel cell's energy and power densities.

Roelofs et al. [255], reported modified inorganic–organic mixed matrix membranes with N-(3-triethoxysilylpro pyl)-4,5-dihydroimidazole (DHIM), which consists of an hydrolyzable inorganic part and a functional organic group. The DHIM silica-SPEEK hybrid's proton diffusion coefficient selectivity to ethanol permeability coefficient was better when compared to pure SPEEK and Nafion-117. In a later study, Roelofs et al. [255] modified a SPEEK membrane with an interconnected inorganic phase of hydrophilic fumed silica particles (Aerosil380), tetra-ethoxysilane (TEOS) and a combination of both silica networks.

Dynamic experiments revealed a notable decrease in ethanol crossover in the Liquid-Gas system with the application of 2 M ethanol, and at 40°C with 4 M ethanol, where the combined Aerosil380-TEOS system performed superbly as a reinforcing feature. Another very promising hybrid electrolyte membrane material was a poly (vinyl alcohol) (PVA) membrane. PVA membrane was capable of

producing films, has a high degree of hydrophilicity, and is readily available sites for the construction of a stable membrane with good mechanical qualities. It is also proven that it has reduced ethanol permeability and low cost, making it attractive for DEFCs [255].

4.4 Degradation

PEMFC encounters certain challenges that affect the further enhancement of the fuel cell. Ethanol crossover and membrane delamination are two of the main problems occurring on ethanol feeding. As it has be mentioned on the working principle of DE PEMFC, electrons flow through the external circuit while protons pass through the membrane to reach the anode. In many cases, ethanol through the membrane reaching, also permits taking place of active surface sites of the cathode, increasing the overpotential decreasing the performance of the fuel cell. Ethanol crossover is crucial for the performance, as it affects the amount of CO_2 and acetic acid that is produced on the cathode [256]. Tsiakaras et al. [137] investigated of behavior of the ethanol's crossover. As it is shown in **Figure 41a** crossover increases linearly with current density up until almost 8.0 mol/L of ethanol feeding, when the current density is 300 mA/cm^2, at 4.0 mol/L of ethanol, crossover rate is 30x10^{-8} (mol cm^{-2}/s), while at the same current at 8.0 mol/L, the crossover rate reaches 90x10^8 (mol cm^{-2}/s).

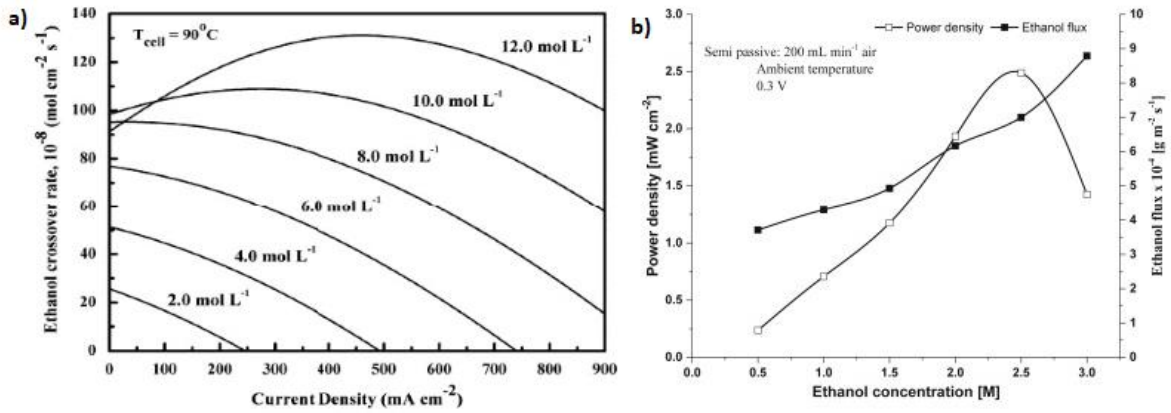

Figure 41. Representation of ethanol crossover with current density for different values of ethanol feeding [137].

Over the 8.0 mol/L, it is observed that the crossover rate has a peak at the middle of the current range and decreases opposite with current density. This phenomenon can be explained as there are two mechanisms that are responsible for crossover diffusion and electro-osmotic drag force. Diffusion occurs at low current densities where, as when current density increases, the oxidation of ethanol increases leading to less concentration difference and less ethanol crossover. On the other hand, over 8.0 mol/L where electro-osmotic drag takes place, higher ethanol concentration leads to higher amount of protons permeation though the membrane which include and ethanol molecules that permeate too. This phenomenon can be explained as there are two mechanism that are responsible for crossover, diffusion, and electro-osmotic drag force. Diffusion occurs at low current densities, as

when it increases, EOR increases leading to less, concentration difference, and ethanol crossover. Electro-osmotic drag takes place over 8.0 mol/L leading higher where elevated ethanol consetration augments permeation of protons and consequently ethanol molecules.

Maab et al. [253], tested membrane made from SPEEK and showed that crossover was 5 times lower than Nafion membrane. Shakeri et al. [257] investigated the key parameters of the fuel cell, temperature, anode-cathode flow rate, ethanol concentration and pressure of oxygen on the cathode. They showed that, the increasing temperature from 35°C to 60°C, resulted in an increase of the power density by 120%. Anode flow rate from 0.025 l/min to 0.1 l/min, showed a bare effect on the performance, while the same effect was also observed on the cathode flow. Kim et al. [258] tested the addition of phosphotungstic acid (PWA) on Nafion membrane from 5 wt.% to 20 wt.%, and proved that the lowest permeability was observed at 20 wt.% of PWA with 12.2% lower ethanol crossover and 22% higher power density. Azam et al. [259], recently studied the parameters that affect fuel cell performance in an ethanol concentration of range 0.5 M – 3.0 M. The results showed that until 2.0 M the OCV was increasing with a peak value at 0.57 V and power density at 5.8 mW/cm^2 and current density at 46.7 mA/cm^2, while better power density was found at 2.5 M (**Figure 41b**) and power density at T=80°C. At concentrations higher than 2.0 M, the effect of byproducts on the anode mostly acetic acid is crucial as far as the performance degradation is concerned, because of the anode's catalyst poisoning. Furthermore, ethanol flow rate is another important parameter that affects performance, as it was shown that power density was increased until 4 mol/L flow rate, at 2.5 M power density reached 12 mW/cm^2.

Membrane degradation can be caused either from mechanical or chemical failure. Mechanical failure usually depends on relative humidity and operation temperature [260]. Membrane needs to be pressurized in a specific range of 75-300 psi which seems to be the optimal in order to provide a solid sealed structure to avoid leakage problems and enhance permeability through the membrane. It has been observed [261] that rising temperature leads to the reduction of elastic modulus which in these values of pressure can lead to mechanical failure. Relative humidity is also essential on MEA fatigue however the effect on failure is three times less than that of temperature. Khorasany et al. [262], showed that cracking on the surface of the catalyst affected integrity of the membrane as it provoked stress which resulted in membrane surface failure. Solasi et al. [263] on a stress strain test on Nafion membrane showed that stress values were reduced over-time when constant strain was applied. They also showed that rupture behavior wasn't affected by temperature variations. Mechanical creep up until final rupture was observed under constant stress even at low stress levels below

yield point. Benziger et al. [264] showed that water absorption lowered the rate of relaxation, while at constant water activity, elastic modulus was increased as temperature also increased. Water absorption and desorption proved to be the reason that provoked cracks on the membrane due to swelling and contraction phenomena [265].

Degradation on the catalyst layer is another important parameter since reactions occur on the surface of the electrode. Electrochemical surface area (ECSA) is used to measure the active surface and its reduction is mainly attributed to Pt dissolution. Zhao et al. [266] studied the development of carbon corrosion and concluded that ESCA's decomposition due to carbon corrosion results in the detachment of Pt sites from the surface. Furthermore, the hydrophobic surface of CL is contrary to the oxygen groups that are created from carbon corrosion and are hydrophilic. Also, CL, can suffer from cracks during fabrication stage, from mechanical stresses on the MEA, when the solvent is evaporated or from insufficient handling. Change et al. [267] showed that swelling and shrinking, enhances the size of the cracks on the catalyst especially after 500 cycles of the fuel cell, the crack length was 300% higher than fresh condition of catalyst. Song et al. [268] referred that inadequate cell performance occurred due to the catalyst delamination, from the surface of the electrolyte. This phenomenon generally results in non-uniform contact of the two materials, which augments overpotential and resistance on mass transfer. Wang et al. [269] conducted experiments on the operation of the PEM FC under subfreezing conditions, and showed that ECSA suffered from severe damage due to freezing conditions. The main reasons reported in this experiment were the alteration between ice and liquid phase damaged that catalyst layer. Furthermore, the presence of ice occupies the triple phase boundary layer of the ionomer on the cathode, blocking the oxygen species and not allowing them to reach the catalyst's layer. ECSA loss is significant, during the first four cycles as, approximately 43% loss of the initial surface was reported while after 10 cycles it ended with total loss of 53% from the initial surface. Zhao et al.[270], reported catalyst degradation which resulting to modification of the microstructure, mainly due to water intrusion. More specifically, ionomers need to be highly humidified to provide elevated conductivity, however incoming water changed the volume of the ionomer, provoking shrinking and swelling. The continuous change in the structure of the ionomer increased fatigue levels that ended up in total failure of the ionomer where the particles of the catalyst loosed-up and were exported from the catalyst through water circulation. Schneider et al.[271] reported that high temperature, of 90 °C and RH 100% had a severe impact on Pt dissolution compared to lower temperature, of 60 °C and RH=30%. The reported explanation was that diffusion rate is

temperature dependent specifically on high temperature. On the other hand, relative humidity enhances the kinetics. Both factors combined, contribute on the faster kinetics rate. At high temperature, higher concentration of the Pt^{2+} on the membrane led to augmentation of the Pt loss rate on the catalyst due to increased diffusion.

Gas diffusion layers are responsible for the removal of water produced, outside the catalyst layer. Sorrentino et al. [272] showed in their research that degradation of the diffusion layer affects water transport due to higher resistance. Abdullah et al. [273], showed that the thickness of the GDL affects the durability on cracking. The main parts that are affected by GDL, slow the mass transport rate which usually occurs because of the existence of non-uniform forces applied on the components. Fatigue from many operation cycles, is responsible for the decrement of porosity. Chen et al. [274], investigated the electrochemical properties of GDL and reviewed the degradation mechanisms of GDL. In their article was reported that over 1.2 V, GDL fibers reduced their diameters resulting on thinner gas diffusion layer. Another form of degradation comes from carbon corrosion, which leads to the reduction of electrochemical surface area (ECSA) and the increase of resistances [275]. Water flooding can happen in the fuel cell at both the anode and the cathode but it is more preferable to occur on the cathode. Flooding results in pore blocking of the gas diffusion layer where molecules of the reaction can't reach the catalyst layer, elevating the demanding levels of performance losses and leading to overpotential [276]. Kumar et al. [277] tested two forms of GDL, carbon paper and carbon cloth under electrochemical degradation of aging up to 100 hours. It was proved that the rigid structure of the carbon paper was lost, increasing residual fatigue under cyclic clamping pressure. Wood et al. [278] referred that, on higher temperatures and flow rates, GDL could lose its hydrophobic character, due to the contact of the reactant with the diffusion surface provoking erosion. Cathode surface was more apt to this kind of erosion since oxygen flow is larger than that of the fuel on the anode. Another important factor is that fuel cell needs to operate in freezing temperatures if it is destined to be utilized in automotive industry. Guo et al. [279] studied the conducted an experiment of 10 freeze-thaw cycles under temperatures from 20°C to -30°C. The results showed that water content in the MEA the delaminated the catalyst layer from membrane and the GDL, while the GDL was seriously cracked.

Bipolar plate (BPP) is another component that can cause degradation on the fuel cell. It is a metal gasket usually made from steel that is placed all over the MEA and between the cells, one plate close to the anode and one close to the cathode. The main tasks of BPP are, the facilitation to the diffusion of gases that enter or retrieve from the fuel cell as reactants, the maintenance of thermal stability and the distribution of water all over the stack. From these tasks, degradation mechanisms are mainly due to

corrosion and low contact of the surfaces. Bipolar plates are exposed to both, oxidation on the anode and reduction on the cathode reactions where, because of these reactions an oxide film is compiled on the surface which erodes the materials [280]. The corrosion that is created results in the development of interfacial contact resistance which increases the overpotential. It is observed that stainless steel has some regions where they favor corrosion. When OPC reaches over 1 V at usually low current density, steel has a transparent region which results to the oxidation of the metal. Similar occasion, occurs at operations where the potential is around 0 – 0.1 V vs RHE where it is called "active" region for steel and again it results in corrosion [281]. Ren et al. [282], tested the behavior of a typical stainless steel, and showed that start-up and shut-down move the potential of the cathode to transparent region. The big range of the potential contributes to the continuous alternation between transparent and passive region which dissolute the outer layer of the metal. El-Hassan et al. [283] reported that the flow channels that direct the reactants and the products on the anode and cathode, caused a back pressure effect which resulted in performance losses and degradation.

CHAPTER V

5. Conclusions

The increased energy consumption, as a consequence of the improved living standards, the expanding industrialization, and the global overpopulation result in the continuous rise of global energy demand. Fossil fuels are the main energy sources used in burning processes although this has severe impacts on the environment since the emissions are hazardous and, the global reserves of fossil fuels are depleting. Therefore, these side effects have led to a multitude of proposed remedies to the existing environmental issues. Among others, fuel cells (FCs), that convert chemical energy to electricity, represent one of the most promising and outstanding options for sustainable energy conversion with low or no environmental impact.

In this thesis, we presented all types of fuel cells and their main features while we also investigated Direct Alcohol Fuel Cells and especially those functioning with ethanol feed in acidic medium and low temperatures. Direct ethanol fuel cells use ethanol as fuel, a renewable biofuel that can be produced from first generation sources, it is non-toxic to humans and via redox reactions it produces electricity. The procedure of electrocatalysis in the cell follows a series of electrochemical processes with features that determine the efficiency and the performance of the FC and complies with basic thermodynamic and kinetic laws. In general, alcohols are reformed before they are used for electricity generation. The main types of reforming are: i) steam reforming, ii) dry reforming, iii) autothermal reforming and iv) partial oxidation that can occur in internal or external reforming processes. Specifically, in direct ethanol fuel cells (DEFCs), ethanol undergoes internal direct reforming.

Direct alcohol fuel cells (DAFCs) can operate in both acidic and alkaline media and their main parts are the electrodes, the catalyst, the membrane, the electrolyte, the bipolar plates, and the diffusion layer as in any other fuel cell. DE-PEMFCS and DE-AEMFCS have some fundamental differences that have been analysed extensively. The working principle, the setup and the performance for, PEM, AEM and SOFC, are some of the outstanding features required in order to understand the operation conditions and performance of each type of fuel cell.

The optimization of DE-PEMFC depends mainly on the anode catalyst material, along with the cathode's material, since they play a key role in the overall fuel cells' efficiency and performance since they facilitate ethanol reaction activity and reduce oxidation potential rates. The identification of a desirable electrocatalyst depends on two basic characteristics: i) contribute in C-C bond cleavage causing the carbon to completely oxidize into carbon dioxide, increasing fuel cell efficiency and fuel use

and, ii) eject the adsorbate intermediate species. Carbon supported Pt and Pt-alloys are commonly used as catalysts in low temperature fuel cells and to date is the most investigated metal. Pt is the most active material for the EOR, however, it is easily poisoned when it is used alone as an anode catalyst, and also achieves higher electrocatalytic activity towards EtOH electrooxidation in acidic media when doping with a second or, a third additive. All the experiments were held in operation-like conditions, in acidic media, medium to low operation temperatures (60-90^{o}C), with Pt cathode materials with different metal loading (1-2 mg/cm^2), while the concentrations of the electrolyte solution (H_2SO_4 or $HClO_4$) and EtOH (anode), as well as O_2 (cathode) feed are not constant.

As far as the report on monometallic electrocatalysts for DE-PEMFCs, the most efficient electrocatalyst was the pure Pt/C with 20 wt.% Pt. The experiment was held in 0.1 mol/l $HClO_4$, 0.1 mol/l EtOH with 1.0 mg/cm^2 Pt metal loading. Although the 30 wt.% Pt catalyst had a higher current density, it also had the greatest negative impact on ORR, which reduced the performance of the entire cell. Platinum has the highest electro-oxidation of ethanol activity; however pure Pt electrode performance is insufficient because highly adsorbed intermediates develop and obstruct the anode surface. The focus of current studies is on using co-catalysts to reduce the quantity of adsorbed intermediates.

According to the reported results regarding binary anode electrocatalysts, some of them stand out for their high electrocatalytic performance for ethanol electrooxidation in acidic medium, proving that the addition of a second metal enhances the cell efficiency. Among Pt-based bimetallic electrocatalysts, Pt-Ru and Pt-Sn are the most promising anode material. When Ru is doped in Pt, it activates water molecules and provides preferential sites for OH_{ads} absorption at lower potential than pure Pt. OH_{ads} completely oxidize the poisoning intermediates to CO_2. The best performance was achieved by Pt_3Ru_2 with 1 M ethanol solution and 0.5 M H_2SO_4 electrolyte solution. Sn also has significant impact on Pt catalyst. More specifically, CO does not prefer to bind with Sn and so Sn active sites are free for OH_{ads}, showing resistance on active site poisoning and also high compatibility. Research proved that the optimal ratio at 90^{o}C with 1 mol/l EtOH anode feed, 20 wt.% Pt and 2.0 mg/cm^2 Pt was found to be 2:1 Pt_2Sn_1 (33 wt.% Sn). Another metal that has been investigated in binary catalysts was Ni that promotes the C-C bond cleavage and decreases the energy of chemisorption of ethanol and its intermediates. The literature review showed that $Pt_{2.3}Ni$ have the higher current density at same potential among others with different atomic ratios in 0.1 M $HClO_4$, 0.2M EtOH and 18% Pt. Combination Pt with Rh has also been tested for its EOR activity. As it was stated, it increases CO_2 selectivity by improving CO_2 yield and decreases the acetaldehyde yield, while the best performance

was achieved by $Pt_{91}Rh_{09}$ in 0.1 mol/l $HClO_4$ and 1.0 M EtOH, although it still has lower performance than the PtRu binary catalyst. $Pt_{09}Rh/TiO_2$ is also a very promising alternative for catalysts. Lastly, as far as the binary Pt-based anode electrocatalysts is concerned, a combined PtPd catalyst has been reviewed. Adsorption of hydroxyl ions and the development of an oxide layer on Pd surfaces have an impact on the electrooxidation of ethanol using Pd catalysts, especially at higher potentials. Out of many investigated, Pt_1Pd_5 showed the best performance in 0.5 M EtOH and 0.5 M H_2SO_4.

According to reports in the open literature of ternary electrocatalysts, most of them are more effective than binary electrocatalysts. On the PtRu based sector the ranking is shown as: PtRuSn > PtRuW > PtRuMo > PtRuRe > PtRuPb. $Pt_{0.8}Ru_{0.1}Sn_{0.1}$ seemed to have the best performance, since the combination of Ru and Sn promotes, the C-C bond cleavage and at the same time, the carbon monoxide and acetic acid oxidation. On the experiment conducted, PtRuSn reached a peak power density of 48 mW/cm^2 at 48 mA/cm^2 and 1 V. W and Mo additives on PtRu enhanced also the electrocatalytic activity by increasing the electrochemical surface area and promoting CO oxidation. As regards PtSn based electrocatalysts, the ranking is depicted as, PtSnNi >PtSnCe > PtSnCo. PtSnNi seemed to be a promising catalyst, since addition of Ni to PtSn, promoted the formation of acetaldehyde and the 2 electrons flow on the circuit. Ni is also a low-cost material which could provide an overall cost reduction of the fuel cell. Ce showed similar properties with Ni on ethanol oxidation providing a large quantity of oxygenated species which promoted the formation of carbon dioxide. More catalysts were reviewed as regards PtSn trimetallic catalysts PtSnX (X= Rh, Re, Mo Pr) however the power density wasn't high enough. Furthermore, rare earth materials were also introduced on PtSn catalysts, including PtSnLa and PtSnTa and showed poor performances.

On the other hand, regarding the Pt-based anode materials, some oxides were synthesized for their potential application in DE-PEMFCS for higher EOR activity and cell performance. Metal oxides are able to adsorb a large number of OH^- species involved in the redox process occurring between different oxidation states of the metal oxide, and improve their catalytic properties. Pt-(RuO_2-PbO_x)/C and $PtRhSnO_2$/C (with an atomic ratio of Pt:Rh:Sn=3:1:4) have provided the highest results in 0.5 M H_2SO_4 and 1 M EtOH feed, while TiO_2 and γ-Fe_2O_3-C have also had remarkable effects on the catalysts' activity towards ethanol oxidation in the same conditions.

Furthermore, iridium is the most investigated among non-platinum catalysts. The bimetallic Ir_3Sn/C showed similar performance to Pt_3Sn/C but it is more active towards ethanol oxidation, making Ir a highly attractive alternative metal for non-platinum materials with performances greater than Pt, in 0.5 M H_2SO_4 and 1 M EtOH with 20 wt.% Pt and 1.5 mg/cm^2 metal loading.

Additionally, porous Ir_3Pb-NDs enhanced durability, CO_2 selectivity, and catalytic activity, with ND-$Ir_3PbAu_{0.05}$/C achieving the highest results. Moreover, $Ir_{77}Ru_{23}$/C was proven to be a very promising low-cost electrocatalyst for DEFC.

In order to reduce the cost of precious metals catalysts, research community investigated some non-precious catalysts. Although the non-precious materials literature study is limited, MOF materials and CoNP/AC/GCE exhibited excellent performance in DEFCs and encouraged further research.

DE-PEMFCs face also challenges as regards performance losses of the fuel cell and degradation of its components. Degradation according to the literature can occur in any part of the fuel cell such as, membrane, catalyst layer, gas diffusion layer, bipolar plates. The mechanisms of degradation are separated into mechanical, chemical and thermal degradation. Membrane degradation mostly comes from all the three mechanisms, notably, elevated temperature, high relative humidity, constant strain on the MEA and water flooding are mainly responsible for degradation. Catalysts suffer mostly from carbon corrosion, freeze/thaw cycles and assembly failures such as highly stresses which result in Pt dissolution, cracking of the surface and ECSA losses. GDL, are vulnerable to carbon corrosion, freeze/thaw cycles, and water flooding while bipolar plates suffer from carbon corrosion and interfacial contact resistances.

Direct ethanol fuel cells have developed significantly over the past few years, and research has progressed to a satisfactory level. However, more research needs to be conducted in the field before DE-PEMFCs can become fully commercialized.

References

1. Walters, E. A.; Wewerka, E. M., An overview of the energy crisis. *Journal of Chemical Education* **1975,** *52*, 282.
2. Liza, Z.; Akhter, H.; Shahibuzzaman, M.; Islam, M., A Path to Renewable Energy from the Energy Crisis in Bangladesh. *Journal of Engineering Research and Reports* **2020**, 6-19.
3. Abdelkareem, M. A.; Elsaid, K.; Wilberforce, T.; Kamil, M.; Sayed, E. T.; Olabi, A., Environmental aspects of fuel cells: A review. *Science of The Total Environment* **2021,** *752*, 141803.
4. Pu, Z.; Zhang, G.; Hassanpour, A.; Zheng, D.; Wang, S.; Liao, S.; Chen, Z.; Sun, S., Regenerative fuel cells: Recent progress, challenges, perspectives and their applications for space energy system. *Applied Energy* **2021,** *283*, 116376.
5. Mohd Azhar, S. H.; Abdulla, R.; Jambo, S. A.; Marbawi, H.; Gansau, J. A.; Mohd Faik, A. A.; Rodrigues, K. F., Yeasts in sustainable bioethanol production: A review. *Biochemistry and Biophysics Reports* **2017,** *10*, 52-61.
6. Dahman, Y.; Syed, K.; Begum, S.; Roy, P.; Mohtasebi, B., 14 - Biofuels: Their characteristics and analysis. In *Biomass, Biopolymer-Based Materials, and Bioenergy*, Verma, D.; Fortunati, E.; Jain, S.; Zhang, X., Eds. Woodhead Publishing: **2019**, 277-325.
7. Manochio, C.; Andrade, B. R.; Rodriguez, R. P.; Moraes, B. S., Ethanol from biomass: A comparative overview. *Renewable and Sustainable Energy Reviews* **2017,** *80*, 743-755.
8. Cajavilca, C.; Varon, J.; Sternbach, G. L., Luigi Galvani and the foundations of electrophysiology. *Resuscitation* **2009,** *80*, 159-162.
9. Bagotsky, V. S., Fuel cells, batteries, and the development of electrochemistry. *Journal of Solid State Electrochemistry* **2011,** *15*, 1559-1562.
10. Katz, E., Electrochemical contributions: William Nicholson (1753–1815). In Wiley Online Library: **2021**, Vol. 1.
11. Breitkopf, C.; Swider-Lyons, K., Electrochemical science—historical review. *Springer Handbook of Electrochemical Energy* **2017**, 1-9.
12. James, F. A., Michael Faraday's first law of electrochemistry: how context develops new knowledge. In ACS Publications: **1989**.
13. Wisniak, J., Electrochemistry and fuel cells: the contribution of William Robert Grove. *Indian Journal of History of Science* **2015,** *50*, 476-490.
14. Mertens, J., From the lecture room to the workshop: John Frederic Daniell, the constant battery and electrometallurgy around 1840. *Annals of science* **1998,** *55*, 241-261.
15. Tull, B., Photovoltaic Cells: Science and Materials. *Columbia University* **2004,** *20*.
16. Barkan, D. L. K., Walther Nernst and the transition to modern physical chemistry. **1992**.
17. Petit, A., Associating Physics and Chemistry to Dissociate Molecules: The History of the Clausius-Williamson Hypothesis. *Historical Studies in the Natural Sciences* **2016,** *46*, 360-391.
18. Καραντώνης, Α., Ηλεκτροχημικές αντιδράσεις. **2016**.
19. Deng, Y.; Wang, D.; Xiao, W.; Jin, X.; Hu, X.; Chen, G. Z., Electrochemistry at conductor/insulator/electrolyte three-phase interlines: a thin layer model. *The Journal of Physical Chemistry B* **2005,** *109*, 14043-14051.
20. Lefrou, C.; Fabry, P.; Poignet, J. C., *Electrochemistry: The Basics, With Examples*. Springer Berlin Heidelberg: **2012**.
21. Zhu, C.; Ang, N. W. J.; Meyer, T. H.; Qiu, Y.; Ackermann, L., Organic Electrochemistry: Molecular Syntheses with Potential. *ACS Central Science* **2021,** *7*, 415-431.
22. Huggins, R. A., Simple method to determine electronic and ionic components of the conductivity in mixed conductors a review. *Ionics* **2002,** *8*, 300-313.
23. Riess, I., Mixed ionic–electronic conductors—material properties and applications. *Solid State Ionics* **2003,** *157*, 1-17.
24. Li, M.; Wang, C.; Chen, Z.; Xu, K.; Lu, J., New concepts in electrolytes. *Chemical Reviews* **2020,** *120*, 6783-6819.
25. Taner, T., *Proton Exchange Membrane Fuel Cell*. IntechOpen: **2018**.
26. Xing, w.; Yin, G.; Zhang, J., *Rotating Electrode Methods and Oxygen Reduction Electrocatalysts*. Elsevier Science: **2014**.
27. Zoski, C. G., *Handbook of Electrochemistry*. Elsevier Science: **2006**.
28. Xu, H.; Ni, M., Numerical simulation of hybrid systems based on solid oxide fuel cells. In *Hybrid Energy System Models*, Elsevier: 2021; pp 91-127.
29. Wang, W.; Wei, X.; Choi, D.; Lu, X.; Yang, G.; Sun, C., Electrochemical cells for medium-and large-scale energy storage: Fundamentals. In *Advances in batteries for medium and large-scale energy storage*, Elsevier: **2015**, 3-28.

30. Perez, N., Mass Transport by Diffusion and Migration. In *Electrochemistry and Corrosion Science*, Springer: **2016**, 151-197.
31. Ki, D.; Popat, S. C.; Torres, C. I., Reduced overpotentials in microbial electrolysis cells through improved design, operation, and electrochemical characterization. *Chemical Engineering Journal* **2016,** *287*, 181-188.
32. Ramachandran, R.; Nosonovsky, M., Coupling of surface energy with electric potential makes superhydrophobic surfaces corrosion-resistant. *Physical Chemistry Chemical Physics* **2015,** *17*, 24988-24997.
33. Strbac, S. B.; Adzic, R. R., Electrocatalysis, Fundamentals - Electron Transfer Process; Current-Potential Relationship; Volcano Plots. In *Encyclopedia of Applied Electrochemistry*, Kreysa, G.; Ota, K.-i.; Savinell, R. F., Eds. Springer New York: New York, NY, **2014**, 417-423.
34. Chan, D. Y. C.; Mitchell, D. J., The free energy of an electrical double layer. *Journal of Colloid and Interface Science* **1983,** *95*, 193-197.
35. Sato, N., *Electrochemistry at Metal and Semiconductor Electrodes*. Elsevier Science: **1998**.
36. Inglezakis, V. J.; Poulopoulos, S. G., 5 - Catalysis. In *Adsorption, Ion Exchange and Catalysis*, Inglezakis, V. J.; Poulopoulos, S. G., Eds. Elsevier: Amsterdam, 2006; pp 355-521.
37. Roduner, E., Selected fundamentals of catalysis and electrocatalysis in energy conversion reactions—A tutorial. *Catalysis Today* **2018,** *309*, 263-268.
38. Chorkendorff, I.; Niemantsverdriet, J. W., *Concepts of modern catalysis and kinetics*. John Wiley & Sons: **2017**.
39. Liu, D.; Song, Z.; Cheng, S.; Wang, Y.; Saad, A.; Deng, S.; Shen, J.; Huang, X.; Cai, X.; Tsiakaras, P., Mesoporous IrNiTa metal glass ribbon as a superior self-standing bifunctional catalyst for water electrolysis. *Chemical Engineering Journal* **2022,** *431*, 134210.
40. Introduction. In *Industrial Catalysis*, **2005**, 1-14.
41. Long, G.-f.; Wan, K.; Liu, M.-y.; Liang, Z.-x.; Piao, J.-h.; Tsiakaras, P., Active sites and mechanism on nitrogen-doped carbon catalyst for hydrogen evolution reaction. *Journal of Catalysis* **2017,** *348*, 151-159.
42. Wells, P. B., Catalysis. In *Encyclopedia of Materials: Science and Technology*, Buschow, K. H. J.; Cahn, R. W.; Flemings, M. C.; Ilschner, B.; Kramer, E. J.; Mahajan, S.; Veyssière, P., Eds. Elsevier: Oxford, **2001**, 1020-1025.
43. Bartholomew, C. H.; Farrauto, R. J., *Fundamentals of Industrial Catalytic Processes*. Wiley: **2011**.
44. Bernard, P.; Stelmachowski, P.; Broś, P.; Makowski, W.; Kotarba, A., Demonstration of the Influence of Specific Surface Area on Reaction Rate in Heterogeneous Catalysis. *Journal of Chemical Education* **2021,** *98*, 935-940.
45. Somorjai, G. A.; Park, J. Y., Molecular Factors of Catalytic Selectivity. *Angewandte Chemie International Edition* **2008,** *47*, 9212-9228.
46. Forzatti, P.; Lietti, L., Catalyst deactivation. *Catalysis Today* **1999,** *52*, 165-181.
47. Bartholomew, C. H., Mechanisms of catalyst deactivation. *Applied Catalysis A: General* **2001,** *212*, 17-60.
48. Cen, J.; Jiang, E.; Zhu, Y.; Chen, Z.; Tsiakaras, P.; Shen, P. K., Enhanced electrocatalytic overall water splitting over novel one-pot synthesized Ru–MoO3-x and Fe3O4–NiFe layered double hydroxide on Ni foam. **2021,** *177*, 1346-1355.
49. Yu, C.; Lu, J.; Luo, L.; Xu, F.; Shen, P. K.; Tsiakaras, P.; Yin, S., Bifunctional catalysts for overall water splitting: CoNi oxyhydroxide nanosheets electrodeposited on titanium sheets. **2019,** *301*, 449-457.
50. Long, G.-f.; Wan, K.; Liu, M.-y.; Liang, Z.-x.; Piao, J.-h.; Tsiakaras, P., Active sites and mechanism on nitrogen-doped carbon catalyst for hydrogen evolution reaction. *Journal of Catalysis* **2017,** *348*, 151-159.
51. Horányi, G., Heterogeneous catalysis and electrocatalysis. *Catalysis Today* **1994,** *19*, 285-311.
52. Lu, J.; Tang, Z.; Luo, L.; Yin, S.; Shen, P. K.; Tsiakaras, P. Worm-like S-doped RhNi alloys as highly efficient electrocatalysts for hydrogen evolution reaction. **2019,** *255*, 117737.
53. Jing, S.; Wang, D.; Yin, S.; Lu, J.; Shen, P. K.; Tsiakaras, P., P-doped CNTs encapsulated nickel hybrids with flower-like structure as efficient catalysts for hydrogen evolution reaction. **2019,** *298*, 142-149.
54. Xu, P.; Qiu, L.; Wei, L.; Liu, Y.; Yuan, D.; Wang, Y.; Tsiakaras, P., Efficient overall water splitting over Mn doped Ni2P microflowers grown on nickel foam. *Catalysis Today* **2020,** *355*, 815-821.
55. Yan, L.; Zhang, B.; Zhu, J.; Li, Y.; Tsiakaras, P.; Shen, P. K., Electronic modulation of cobalt phosphide nanosheet arrays via copper doping for highly efficient neutral-pH overall water splitting. *Applied Catalysis B: Environmental* **2020,** *265*, 118555.
56. Zhang, B.; Shan, J.; Wang, W.; Tsiakaras, P.; Li, Y., Oxygen Vacancy and Core–Shell Heterojunction Engineering of Anemone-Like CoP@ CoOOH Bifunctional Electrocatalyst for Efficient Overall Water Splitting. **2022,** *18*, 2106012.
57. Saad, A.; Gao, Y.; Owusu, K. A.; Liu, W.; Wu, Y.; Ramiere, A.; Guo, H.; Tsiakaras, P.; Cai, X., Ternary Mo2NiB2 as a superior bifunctional electrocatalyst for overall water splitting. **2022,** *18*, 2104303.

58. Yan, L.; Zhang, B.; Zhu, J.; Li, Y.; Tsiakaras, P.; Shen, P. K., Electronic modulation of cobalt phosphide nanosheet arrays via copper doping for highly efficient neutral-pH overall water splitting. **2020,** *265*, 118555.
59. Qi, L.; Li, J., Adsorbate interactions on surface lead to a flattened Sabatier volcano plot in reduction of oxygen. *Journal of Catalysis* **2012,** *295*, 59-69.
60. Zhang, Y.; Huang, J.; Eikerling, M., Criterion for finding the optimal electrocatalyst at any overpotential. *Electrochimica Acta* **2021,** *400*, 139413.
61. Ooka, H.; Huang, J.; Exner, K. S., The sabatier principle in electrocatalysis: Basics, limitations, and extensions. *Frontiers in Energy Research* **2021,** *9*, 155.
62. Wang, K.; Chen, H.; Zhang, X.; Tong, Y.; Song, S.; Tsiakaras, P.; Wang, Y., Iron oxide@ graphitic carbon core-shell nanoparticles embedded in ordered mesoporous N-doped carbon matrix as an efficient cathode catalyst for PEMFC. **2020,** *264*, 118468.
63. Zhang, L.; Lu, J.; Yin, S.; Luo, L.; Jing, S.; Brouzgou, A.; Chen, J.; Shen, P. K.; Tsiakaras, P., One-pot synthesized boron-doped RhFe alloy with enhanced catalytic performance for hydrogen evolution reaction. **2018,** *230*, 58-64.
64. Goula, M. A.; Kontou, S. K.; Tsiakaras, P., Hydrogen production by ethanol steam reforming over a commercial Pd/γ-Al2O3 catalyst. **2004,** *49*, 135-144.
65. Yu, C.; Xu, F.; Luo, L.; Abbo, H. S.; Titinchi, S. J.; Shen, P. K.; Tsiakaras, P.; Yin, S., Bimetallic Ni–Co phosphide nanosheets self-supported on nickel foam as high-performance electrocatalyst for hydrogen evolution reaction. **2019,** *317*, 191-198.
66. Long, B.; Yang, H.; Li, M.; Balogun, M.-S.; Mai, W.; Ouyang, G.; Tong, Y.; Tsiakaras, P.; Song, S., Interface charges redistribution enhanced monolithic etched copper foam-based Cu2O layer/TiO2 nanodots heterojunction with high hydrogen evolution electrocatalytic activity. **2019,** *243*, 365-372.
67. Armand, M.; Tarascon, J. M., Building better batteries. *Nature* **2008,** *451*, 652-657.
68. Najam, T.; Shah, S. S. A.; Peng, L.; Javed, M. S.; Imran, M.; Zhao, M.-Q.; Tsiakaras, P., Synthesis and nano-engineering of MXenes for energy conversion and storage applications: Recent advances and perspectives. *Coordination Chemistry Reviews* **2022,** *454*, 214339.
69. Shah, S. S.; Najam, T.; Brouzgou, A.; Tsiakaras, P., Alkaline Oxygen Electrocatalysis for Fuel Cells and Metal–Air Batteries. **2007**, 1-28.
70. Liang, H.; Gong, X.; Jia, L.; Chen, F.; Rao, Z.; Jing, S.; Tsiakaras, P., Highly efficient Li-O2 batteries based on self-standing NiFeP@ NC/BC cathode derived from biochar supported Prussian blue analogues. **2020,** *867*, 114124.
71. Lyu, D.; Yao, S.; Ali, A.; Tian, Z.; Tsiakaras, P.; Shen, P. Codoped Carbon Matrix-Encapsulated Co9S8 Nanoparticles as a Highly Efficient and Durable Bifunctional Oxygen Redox Electrocatalyst for Rechargeable Zn-Air Batteries [J]. **2021,** *11*, 2101249.
72. Jing, S.; Ding, P.; Zhang, Y.; Liang, H.; Yin, S.; Tsiakaras, P., Lithium-sulfur battery cathodes made of porous biochar support CoFe@ NC metal nanoparticles derived from Prussian blue analogues. **2019,** *25*, 5297-5304.
73. Jing, S.; Zhang, Y.; Chen, F.; Liang, H.; Yin, S.; Tsiakaras, P., Novel and highly efficient cathodes for Li-O2 batteries: 3D self-standing NiFe@ NC-functionalized N-doped carbon nanonet derived from Prussian blue analogues/biomass composites. **2019,** *245*, 721-732.
74. Liang, H.; Zhang, Y.; Chen, F.; Jing, S.; Yin, S.; Tsiakaras, P., A novel NiFe@ NC-functionalized N-doped carbon microtubule network derived from biomass as a highly efficient 3D free-standing cathode for Li-CO2 batteries. **2019,** *244*, 559-567.
75. Liang, H.; Chen, F.; Zhang, M.; Jing, S.; Shen, B.; Yin, S.; Tsiakaras, P., Highly performing free standing cathodic electrocatalysts for Li-O2 batteries: CoNiO2 nanoneedle arrays supported on N-doped carbon nanonet. **2019,** *574*, 114-121.
76. Zhang, G.; Shi, Y.; Wang, H.; Jiang, L.; Yu, X.; Jing, S.; Xing, S.; Tsiakaras, P., A facile route to achieve ultrafine Fe2O3 nanorods anchored on graphene oxide for application in lithium-ion battery. **2019,** *416*, 118-124.
77. Goodenough, J. B., How we made the Li-ion rechargeable battery. *Nature Electronics* **2018,** *1*, 204-204.
78. Winter, M.; Brodd, R. J., What Are Batteries, Fuel Cells, and Supercapacitors? *Chemical Reviews* **2004,** *104*, 4245-4270.
79. Frackowiak, E., Carbon materials for supercapacitor application. *Physical Chemistry Chemical Physics* **2007,** *9*, 1774-1785.
80. Tan, A.-d.; Wang, Y.-f.; Fu, Z.-y.; Tsiakaras, P.; Liang, Z.-x., Highly effective oxygen reduction reaction electrocatalysis: Nitrogen-doped hierarchically mesoporous carbon derived from interpenetrated nonporous metal-organic frameworks. *Applied Catalysis B: Environmental* **2017,** *218*, 260-266.

81. Andreadis, G.; Podias, A.; Tsiakaras, P., The effect of the parasitic current on the direct ethanol PEM fuel cell operation. **2008,** *181*, 214-227.
82. Wang, Y.; He, C.; Brouzgou, A.; Liang, Y.; Fu, R.; Wu, D.; Tsiakaras, P.; Song, S., A facile soft-template synthesis of ordered mesoporous carbon/tungsten carbide composites with high surface area for methanol electrooxidation. **2012,** *200*, 8-13.
83. Lagaeva, J.; Medvedev, D.; Demin, A.; Tsiakaras, P., Insights on thermal and transport features of BaCe0. 8− xZrxY0. 2O3− δ proton-conducting materials. **2015,** *278*, 436-444.
84. Wu, R.; Tsiakaras, P.; Shen, P. K., Facile synthesis of bimetallic Pt-Pd symmetry-broken concave nanocubes and their enhanced activity toward oxygen reduction reaction. *Applied Catalysis B: Environmental* **2019,** *251*, 49-56.
85. Chen, Q.; Chen, Z.; Ali, A.; Luo, Y.; Feng, H.; Luo, Y.; Tsiakaras, P.; Kang Shen, P., Shell-thickness-dependent Pd@PtNi core–shell nanosheets for efficient oxygen reduction reaction. *Chemical Engineering Journal* **2022,** *427*, 131565.
86. Brouzgou, A.; Seretis, A.; Song, S.; Shen, P. K.; Tsiakaras, P., CO tolerance and durability study of PtMe (Me= Ir or Pd) electrocatalysts for H2-PEMFC application. **2021,** *46*, 13865-13877.
87. Zhu, X.; Huang, L.; Wei, M.; Tsiakaras, P.; Shen, P., Highly stable Pt-Co nanodendrite in nanoframe with Pt skin structured catalyst for oxygen reduction electrocatalysis. **2021,** *281*, 119460.
88. Molochas, C.; Tsiakaras, P. Carbon Monoxide Tolerant Pt-Based Electrocatalysts for H2-PEMFC Applications: Current Progress and Challenges. **2021,** *11*, 1127.
89. Jain, N.; Roy, A.; Jain, R.; Karmakar, N., Polymer Electrolyte Membrane Fuel Cells: Alternative to fossil fuels for power supply to Heavy Earth Moving and Allied Machinery in Mining and Civil Engineering Industry. In Dec: **2013**.
90. Vaghari, H.; Jafarizadeh-Malmiri, H.; Berenjian, A.; Anarjan, N., Recent advances in application of chitosan in fuel cells. **2013,** *1*, 1-12.
91. Luo, Y.; Shi, Y.; Cai, N., Chapter 3 - Bridging a bi-directional connection between electricity and fuels in hybrid multienergy systems. In *Hybrid Systems and Multi-energy Networks for the Future Energy Internet*, Luo, Y.; Shi, Y.; Cai, N., Eds. Academic Press: **2021**, 41-84.
92. Sudhakar, Y. N.; Selvakumar, M.; Bhat, D. K., Chapter 5 - Biopolymer Electrolytes for Fuel Cell Applications. In *Biopolymer Electrolytes*, Sudhakar, Y. N.; Selvakumar, M.; Bhat, D. K., Eds. Elsevier: **2018**, 151-166.
93. Taroco, H.; Santos, J.; Domingues, R.; Matencio, T., Ceramic materials for solid oxide fuel cells. *Advances in ceramics-Synthesis and Characterization, processing and specific applications* **2011**, 423-446.
94. Dincer, I.; Rosen, M. A., Chapter 18 - Exergy analyses of fuel cell systems. In *Exergy (Third Edition)*, Dincer, I.; Rosen, M. A., Eds. Elsevier: **2021**, 479-514.
95. Vaghari, H.; Jafarizadeh-Malmiri, H.; Berenjian, A.; Anarjan, N., Recent advances in application of chitosan in fuel cells. *Sustainable Chemical Processes* **2013,** *1*, 1-12.
96. Jiang, L.; Sun, G., FUEL CELLS – DIRECT ALCOHOL FUEL CELLS | Direct Ethanol Fuel Cells. In *Encyclopedia of Electrochemical Power Sources*, Garche, J., Ed. Elsevier: Amsterdam, **2009**, 390-401.
97. Balkourani, G.; Brouzgou, A.; Vecchio, C. L.; Aricò, A. S.; Baglio, V.; Tsiakaras, P., Selective electro-oxidation of dopamine on Co or Fe supported onto N-doped ketjenblack. *Electrochimica Acta* **2022,** *409*, 139943.
98. Sharma, N.; Mutreja, V.; Kaur, H., Electrochemical sensors. *European Journal of Molecular & Clinical Medicine* **2020,** *7*, 2020.
99. Coutelieris, F.; Douvartzides, S.; Tsiakaras, P., The importance of the fuel choice on the efficiency of a solid oxide fuel cell system. **2003,** *123*, 200-205.
100. Song, S.; Maragou, V.; Tsiakaras, P., How far are direct alcohol fuel cells from our energy future? **2007**.
101. Iulianelli, A.; Ribeirinha, P.; Mendes, A.; Basile, A., Methanol steam reforming for hydrogen generation via conventional and membrane reactors: A review. *Renewable and Sustainable Energy Reviews* **2014,** *29*, 355-368.
102. Vidal Vázquez, F.; Simell, P.; Pennanen, J.; Lehtonen, J., Reactor design and catalysts testing for hydrogen production by methanol steam reforming for fuel cells applications. *International Journal of Hydrogen Energy* **2016,** *41*, 924-935.
103. Sharma, Y. C.; Kumar, A.; Prasad, R.; Upadhyay, S. N., Ethanol steam reforming for hydrogen production: Latest and effective catalyst modification strategies to minimize carbonaceous deactivation. *Renewable and Sustainable Energy Reviews* **2017,** *74*, 89-103.
104. Wang, F. In *Hydrogen production from steam reforming of ethanol over an Ir/ceria-based catalyst : catalyst ageing analysis and performance improvement upon ceria doping*, *Université Claude Bernard - Lyon I, 2012. English,* ***2012***.

105. Dimitrova, Z. In *Fuel cell electric vehicles. Investigation of the energy balance for optimal reforming process of bio-ethanol*, IOP Conference Series: Materials Science and Engineering, 2020; IOP Publishing: **2020**, 120-125.
106. Ma, S.; Lin, M.; Lin, T.-E.; Lan, T.; Liao, X.; Maréchal, F.; Van herle, J.; Yang, Y.; Dong, C.; Wang, L., Fuel cell-battery hybrid systems for mobility and off-grid applications: A review. *Renewable and Sustainable Energy Reviews* **2021,** *135*, 110119.
107. Acar, C.; Dincer, I., 3.1 Hydrogen Production. In *Comprehensive Energy Systems*, Dincer, I., Ed. Elsevier: Oxford, **2018**, 1-40.
108. Dou, B.; Song, Y.; Wang, C.; Chen, H.; Xu, Y. J. R.; Reviews, S. E., Hydrogen production from catalytic steam reforming of biodiesel byproduct glycerol: Issues and challenges. **2014,** *30*, 950-960.
109. Kaiwen, L.; Bin, Y.; Tao, Z. J. E. S., Part B: Economics, Planning,; Policy, Economic analysis of hydrogen production from steam reforming process: A literature review. **2018,** *13*, 109-115.
110. Contreras, J. L.; Salmones, J.; Colín-Luna, J. A.; Nuño, L.; Quintana, B.; Córdova, I.; Zeifert, B.; Tapia, C.; Fuentes, G. A., Catalysts for H2 production using the ethanol steam reforming (a review). *International Journal of Hydrogen Energy* **2014,** *39*, 18835-18853.
111. Sá, S.; Silva, H.; Brandão, L.; Sousa, J. M.; Mendes, A., Catalysts for methanol steam reforming—A review. *Applied Catalysis B: Environmental* **2010,** *99*, 43-57.
112. Minh, D. P.; Siang, T. J.; Vo, D.-V. N.; Phan, T. S.; Ridart, C.; Nzihou, A.; Grouset, D., Hydrogen production from biogas reforming: An overview of steam reforming, dry reforming, dual reforming, and tri-reforming of methane. **2018**, 111-166.
113. Gangadharan, P.; Kanchi, K. C.; Lou, H. H., Evaluation of the economic and environmental impact of combining dry reforming with steam reforming of methane. *Chemical Engineering Research and Design* **2012,** *90*, 1956-1968.
114. Bahari, M. B.; Phuc, N. H. H.; Abdullah, B.; Alenazey, F.; Vo, D.-V. N., Ethanol dry reforming for syngas production over Ce-promoted Ni/Al2O3 catalyst. **2016,** *4*, 4830-4838.
115. Kang, I.; Bae, J.; Bae, G., Performance comparison of autothermal reforming for liquid hydrocarbons, gasoline and diesel for fuel cell applications. *Journal of Power Sources* **2006,** *163*, 538-546.
116. Balopi, B.; Moyo, M.; Gorimbo, J., Autothermal Reforming of Bio-ethanol: A Short Review of Strategies Used to Synthesize Coke-Resistant Nickel-Based Catalysts. **2022**, 1-13.
117. Hohn, K. L.; Lin, Y. C.; Energy, S.; Materials, Catalytic partial oxidation of methanol and ethanol for hydrogen generation. **2009,** *2*, 927-940.
118. Salge, J.; Deluga, G.; Schmidt, L., Catalytic partial oxidation of ethanol over noble metal catalysts. **2005,** *235*, 69-78.
119. Arku, P.; Regmi, B.; Dutta, A., A review of catalytic partial oxidation of fossil fuels and biofuels: Recent advances in catalyst development and kinetic modelling. *Chemical Engineering Research and Design* **2018,** *136*, 385-402.
120. Avgouropoulos, G.; Ioannides, T.; Kallitsis, J. K.; Neophytides, S., Development of an internal reforming alcohol fuel cell: Concept, challenges and opportunities. *Chemical Engineering Journal* **2011,** *176-177*, 95-101.
121. Cimenti, M.; Hill, J. M., Direct Utilization of Liquid Fuels in SOFC for Portable Applications: Challenges for the Selection of Alternative Anodes. *Energies* **2009,** *2*, 377-410.
122. Aguiar, P.; Adjiman, C. S.; Brandon, N. P., Anode-supported intermediate temperature direct internal reforming solid oxide fuel cell. I: model-based steady-state performance. *Journal of Power Sources* **2004,** *138*, 120-136.
123. Clarke, S. H.; Dicks, A. L.; Pointon, K.; Smith, T. A.; Swann, A., Catalytic aspects of the steam reforming of hydrocarbons in internal reforming fuel cells. *Catalysis Today* **1997,** *38*, 411-423.
124. Aguiar, P.; Chadwick, D.; Kershenbaum, L., Modelling of an indirect internal reforming solid oxide fuel cell. *Chemical Engineering Science* **2002,** *57*, 1665-1677.
125. Dicks, A. L., Advances in catalysts for internal reforming in high temperature fuel cells. *Journal of Power Sources* **1998,** *71*, 111-122.
126. Santoro, M.; Di Bartolomeo, E.; Luisetto, I.; Aricò, A. S.; Squadrito, G.; Zignani, S. C.; Lo Faro, M., Insights on the electrochemical performance of indirect internal reforming of biogas into a solid oxide fuel cell. *Electrochimica Acta* **2022,** *409*, 139-940.
127. Dokamaingam, P.; Assabumrungrat, S.; Soottitantawat, A.; Sramala, I.; Laosiripojana, N., Modeling of SOFC with indirect internal reforming operation: Comparison of conventional packed-bed and catalytic coated-wall internal reformer. *International Journal of Hydrogen Energy* **2009,** *34*, 410-421.

128. Chatrattanawet, N.; Saebea, D.; Authayanun, S.; Arpornwichanop, A.; Patcharavorachot, Y., Performance and environmental study of a biogas-fuelled solid oxide fuel cell with different reforming approaches. *Energy* **2018,** *146*, 131-140.
129. Long, G.-f.; Wan, K.; Liu, M.-y.; Liang, Z.-x.; Piao, J.-h.; Tsiakaras, P., Active sites and mechanism on nitrogen-doped carbon catalyst for hydrogen evolution reaction. **2017,** *348*, 151-159.
130. Prykhodko, Y.; Fatyeyeva, K.; Hespel, L.; Marais, S., Progress in hybrid composite Nafion®-based membranes for proton exchange fuel cell application. *Chemical Engineering Journal* **2021,** *409*, 127329.
131. Zhang, H.; Shen, P. K., Recent Development of Polymer Electrolyte Membranes for Fuel Cells. *Chemical Reviews* **2012,** *112*, 2780-2832.
132. Song, S.; Tsiakaras, P., Recent progress in direct ethanol proton exchange membrane fuel cells (DE-PEMFCs). *Applied Catalysis B: Environmental* **2006,** *63*, 187-193.
133. Monyoncho, E. A.; Steinmann, S. N.; Michel, C.; Baranova, E. A.; Woo, T. K.; Sautet, P., Ethanol Electro-oxidation on Palladium Revisited Using Polarization Modulation Infrared Reflection Absorption Spectroscopy (PM-IRRAS) and Density Functional Theory (DFT): Why Is It Difficult To Break the C–C Bond? *ACS Catalysis* **2016,** *6*, 4894-4906.
134. Sheng, W.; Zheng, L.; Liu, Y.; Zhao, X.; Weng, J.; Zhang, Y., Sensitive detection of dopamine via leucodopaminechrome on polyacrylic acid-coated ceria nanorods. *Nanotechnology* **2017,** *28*, 365504.
135. Colmati, F.; Tremiliosi-Filho, G.; Gonzalez, E. R.; Berná, A.; Herrero, E.; Feliu, J. M., The role of the steps in the cleavage of the C–C bond during ethanol oxidation on platinum electrodes. *Physical Chemistry Chemical Physics* **2009,** *11*, 9114-9123.
136. Song, S. Q.; Zhou, W. J.; Zhou, Z. H.; Jiang, L. H.; Sun, G. Q.; Xin, Q.; Leontidis, V.; Kontou, S.; Tsiakaras, P., Direct ethanol PEM fuel cells: The case of platinum based anodes. *International Journal of Hydrogen Energy* **2005,** *30*, 995-1001.
137. Andreadis, G.; Tsiakaras, P., Ethanol crossover and direct ethanol PEM fuel cell performance modeling and experimental validation. *Chemical Engineering Science* **2006,** *61*, 7497-7508.
138. Kamarudin, M. Z. F.; Kamarudin, S. K.; Masdar, M. S.; Daud, W. R. W., Review: Direct ethanol fuel cells. *International Journal of Hydrogen Energy* **2013,** *38*, 9438-9453.
139. Pereira, J. P.; Falcão, D. S.; Oliveira, V. B.; Pinto, A. M. F. R., Performance of a passive direct ethanol fuel cell. *Journal of Power Sources* **2014,** *256*, 14-19.
140. Zheng, Y.; Wan, X.; Cheng, X.; Cheng, K.; Dai, Z.; Liu, Z., Advanced Catalytic Materials for Ethanol Oxidation in Direct Ethanol Fuel Cells. *Catalysts* **2020,** *10*, 166.
141. Gottesfeld, S.; Dekel, D. R.; Page, M.; Bae, C.; Yan, Y.; Zelenay, P.; Kim, Y. S., Anion exchange membrane fuel cells: Current status and remaining challenges. *Journal of Power Sources* **2018,** *375*, 170-184.
142. Tsiakaras, P.; Vayenas, C., Oxidative coupling of CH4 on Ag catalyst-electrodes deposited on ZrO2 (8 mol% Y2O3). **1993,** *144*, 333-347.
143. Wang, K.; Wang, Y.; Liang, Z.; Liang, Y.; Wu, D.; Song, S.; Tsiakaras, P., Ordered mesoporous tungsten carbide/carbon composites promoted Pt catalyst with high activity and stability for methanol electrooxidation. **2014,** *147*, 518-525.
144. Brouzgou, A.; Song, S.; Tsiakaras, P., Carbon-supported PdSn and Pd3Sn2 anodes for glucose electrooxidation in alkaline media. **2014,** *158*, 209-216.
145. An, L.; Zhao, T. J. E.; Science, E., An alkaline direct ethanol fuel cell with a cation exchange membrane. **2011,** *4*, 2213-2217.
146. An, L.; Zhao, T., *Anion Exchange Membrane Fuel Cells*. Springer: **2018**.
147. Hou, H.; Sun, G.; He, R.; Wu, Z.; Sun, B., Alkali doped polybenzimidazole membrane for high performance alkaline direct ethanol fuel cell. **2008,** *182*, 95-99.
148. Hickner, M. A.; Herring, A. M.; Coughlin, E. B., Anion exchange membranes: Current status and moving forward. **2013,** *51*, 1727-1735.
149. Singh, P.; Minh, N. Q., Solid oxide fuel cells: technology status. *International Journal of Applied Ceramic Technology* **2004,** *1*, 5-15.
150. Singhal, S. C., Advances in solid oxide fuel cell technology. *Solid State Ionics* **2000,** *135*, 305-313.
151. Yamamoto, O., Solid oxide fuel cells: fundamental aspects and prospects. *Electrochimica Acta* **2000,** *45*, 2423-2435.
152. Sønderby, S. In *Yttria-Stabilized Zirconia and Gadolinia-Doped Ceria Thin Films for Fuel Cell Applications*, **2014**.
153. Fergus, J. W., Electrolytes for solid oxide fuel cells. *Journal of Power Sources* **2006,** *162*, 30-40.

154. Ormerod, R. M., Solid oxide fuel cells. *Chemical Society Reviews* **2003,** *32*, 17-28.
155. Jacobson, A. J., Materials for Solid Oxide Fuel Cells. *Chemistry of Materials* **2010,** *22*, 660-674.
156. Brouzgou, A.; Tzorbatzoglou, F.; Tsiakaras, P. In *Direct Alcohol Fuel Cells: Challenges and future trends*, Proceedings of the 2011 3rd International Youth Conference on Energetics (IYCE), 7-9 July **2011**, 1-6.
157. Steil, M.; Nobrega, S.; Georges, S.; Gelin, P.; Uhlenbruck, S.; Fonseca, F., Durable direct ethanol anode-supported solid oxide fuel cell. **2017,** *199*, 180-186.
158. Ye, X.-F.; Wang, S. R.; Hu, Q.; Wang, Z. R.; Wen, T. L.; Wen, Z. Y., Improvement of multi-layer anode for direct ethanol Solid Oxide Fuel Cells. *Electrochemistry Communications* **2009,** *11*, 823-826.
159. Nobrega, S. D.; Galesco, M. V.; Girona, K.; de Florio, D. Z.; Steil, M. C.; Georges, S.; Fonseca, F. C., Direct ethanol solid oxide fuel cell operating in gradual internal reforming. *Journal of Power Sources* **2012,** *213*, 156-159.
160. Singh, M.; Zappa, D.; Comini, E., Solid oxide fuel cell: Decade of progress, future perspectives and challenges. *International Journal of Hydrogen Energy* **2021,** *46*, 27643-27674.
161. Wang, W.; Su, C.; Ran, R.; Zhao, B.; Shao, Z.; Tade, M.; Liu, S., Nickel-Based Anode with Water Storage Capability to Mitigate Carbon Deposition for Direct Ethanol Solid Oxide Fuel Cells. *ChemSusChem* **2014,** *7*.
162. Steil, M. C.; Nobrega, S. D.; Georges, S.; Gelin, P.; Uhlenbruck, S.; Fonseca, F. C., Durable direct ethanol anode-supported solid oxide fuel cell. *Applied Energy* **2017,** *199*, 180-186.
163. Xie, Z.; Xia, C.; Zhang, M.; Zhu, W.; Wang, H., Ni1−xCux alloy-based anodes for low-temperature solid oxide fuel cells with biomass-produced gas as fuel. *Journal of Power Sources* **2006,** *161*, 1056-1061.
164. Malavasi, L.; Fisher, C. A. J.; Islam, M. S., Oxide-ion and proton conducting electrolyte materials for clean energy applications: structural and mechanistic features. *Chemical Society Reviews* **2010,** *39*, 4370-4387.
165. Yang, L.; Wang, S.; Blinn, K.; Liu, M.; Liu, Z.; Cheng, Z.; Liu, M., Enhanced Sulfur and Coking Tolerance of a Mixed Ion Conductor for SOFCs. *Science* **2009,** *326*, 126-129.
166. Burhan, H.; Yılmaz, M.; Cellat, K.; Zeytun, A.; Yılmaz, G.; Şen, F., Chapter 4 - Direct ethanol fuel cells (DEFCs). In *Direct Liquid Fuel Cells*, Akay, R. G.; Yurtcan, A. B., Eds. Academic Press: **2021**, 95-113.
167. Akay, R. G.; Yurtcan, A. B., *Direct Liquid Fuel Cells: Fundamentals, Advances and Future*. Elsevier Science: 2020.
168. Taymaz, I.; Benli, M., Numerical study of assembly pressure effect on the performance of proton exchange membrane fuel cell. *Energy* **2010,** *35*, 2134-2140.
169. Tayal, J.; Rawat, B.; Basu, S., Effect of addition of rhenium to Pt-based anode catalysts in electro-oxidation of ethanol in direct ethanol PEM fuel cell. *International Journal of Hydrogen Energy* **2012,** *37*, 4597-4605.
170. Chen, A.; Holt-Hindle, P., Platinum-Based Nanostructured Materials: Synthesis, Properties, and Applications. *Chemical Reviews* **2010,** *110*, 3767-3804.
171. Liu, C.-W.; Chang, Y.-W.; Wei, Y.-C.; Wang, K.-W., The effect of oxygen containing species on the catalytic activity of ethanol oxidation for PtRuSn/C catalysts. *Electrochimica Acta* **2011,** *56*, 2574-2581.
172. Figueiredo, M. C.; Sorsa, O.; Arán-Ais, R. M.; Doan, N.; Feliu, J. M.; Kallio, T., Trimetallic catalyst based on PtRu modified by irreversible adsorption of Sb for direct ethanol fuel cells. *Journal of Catalysis* **2015,** *329*, 69-77.
173. Akhairi, M. A. F.; Kamarudin, S. K., Catalysts in direct ethanol fuel cell (DEFC): An overview. *International Journal of Hydrogen Energy* **2016,** *41*, 4214-4228.
174. Perez, J.; Paganin, V. A.; Antolini, E., Particle size effect for ethanol electro-oxidation on Pt/C catalysts in half-cell and in a single direct ethanol fuel cell. *Journal of Electroanalytical Chemistry* **2011,** *654*, 108-115.
175. Tayal, J.; Rawat, B.; Basu, S., Effect of addition of rhenium to Pt-based anode catalysts in electro-oxidation of ethanol in direct ethanol PEM fuel cell. **2012,** *37*, 4597-4605.
176. Anwar, M. T.; Yan, X.; Shen, S.; Husnain, N.; Zhu, F.; Luo, L.; Zhang, J., Enhanced durability of Pt electrocatalyst with tantalum doped titania as catalyst support. *International Journal of Hydrogen Energy* **2017,** *42*, 30750-30759.
177. Zhou, W.; Zhou, Z.; Song, S.; Li, W.; Sun, G.; Tsiakaras, P.; Xin, Q., Pt based anode catalysts for direct ethanol fuel cells. *Applied Catalysis B: Environmental* **2003,** *46*, 273-285.
178. Chelaghmia, M.; Nacef, M.; Fisli, H.; Affoune, A.; Pontié, M.; Makhlouf, A.; Derabla, T.; Khelifi, O.; Aissat, F., Electrocatalytic performance of Pt–Ni nanoparticles supported on an activated graphite electrode for ethanol and 2-propanol oxidation. *RSC advances* **2020,** *10*, 36941-36948.
179. Zhou, W. J.; Song, S. Q.; Li, W. Z.; Zhou, Z. H.; Sun, G. Q.; Xin, Q.; Douvartzides, S.; Tsiakaras, P., Direct ethanol fuel cells based on PtSn anodes: the effect of Sn content on the fuel cell performance. *Journal of Power Sources* **2005,** *140*, 50-58.

180. Neto, A. O.; Dias, R. R.; Tusi, M. M.; Linardi, M.; Spinacé, E. V., Electro-oxidation of methanol and ethanol using PtRu/C, PtSn/C and PtSnRu/C electrocatalysts prepared by an alcohol-reduction process. *Journal of Power Sources* **2007,** *166*, 87-91.
181. Atbas, D.; Çağlar, A.; Kivrak, H.; Kivrak, A., Microwave assisted synthesis of Sn promoted Pt catalysts and their ethanol electro-oxidation activities. *Am. J. Nanomater* **2016,** *4*, 8-11.
182. Wnuk, P.; Jurczakowski, R.; Lewera, A., Electrochemical Characterization of Low-Temperature Direct Ethanol Fuel Cells using Direct and Alternate Current Methods. *Electrocatalysis* **2020,** *11*, 121-132.
183. Bergamaski, K.; Gonzalez, E. R.; Nart, F. C., Ethanol oxidation on carbon supported platinum-rhodium bimetallic catalysts. *Electrochimica Acta* **2008,** *53*, 4396-4406.
184. Wala, M.; Simka, W., Effect of Anode Material on Electrochemical Oxidation of Low Molecular Weight Alcohols—A Review. *Molecules* **2021,** *26*, 2144.
185. González Pereira, M.; Dávila Jiménez, M.; Elizalde, M. P.; Manzo-Robledo, A.; Alonso-Vante, N., Study of the electrooxidation of ethanol on hydrophobic electrodes by DEMS and HPLC. *Electrochimica Acta* **2004,** *49*, 3917-3925.
186. Antolini, E., Catalysts for direct ethanol fuel cells. *Journal of Power Sources* **2007,** *170*, 1-12.
187. Camara, G. A.; de Lima, R. B.; Iwasita, T., Catalysis of ethanol electrooxidation by PtRu: the influence of catalyst composition. *Electrochemistry Communications* **2004,** *6*, 812-815.
188. Lima, F.; Gonzalez, E., Ethanol electro-oxidation on carbon-supported Pt–Ru, Pt–Rh and Pt–Ru–Rh nanoparticles. *Electrochimica Acta* **2008,** *53*, 2963-2971.
189. Silva-Junior, L. C.; Maia, G.; Passos, R. R.; de Souza, E. A.; Camara, G. A.; Giz, M. J., Analysis of the selectivity of PtRh/C and PtRhSn/C to the formation of CO2 during ethanol electrooxidation. *Electrochimica Acta* **2013,** *112*, 612-619.
190. Wang, P.; Wen, Y.; Yin, S.; Wang, N.; Shen, P. K., PtRh alloys on hybrid TiO2–Carbon support as high efficiency catalyst for ethanol oxidation. *International Journal of Hydrogen Energy* **2017,** *42*, 24689-24696.
191. Kadirgan, F.; Beyhan, S.; Atilan, T., Preparation and characterization of nano-sized Pt–Pd/C catalysts and comparison of their electro-activity toward methanol and ethanol oxidation. *International Journal of Hydrogen Energy* **2009,** *34*, 4312-4320.
192. dos Santos Almeida, T.; De Andrade, A. R., *New and Future Developments in Catalysis: Chapter 15. New Trends in Direct Ethanol Fuel Cells*. Elsevier Science: **2013**.
193. Altarawneh, R. M.; Brueckner, T. M.; Chen, B.; Pickup, P. G., Product distributions and efficiencies for ethanol oxidation at PtNi octahedra. *Journal of Power Sources* **2018,** *400*, 369-376.
194. Sulaiman, J. E.; Zhu, S.; Xing, Z.; Chang, Q.; Shao, M., Pt–Ni octahedra as electrocatalysts for the ethanol electro-oxidation reaction. *ACS Catalysis* **2017,** *7*, 5134-5141.
195. Zheng, Y.; Qiao, J.; Yuan, J.; Shen, J.; Wang, A.-j.; Huang, S., Controllable synthesis of PtPd nanocubes on graphene as advanced catalysts for ethanol oxidation. *International Journal of Hydrogen Energy* **2018,** *43*, 4902-4911.
196. Liu, J.; Cao, L.; Huang, W.; Li, Z., Direct electrodeposition of PtPd alloy foams comprised of nanodendrites with high electrocatalytic activity for the oxidation of methanol and ethanol. *Journal of Electroanalytical Chemistry* **2012,** *686*, 38-45.
197. Wu, D.; Shen, X.; Pan, Y.; Yao, L.; Peng, Z., Platinum alloy catalysts for oxygen reduction reaction: Advances, challenges and perspectives. *ChemNanoMat* **2020,** *6*, 32-41.
198. Zhou, W.; Zhou, Z.; Song, S.; Li, W.; Sun, G.; Tsiakaras, P.; Xin, Q., Pt based anode catalysts for direct ethanol fuel cells. **2003,** *46*, 273-285.
199. Tanaka, S.; Umeda, M.; Ojima, H.; Usui, Y.; Kimura, O.; Uchida, I., Preparation and evaluation of a multi-component catalyst by using a co-sputtering system for anodic oxidation of ethanol. *Journal of Power Sources* **2005,** *152*, 34-39.
200. Li, G.; Pickup, P. G., The promoting effect of Pb on carbon supported Pt and Pt/Ru catalysts for electro-oxidation of ethanol. *Electrochimica Acta* **2006,** *52*, 1033-1037.
201. Spinacé, E.; Dias, R. R.; Brandalise, M.; Linardi, M.; Neto, A. O., Electro-oxidation of ethanol using PtSnRh/C electrocatalysts prepared by an alcohol-reduction process. *Ionics* **2010,** *16*, 91-95.
202. Cunha, E. M.; Ribeiro, J.; Kokoh, K. B.; de Andrade, A. R., Preparation, characterization and application of Pt–Ru–Sn/C trimetallic electrocatalysts for ethanol oxidation in direct fuel cell. *International Journal of Hydrogen Energy* **2011,** *36*, 11034-11042.

203. Thepkaew, J.; Therdthianwong, S.; Therdthianwong, A.; Kucernak, A.; Wongyao, N., Promotional roles of Ru and Sn in mesoporous PtRu and PtRuSn catalysts toward ethanol electrooxidation. *International Journal of Hydrogen Energy* **2013,** *38*, 9454-9463.
204. García, G.; Tsiouvaras, N.; Pastor, E.; Peña, M. A.; Fierro, J. L. G.; Martínez-Huerta, M. V., Ethanol oxidation on PtRuMo/C catalysts: In situ FTIR spectroscopy and DEMS studies. *International Journal of Hydrogen Energy* **2012,** *37*, 7131-7140.
205. Nakagawa, N.; Watanabe, T.; Wagatsuma, M.; Tsujiguchi, T. In *Carbon-Supported PtRuRh Nanoparticles as a Catalyst for Direct Ethanol Fuel Cells*, Key Engineering Materials, 2012; Trans Tech Publ: 2012; pp 67-72.
206. Antolini, E., Iron-containing platinum-based catalysts as cathode and anode materials for low-temperature acidic fuel cells: a review. *RSC advances* **2016,** *6*, 3307-3325.
207. Choudhary, A. K.; Pramanik, H., Addition of rhenium (Re) to Pt-Ru/f-MWCNT anode electrocatalysts for enhancement of ethanol electrooxidation in half cell and single direct ethanol fuel cell. *International Journal of Hydrogen Energy* **2020,** *45*, 13300-13321.
208. Spinacé, E. V.; Linardi, M.; Neto, A. O., Co-catalytic effect of nickel in the electro-oxidation of ethanol on binary Pt–Sn electrocatalysts. **2005,** *7*, 365-369.
209. Spinacé, E.; Neto, A. O.; Linardi, M., Electro-oxidation of methanol and ethanol using PtRu/C electrocatalysts prepared by spontaneous deposition of platinum on carbon-supported ruthenium nanoparticles. *Journal of Power Sources* **2004,** *129*, 121-126.
210. Beyhan, S.; Léger, J.-M.; Kadırgan, F., Pronounced synergetic effect of the nano-sized PtSnNi/C catalyst for ethanol oxidation in direct ethanol fuel cell. *Applied Catalysis B: Environmental* **2013,** *130-131*, 305-313.
211. Almeida, T.; Palma, L.; Morais, C.; Kokoh, K.; De Andrade, A., Effect of adding a third metal to carbon-supported PtSn-based nanocatalysts for direct ethanol fuel cell in acidic medium. **2013,** *160*, F965.
212. Rousseau, S.; Coutanceau, C.; Lamy, C.; Léger, J. M., Direct ethanol fuel cell (DEFC): Electrical performances and reaction products distribution under operating conditions with different platinum-based anodes. *Journal of Power Sources* **2006,** *158*, 18-24.
213. Antolini, E.; Colmati, F.; Gonzalez, E. R., Effect of Ru addition on the structural characteristics and the electrochemical activity for ethanol oxidation of carbon supported Pt–Sn alloy catalysts. *Electrochemistry Communications* **2007,** *9*, 398-404.
214. Ribeiro, J.; Dos Anjos, D.; Kokoh, K. B.; Coutanceau, C.; Léger, J.-M.; Olivi, P.; De Andrade, A.; Tremiliosi-Filho, G., Carbon-supported ternary PtSnIr catalysts for direct ethanol fuel cell. *Electrochimica Acta* **2007,** *52*, 6997-7006.
215. De Souza, R. F. B.; Parreira, L. S.; Silva, J. C. M.; Simões, F. C.; Calegaro, M. L.; Giz, M. J.; Camara, G. A.; Neto, A. O.; Santos, M. C., PtSnCe/C electrocatalysts for ethanol oxidation: DEFC and FTIR "in-situ" studies. *International Journal of Hydrogen Energy* **2011,** *36*, 11519-11527.
216. Ribeiro, J.; Dos Anjos, D.; Léger, J.-M.; Hahn, F.; Olivi, P.; De Andrade, A.; Tremiliosi-Filho, G.; Kokoh, K., Effect of W on PtSn/C catalysts for ethanol electrooxidation. **2008,** *38*, 653-662.
217. de Souza, E. A.; Giz, M. J.; Camara, G. A.; Antolini, E.; Passos, R. R., Ethanol electro-oxidation on partially alloyed Pt-Sn-Rh/C catalysts. *Electrochimica Acta* **2014,** *147*, 483-489.
218. Corradini, P. G.; Antolini, E.; Perez, J., Electro-oxidation of ethanol on ternary non-alloyed Pt–Sn–Pr/C catalysts. *Journal of Power Sources* **2015,** *275*, 377-383.
219. Jacob, J. M.; Corradini, P. G.; Antolini, E.; Santos, N. A.; Perez, J., Electro-oxidation of ethanol on ternary Pt–Sn–Ce/C catalysts. *Applied Catalysis B: Environmental* **2015,** *165*, 176-184.
220. Queiroz, M. A. R.; Ribeiro, J., Catalysts of PtSn/C modified with Ru and Ta for electrooxidation of ethanol. **2019,** *9*, 277.
221. Corradini, P. G.; Perez, J., Activity, mechanism, and short-term stability evaluation of PtSn-rare earth/C electrocatalysts for the ethanol oxidation reaction. **2018,** *22*, 1525-1537.
222. Lee, E.; Murthy, A.; Manthiram, A., Effect of Mo addition on the electrocatalytic activity of Pt–Sn–Mo/C for direct ethanol fuel cells. *Electrochimica Acta* **2011,** *56*, 1611-1618.
223. Rizo, R.; Bergmann, A.; Timoshenko, J.; Scholten, F.; Rettenmaier, C.; Jeon, H. S.; Chen, Y.-T.; Yoon, A.; Bagger, A.; Rossmeisl, J.; Roldan Cuenya, B., Pt-Sn-Co nanocubes as highly active catalysts for ethanol electro-oxidation. *Journal of Catalysis* **2021,** *393*, 247-258.
224. Suffredini, H. B.; Salazar-Banda, G. R.; Avaca, L. A., Enhanced ethanol oxidation on PbOx-containing electrode materials for fuel cell applications. *Journal of Power Sources* **2007,** *171*, 355-362.

225. Xu, X.; Lin, Q.; Liu, A.; Chen, W.; Weng, X.; Wang, C.; Lin, X., Simultaneous Voltammetric Determination of Ascorbic Acid, Dopamine and Uric Acid Using Polybromothymol Blue Film-Modified Glassy Carbon Electrode. *Chemical and Pharmaceutical Bulletin* **2010,** *58*, 788-793.
226. Comignani, V.; Sieben, J. M.; Brigante, M. E.; Duarte, M. M. E., Carbon supported Pt–NiO nanoparticles for ethanol electro-oxidation in acid media. *Journal of Power Sources* **2015,** *278*, 119-127.
227. Zignani, S. C.; Baglio, V.; Sebastián, D.; Siracusano, S.; Aricò, A. S., Enhancing ethanol oxidation rate at PtRu electro-catalysts using metal-oxide additives. *Electrochimica Acta* **2016,** *191*, 183-191.
228. Almeida, T. S.; Garbim, C.; Silva, R. G.; De Andrade, A. R., Addition of iron oxide to Pt-based catalyst to enhance the catalytic activity of ethanol electrooxidation. *Journal of Electroanalytical Chemistry* **2017,** *796*, 49-56.
229. Antolini, E., Iridium Application in Low-Temperature Acidic Fuel Cells: Pt-Free Ir-Based Catalysts or Second/Third Promoting Metal in Pt-Based Catalysts? *ChemElectroChem* **2014,** *1*, 318-328.
230. Cao, L.; Sun, G.; Li, H.; Xin, Q., Carbon-supported IrSn catalysts for a direct ethanol fuel cell. *Electrochemistry Communications* **2007,** *9*, 2541-2546.
231. Cao, L.; Sun, G.; Li, H.; Xin, Q., Carbon-supported IrSn catalysts for direct ethanol fuel cell. *Fuel Cells Bulletin* **2007**, 12-16.
232. Zhang, G.; Zhang, Z., Ir 3 Pb alloy nanodendrites with high performance for ethanol electrooxidation and their enhanced durability by alloying trace Au. *Inorganic Chemistry Frontiers* **2020,** *7*, 2231-2240.
233. Du, W.; Deskins, N. A.; Su, D.; Teng, X., Iridium–Ruthenium Alloyed Nanoparticles for the Ethanol Oxidation Fuel Cell Reactions. *ACS Catalysis* **2012,** *2*, 1226-1231.
234. Yang, L.; Kinoshita, S.; Yamada, T.; Kanda, S.; Kitagawa, H.; Tokunaga, M.; Ishimoto, T.; Ogura, T.; Nagumo, R.; Miyamoto, A., A metal–organic framework as an electrocatalyst for ethanol oxidation. *Angewandte Chemie* **2010,** *122*, 5476-5479.
235. Rohani, T.; Mohammadi, S. Z.; Beheshti-Marnani, A.; Taghizadeh, H., Cobalt nanoparticles introduced to activated carbon, CoNP/AC, as an effective electrocatalyst for oxidation and determination of methanol and ethanol. *International Journal of Hydrogen Energy* **2022,** *47*, 6837-6847.
236. Akhairi, M.; Kamarudin, S. K., Catalysts in direct ethanol fuel cell (DEFC): An overview. *International Journal of Hydrogen Energy* **2016,** *41*, 4214-4228.
237. Lopes, T.; Antolini, E.; Colmati, F.; Gonzalez, E. R., Carbon supported Pt–Co (3:1) alloy as improved cathode electrocatalyst for direct ethanol fuel cells. *Journal of Power Sources* **2007,** *164*, 111-114.
238. Lopes, T.; Antolini, E.; Gonzalez, E. R., Carbon supported Pt–Pd alloy as an ethanol tolerant oxygen reduction electrocatalyst for direct ethanol fuel cells. *International Journal of Hydrogen Energy* **2008,** *33*, 5563-5570.
239. Esfandiari, A.; Kazemeini, M.; Bastani, D., Synthesis, characterization and performance determination of an Ag@Pt/C electrocatalyst for the ORR in a PEM fuel cell. *International Journal of Hydrogen Energy* **2016,** *41*, 20720-20730.
240. Ma, K.-B.; Kwak, D.-H.; Han, S.-B.; Park, H.-S.; Kim, D.-H.; Won, J.-E.; Kwon, S.-H.; Kim, M.-C.; Moon, S.-H.; Park, K.-W.; Engineering, Direct ethanol fuel cells with superior ethanol-tolerant nonprecious metal cathode catalysts for oxygen reduction reaction. **2018,** *6*, 7609-7618.
241. Wei, Y.-C.; Liu, C.-W.; Lee, H.-W.; Chung, S.-R.; Lee, S.-L.; Chan, T.-S.; Lee, J.-F.; Wang, K.-W., Synergistic effect of Co alloying and surface oxidation on oxygen reduction reaction performance for the Pd electrocatalysts. *International Journal of Hydrogen Energy* **2011,** *36*, 3789-3802.
242. Osmieri, L.; Escudero-Cid, R.; Armandi, M.; Monteverde Videla, A. H. A.; García Fierro, J. L.; Ocón, P.; Specchia, S., Fe-N/C catalysts for oxygen reduction reaction supported on different carbonaceous materials. Performance in acidic and alkaline direct alcohol fuel cells. *Applied Catalysis B: Environmental* **2017,** *205*, 637-653.
243. Salomé, S.; Ferraria, A. M.; Botelho do Rego, A. M.; Alcaide, F.; Savadogo, O.; Rego, R., Enhanced activity and durability of novel activated carbon-supported PdSn heat-treated cathode catalyst for polymer electrolyte fuel cells. *Electrochimica Acta* **2016,** *192*, 268-282.
244. Chandran, P.; Puthusseri, D.; Ramaprabhu, S., 1D-2D integrated hybrid carbon nanostructure supported bimetallic alloy catalyst for ethanol oxidation and oxygen reduction reactions. *International Journal of Hydrogen Energy* **2019,** *44*, 4951-4961.
245. Wang, K.; Wang, F.; Zhao, Y.; Zhang, W., Surface-tailored PtPdCu ultrathin nanowires as advanced electrocatalysts for ethanol oxidation and oxygen reduction reaction in direct ethanol fuel cell. *Journal of Energy Chemistry* **2021,** *52*, 251-261.

246. Peighambardoust, S. J.; Rowshanzamir, S.; Amjadi, M., Review of the proton exchange membranes for fuel cell applications. *International Journal of Hydrogen Energy* **2010,** *35*, 9349-9384.
247. Zakaria, Z.; Kamarudin, S. K.; Timmiati, S., Membranes for direct ethanol fuel cells: an overview. *Applied Energy* **2016,** *163*, 334-342.
248. Casciola, M.; Alberti, G.; Sganappa, M.; Narducci, R., On the decay of Nafion proton conductivity at high temperature and relative humidity. *Journal of Power Sources* **2006,** *162*, 141-145.
249. Jablonski, A.; Kulesza, P. J.; Lewera, A., Oxygen permeation through Nafion 117 membrane and its impact on efficiency of polymer membrane ethanol fuel cell. *Journal of Power Sources* **2011,** *196*, 4714-4718.
250. Battirola, L. C.; Schneider, J. F.; Torriani, Í. C. L.; Tremiliosi-Filho, G.; Rodrigues-Filho, U. P., Improvement on direct ethanol fuel cell performance by using doped-Nafion® 117 membranes with Pt and Pt–Ru nanoparticles. *International Journal of Hydrogen Energy* **2013,** *38*, 12060-12068.
251. Matos, B. R.; Isidoro, R. A.; Santiago, E. I.; Fonseca, F. C., Performance enhancement of direct ethanol fuel cell using Nafion composites with high volume fraction of titania. *Journal of Power Sources* **2014,** *268*, 706-711.
252. Zakaria, Z.; Kamarudin, S. K.; Timmiati, S. N., Membranes for direct ethanol fuel cells: An overview. *Applied Energy* **2016,** *163*, 334-342.
253. Maab, H.; Nunes, S. P., Modified SPEEK membranes for direct ethanol fuel cell. *Journal of Power Sources* **2010,** *195*, 4036-4042.
254. Fu, R. Q.; Hong, L.; Lee, J. Y., Membrane Design for Direct Ethanol Fuel Cells: A Hybrid Proton-Conducting Interpenetrating Polymer Network. *Fuel Cells* **2008,** *8*, 52-61.
255. Roelofs, K. S.; Hirth, T.; Schiestel, T., Dihydrogenimidazole modified silica-sulfonated poly(ether ether ketone) hybrid materials as electrolyte membranes for direct ethanol fuel cells. *Materials Science and Engineering: B* **2011,** *176*, 727-735.
256. James, D. D.; Pickup, P. G., Effects of crossover on product yields measured for direct ethanol fuel cells. *Electrochimica Acta* **2010,** *55*, 3824-3829.
257. Heysiattalab, S.; Shakeri, M.; Safari, M.; Keikha, M. M., Investigation of key parameters influence on performance of direct ethanol fuel cell (DEFC). *Journal of Industrial and Engineering Chemistry* **2011,** *17*, 727-729.
258. Kim, H.; Lee, S.; Kim, S.; Oh, C.; Ryu, J.; Kim, J.; Park, E.; Hong, S.; No, K., Membrane crystallinity and fuel crossover in direct ethanol fuel cells with Nafion composite membranes containing phosphotungstic acid. *Journal of Materials Science* **2017,** *52*, 2400-2412.
259. Azam, A. M. I. N.; Lee, S. H.; Masdar, M. S.; Zainoodin, A. M.; Kamarudin, S. K., Parametric study on direct ethanol fuel cell (DEFC) performance and fuel crossover. *International Journal of Hydrogen Energy* **2019,** *44*, 8566-8574.
260. Sridhar, R. L.; Krishnan, R., PEMFC membrane electrode assembly degradation study based on its mechanical properties. **2013,** *104*, 892-898.
261. Hamrock, S. J.; Yandrasits, M. A., Proton Exchange Membranes for Fuel Cell Applications. *Journal of Macromolecular Science, Part C* **2006,** *46*, 219-244.
262. M.H. Khorasany, R.; Sadeghi Alavijeh, A.; Kjeang, E.; Wang, G. G.; Rajapakse, R. K. N. D., Mechanical degradation of fuel cell membranes under fatigue fracture tests. *Journal of Power Sources* **2015,** *274*, 1208-1216.
263. Solasi, R.; Zou, Y.; Huang, X.; Reifsnider, K., A time and hydration dependent viscoplastic model for polyelectrolyte membranes in fuel cells. *Mechanics of Time-Dependent Materials* **2008,** *12*, 15-30.
264. Satterfield, M. B.; Benziger, J. B., Viscoelastic properties of Nafion at elevated temperature and humidity. **2009,** *47*, 11-24.
265. Khorasany, R. M.; Goulet, M.-A.; Alavijeh, A. S.; Kjeang, E.; Wang, G. G.; Rajapakse, R., On the constitutive relations for catalyst coated membrane applied to in-situ fuel cell modeling. **2014,** *252*, 176-188.
266. Zhao, J.; Tu, Z.; Chan, S. H., Carbon corrosion mechanism and mitigation strategies in a proton exchange membrane fuel cell (PEMFC): A review. *Journal of Power Sources* **2021,** *488*, 229434.
267. Chang, Y.; Liu, J.; Li, R.; Zhao, J.; Qin, Y.; Zhang, J.; Yin, Y.; Li, X., Effect of humidity and thermal cycling on the catalyst layer structural changes in polymer electrolyte membrane fuel cells. *Energy Conversion and Management* **2019,** *189*, 24-32.
268. Song, S.; Wang, G.; Zhou, W.; Zhao, X.; Sun, G.; Xin, Q.; Kontou, S.; Tsiakaras, P., The effect of the MEA preparation procedure on both ethanol crossover and DEFC performance. *Journal of Power Sources* **2005,** *140*, 103-110.
269. Mishler, J.; Wang, Y.; Mukherjee, P. P.; Mukundan, R.; Borup, R. L., Subfreezing operation of polymer electrolyte fuel cells: Ice formation and cell performance loss. *Electrochimica Acta* **2012,** *65*, 127-133.

270. Zhao, J.; Shahgaldi, S.; Li, X.; Liu, Z., Experimental Observations of Microstructure Changes in the Catalyst Layers of Proton Exchange Membrane Fuel Cells under Wet-Dry Cycles. *Journal of The Electrochemical Society* **2018,** *165*, 3337-3345.
271. Schneider, P.; Sadeler, C.; Scherzer, A.-C.; Zamel, N.; Gerteisen, D., Fast and Reliable State-of-Health Model of a PEM Cathode Catalyst Layer. *Journal of The Electrochemical Society* **2019,** *166*, 322-333.
272. Sorrentino, A.; Sundmacher, K.; Vidakovic-Koch, T., Polymer Electrolyte Fuel Cell Degradation Mechanisms and Their Diagnosis by Frequency Response Analysis Methods: A Review. **2020,** *13*, 5825.
273. Zhao, J.; Li, X., A review of polymer electrolyte membrane fuel cell durability for vehicular applications: Degradation modes and experimental techniques. *Energy Conversion and Management* **2019,** *199*, 112022.
274. Chen, G.; Zhang, H.; Ma, H.; Zhong, H., Electrochemical durability of gas diffusion layer under simulated proton exchange membrane fuel cell conditions. *International Journal of Hydrogen Energy* **2009,** *34*, 8185-8192.
275. Schmittinger, W.; Vahidi, A., A review of the main parameters influencing long-term performance and durability of PEM fuel cells. *Journal of Power Sources* **2008,** *180*, 1-14.
276. He, W.; Lin, G.; Van Nguyen, T., Diagnostic tool to detect electrode flooding in proton-exchange-membrane fuel cells. **2003,** *49*, 3221-3228.
277. John Felix Kumar, R.; Radhakrishnan, V.; Haridoss, P., Effect of electrochemical aging on the interaction between gas diffusion layers and the flow field in a proton exchange membrane fuel cell. *International Journal of Hydrogen Energy* **2011,** *36*, 7207-7211.
278. Wood, D.; Xie, J.; Pacheco, S.; Davey, J.; Borup, R. *Durability issues of the PEMFC GDL and MEA under steady-state and drive-cycle operating conditions*; Los Alamos National Lab.(LANL), Los Alamos, NM (United States): **2004**.
279. Guo, Q.; Qi, Z., Effect of freeze-thaw cycles on the properties and performance of membrane-electrode assemblies. *Journal of Power Sources* **2006,** *160*, 1269-1274.
280. Büchi, F. N.; Inaba, M.; Schmidt, T. J., *Polymer electrolyte fuel cell durability*. Springer: **2009**.
281. Jahnke, T.; Futter, G.; Latz, A.; Malkow, T.; Papakonstantinou, G.; Tsotridis, G.; Schott, P.; Gérard, M.; Quinaud, M.; Quiroga, M.; Franco, A. A.; Malek, K.; Calle-Vallejo, F.; Ferreira de Morais, R.; Kerber, T.; Sautet, P.; Loffreda, D.; Strahl, S.; Serra, M.; Polverino, P.; Pianese, C.; Mayur, M.; Bessler, W. G.; Kompis, C., Performance and degradation of Proton Exchange Membrane Fuel Cells: State of the art in modeling from atomistic to system scale. *Journal of Power Sources* **2016,** *304*, 207-233.
282. Ren, P.; Pei, P.; Chen, D.; Zhang, L.; Li, Y.; Song, X.; Wang, M.; Wang, H., Corrosion of metallic bipolar plates accelerated by operating conditions in a simulated PEM fuel cell cathode environment. *Renewable Energy* **2022,** *194*, 1277-1287.
283. Wilberforce, T.; El-Hassan, Z.; Khatib, F. N.; Al Makky, A.; Mooney, J.; Barouaji, A.; Carton, J. G.; Olabi, A.-G., Development of Bi-polar plate design of PEM fuel cell using CFD techniques. *International Journal of Hydrogen Energy* **2017,** *42*, 25663-25685.